UNIVERSITA' DI PADOVA
DIPARTIMENTO DI INGEGNERIA
DELL'INFORMAZIONE

DOTTORATO DI RICERCA IN INGEGNERIA INFORMATICA
ED ELETTRONICA INDUSTRIALI - XV CICLO

OMNIDIRECTIONAL VISION FOR MOBILE ROBOTS

Coordinatore: Prof.ssa Concettina Guerra

Tutore: Prof. Enrico Pagello

Emanuele Menegatti

Padova - 31 Dicembre 2002

Abstract

This dissertation describes the work done by the author in the period of his Ph.D. in the field of omnidirectional vision.

After a general presentation on omnidirectional vision, the dissertation focuses on omnidirectional vision for mobile robotics. Each chapter of the dissertation covers a different topic in omnidirectional vision for mobile robotics. The three main chapters describe the evolution of an omnidirectional vision system to be mounted on a mobile robot. First, a new simple algorithm used to produce low-cost omnidirectional mirrors with custom profiles is presented. Second, a new method of hierarchical localisation is described. Hierarchical localisation is defined as the determination of the robot's position with different accuracies depending on the environment structure. Third, the implementation of the Spatial Semantic Hierarchy is described in detail. The Spatial Semantic Hierarchy of B. Kuipers has been previously implemented only on simulated robots or on robots with sonar in very simple environments. The described implementation deals with a real robot, in a real-world environment, equipped with an omnidirectional vision sensor only.

The last chapter describes an extension of omnidirectional vision from single robot domain to multi-robot domain. The aim is to build an Omnidirectional Distributed Vision System. In a Distributed Vision System, the different sensors are networked. The interaction and the communication between the sensors enables intelligent behaviours not achievable with a single sensor. This last section should be considered as an overview of the current work of the author, in which preliminary results and preliminary experiments are reported.

Abstract

Questa tesi descrive il lavoro svolto dall'autore nel campo della visione omnidirezionale durante il suo adottarti.

La tesi, dopo una presentazione generale sulla visione omnidirezionale, si concentra sulla visione omnidirezionale per robot mobili. Ogni capitolo affronta un diverso argomento di visione omnidirezionale per robotica mobile. I tre capitoli principali descrivono l'evoluzione di un sistema di visione omnidirezionale per un robot mobile. Dapprima presentato un nuovo algoritmo per la produzione di specchi omnidirezionali a basso costo con profilo variabile. Poi si passa alla descrizione di un nuovo metodo di localizzazione gerarchica per il robot: l'idea quella di determinare la posizione del robot con un'accuratezza che dipende dalla struttura dell'ambiente che circonda il robot. In fine viene descritta in dettaglio l'implementazione della *Spatial Semantic Hierarchy* di B. Kuipers su un robot reale. La *Spatial Semantic Hierarchy* era stata testata precedentemente solo su robot simulati o robot dotati di sonar che operano in ambienti molto semplici. L'implementazione descritta stata realizzata su un robot reale, che opera in un ambiente reale ed dotato solo di un sensore di visione omnidirezionale.

L'ultimo capitolo riporta il lavoro svolto per applicare la visione omnidirezionale a sistemi multi-robot. L'obiettivo quello di realizzare un *Omnidirectional Distributed Vision System* in cui i vari sensori omnidirezionali siano collegati in rete tra loro e in cui l'interazione tra i singoli sensori genera dei comportamenti intelligenti che non possono essere ottenuti con un singolo sensore. L'ultimo capitolo dovrebbe essere considerato come una panoramica del lavoro attuale dell'autore, in cui vengono riportati risultati ed esperimenti preliminari.

Al Mio Amore,
"…viaggiare io e te
con la stessa valigia in due
dividendo tutto sempre"
(Tiromancino)

Alla Mia Mamma e al Mio Papà,
"…dammi ancora la mano, anche se quello stringerla è solo un pretesto per sentire la fiducia totale che nessuno mi ha dato o mi ha mai chiesto… (F. Guccini)

Acknowledgement

To compress in one page all the people I met in three years of Ph.D. is not easy. There are so many people I wish to thank for their support and their help. First of all I wish to mention my wife Maria Grazia that forwent three years of beach holidays for following me around the world. My parents always present and ready to support me. I wish to remember my mother always worried about my health especially when I was on the other side of the world. My friends, they were close even if I was on the other side of the world: Samuele, Matteo, Marco, Carlo, Nico, Daniel, Justin.

I wish to thank all the scientists I met, for the marvellous things they taught me: my supervisor Enrico Pagello, Bob Fisher, Mark Right and John Hallam of the University of Edinburgh (U.K.), Hiroshi Ishiguro and Takayuki Nakamura of the University of Wakayama (Japan), Wolfram Burgard of the University of Freibur (Germany), Ben Kröse of the University of Amsterdam (The Nederlands), Ryad Benosman of the University of Paris 6 (France).

A special thank goes to Hiroshi Ishiguro for the invitation in his laboratory at Wakayama University (Japan), for the wonderful atmosphere he created there for me and for the support he kindly provided me.

Last but not least, I wish to mention my colleagues of the *box dottorandi* at the University of Padua. Thank to them, lunch was a relief from work and coffee was an extra pleasure: Barbara, Chiara, Marco, Enrico, Andrea, Gianluigi, Stefano, Francesco.

This research has been supported by: the PRASSI project of ENEA (the

Italian National Agency for New Technologies, Energy and Environment), Padova Richerche s.c.p.a. (Padova - ITALY), Tecnogamma s.p.a. (Traviso - ITALY), the Scottish Award Agency (U.K.), the University of Wakayama (Japan), Progetto sui Sistemi Multi-Robot of The University of Padua, the Ph.D. School of the University of Padua.

Contents

List of Figures

List of Tables

Chapter 1

Introduction

The sense of vision is one of the most effective way of collecting information on the surrounding environment. This is true both for animals and for machines. Since the beginning of research on mobile robotics the scientists tried to give the robots the *sense of vision*. Many times the progress of science and technology was inspired by the observation of the Nature. We will introduce the omnidirectional vision and its advantages by looking at the world of nature. From these observations, it will be evident the need to design different vision systems for robots performing different tasks.

1.1 The Sense of Vision

The knowledge of the surroundings in Nature is essential to survive. For instance, the ability to effectively track the motion of a pray or the ability to spot a predator while it is far away are essential skills in the struggle for survival. The natural distinction of animals into preys and predators brought to the development of two different kind of vision systems.

The vision systems of preys is "designed" with the largest possible vision field in order to survey the widest area around them. This brought to very large eyes positioned on the opposing sides of the snout. This arrangement

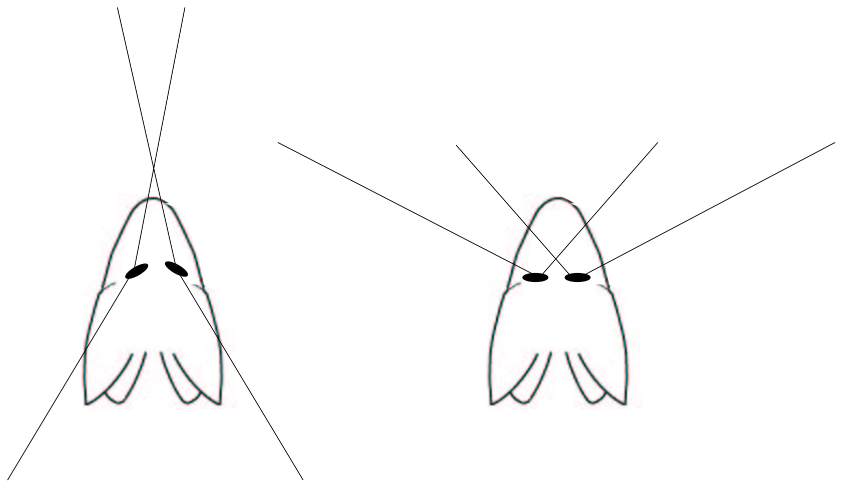

Figure 1.1: The field of view of preys (left) and predators (right).

assures the maximum coverage of the environment, because the field of views of the two eyes have a very little overlap or do not overlap at all. With this arrangement preys can achieve up to 360° of field of view.

The vision system of predators is designed with the highest acuity in order to accurately locate their preys. This brought to eyes positioned on the forward part of the snout with a big overlap of the vision fields of the two eyes in order to perform stereoscopic vision enabling the accurate estimation of the pose of objects of interest. The resolution achievable by animals is impressive, e.g. an eagle can spot an hare from two kilometres away.

The two tracks followed by the evolution are evidences of the trade off we face when building an artificial vision system: should we privilege the high resolution or should we privilege the wide field of view? The two approaches can be combined only to some extent. In fact, increasing the resolution of the vision sensor and extending the vision field of the sensor, both increase the amount of information gathered from the sensor. This information then should be processed. If the amount of information is too high this processing is too burdensome and there is no advantage. This is true for the vision organs of the animals and for the artificial vision systems we can build.

In this dissertation, we will present our efforts for building an artificial vision system with a very large field of view. We will focus on the design of sensors that can grab images with 360° of horizontal field of view and on the techniques developed by the author for extracting from omnidirectional images the information needed by a mobile robot.

1.2 Omnidirectional Vision

The term Omnidirectional Vision refers to vision sensor with a very large field of view, i.e. sensor with a horizontal field of view of 360° and a variable vertical field of view usually between 60° and 150° .

Usually animals achieve a 360° field of view with two eyes. The field of view of every eye is limited to 140–220° , but some animal presents eyes with a 360° of horizontal field of view. These eyes can be considered as omnidirectional sensors. When the mankind started to reproduce the world into paintings, it tried to give the sense of "*reality*" by generating very large sight of the represented environment. Lately, machine vision researchers discovered that the imaging techniques developed as a form of art or *"divertissment"* could be used also in scientific domains and new generations of omnidirectional sensors sprouted out.

Omnidirectional vision is a new technique and probably is not mature yet for commercial and market application, but its use is growing very fast. More and more laboratory around the world are developing new sensors and new applications of omnidirectional vision.[1] Today, omnidirectional vision is used in tasks as: wide area surveillance [32], video-conferencing [25], remote reality [11], non-destructive inspections [30] [5], 3D environment re-

[1]As an example of the rate of growth, consider the web page "The Page of Omnidirectional Vision" (www.cis.upenn.edu/ kostas/omni.html). This page links to Universities and Companies working in the field of omnidirectional vision. When the author started his work on omnidirectional vision in 2000, this page had only 10 links to Universities and 5 or 6 links to companies. Now the links present in the page are more than doubled.

construction [15], etc. Probably, the domain where omnidirectional vision found the largest application is the mobile robotics domain. This dissertation will illustrate the work of the author in several fields of applications of omnidirectional vision to mobile robotics.

1.3 Omnidirectional Vision for Mobile Robotics

Usually the cameras used in machine vision tasks are off-the-shelf cameras. These cameras are designed for television purpose or for grabbing still pictures. In order to apply them to Computer Vision or Robot Vision tasks, the researchers developed several workarounds to overcome the limitations of these systems. On the contrary, we believe that, as nature designed different kind of eyes for different tasks, we should employ (or design, as well) different imaging sensors for the different tasks assigned to the machines. This is not always possible due to external constraints (like costs and technological limitations), but omnidirectional cameras, and in particular catadioptric camera, greatly extended the flexibility of the imaging systems.

Omnidirectional vision is a relatively new technique for mobile robotics. Its range of applications and the new possibilities offered are not fully understood. In fact, despite the fact that the first works that used omnidirectional vision sensors mounted on mobile robots date back to the early 90's, there are no public available software libraries dedicated to omnidirectional vision.[2]

Omnidirectional vision sensors are valuable sensors in the field of mobile robotics, because they offer in one shot a global view of the area surrounding the robot. For instance, the knowledge of the positions of the objects at 360° around the robot is essential in tasks like map matching or image-based navigation. The field of view at 360° greatly reduces the perceptual aliasing

[2]At the time of writing, at the Intelligent Autonomous System Laboratory (IAS-Lab) of the University of Padua we are working on the first release of *V2* our omnidirectional vision software suite

(i.e. the possibility that two distinct places offer the same sensory reading). In addition, in highly dynamic environment, the continuous view of the area surrounding the robot enable simple tracking techniques to follow the objects of interest.

Moreover, the impact of omnidirectional vision is not fully understood also by people working with omnidirectional vision sensor. The use of an omnidirectional vision sensor should influence the entire robot. Omnidirectional vision sensors should be considered as a totally different sensors with respect to a standard perspective cameras. The completeness of their 360° field of view should influence the complete robot: the whole body, the driving system and the software controlling the robot. There should be a complete synergy between the omnidirectional sensor and the body of the robot . The body should not impair the omnidirectional vision sensor. For instance, the body should have a rotational symmetry and be shaped in order not to occlude the sensor preventing the observation of some areas around the robot. This recommendation is not followed by many researchers. For instance, in the RoboCup competitions almost every team is using omnidirectional vision sensors, but only few of them have robots with a circular symmetry and behaviours that fully exploit the omnidirectional sensor.

1.4 The dissertation overview

This dissertation is intended as a description of the work done by the author in the field of omnidirectional vision during his Ph.D.

Chapter 2 presents a general overview of the different techniques used to grab omnidirectional images. The chapter starts with an overview on omnidirectional vision in animals, then gives a brief panoramic of omnidirectional vision in arts, concluding with the different techniques used at the moment in the scientific laboratories around the world to capture omnidirectional images. The aim of the chapter is to identify the roots of the modern omnidirectional vision used in mobile robotics.

Chapter 3 proposes the idea that the omnidirectional vision sensor mounted on a mobile robot should be customised on the robot's task and on the robot's body. In the chapter, we also detailed the technique used to design and produce low-cost omnidirectional mirrors with custom profile. Some examples of realised mirrors are proposed.

Chapter 4 discusses the main scientific result: a method for the *hierarchical localisation* of a mobile robot within the image-based localisation frame. We realised this work when we were visiting researcher at The Intelligent Robotics Laboratory of Prof. **H. Ishiguro** at Wakayama University (Japan). The second part of the chapter discusses the integration of a Monte-Carlo localisation method with our method of image-based localisation in order to solve the main problem that affects image-based localisation, i.e. the *perceptual aliasing*. Experimental results are presented.

Chapter 5 presents another main scientific result: the implementation of the Spatial Semantic Hierarchy of Prof. **B. Kuipers** on a real robot fitted only with an omnidirectional vision sensor. The chapter describes why the omnidirectional vision sensor is a good sensor to implement the Spatial Semantic Hierarchy. This work started when we were a Master Student in Artificial Intelligence at the University of Edinburgh (U.K.) during the first year of our Ph.D and then continued in Padua.

Chapter 6 presents some new topics we are working on. This chapter should be considered as a kind of "work-in-progress" section even if the ideas and the first experiments presented have been published in some conferences. In the first part of the chapter, we present the concept of Distributed Vision System and Vision Agents. Then we explore how these concepts can be exploited with omnidirectional vision. In the end we present the first stage of an Omnidirectional Distributed Vision system composed of uncalibrated omnidirectional cameras that can learn to control a mobile robot.

Chapter 2

Omnidirectional Imaging

In this chapter, we will give an overview of the omnidirectional vision sensors. We will start introducing some examples of omnidirectional vision in animals showing that different eyes evolved for different tasks. Then, we will discuss how the mankind approached the idea of omnidirectional vision within arts in order expand the perceptive experience of the observer. We will discuss some of the philosophical implication of this. In the end of the chapter we will present a brief survey of the modern technique to capture omnidirectional images and how these are used in science to build more effective artificial vision systems.

2.1 Omnidirectional Vision in Animals

Several times, the progress of science has been inspired by the observation of the Nature, so we will start this overview on omnidirectional vision sensors by analysing some examples of omnidirectional eyes in animals.

One of the first examples of omnidirectional vision sensor appeared on Earth about 50 Million of years ago. Fig. 2.1 shows a picture of the fossil eye of a trilobite. This was a compound eye similar to the one of the modern insects.

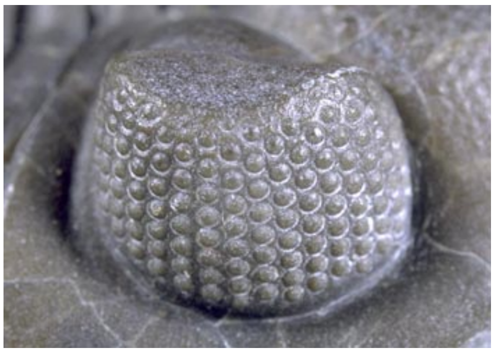

Figure 2.1: The close-up view of the eye of a fossil trilobite. One of the first examples of omnidirectional vision system.

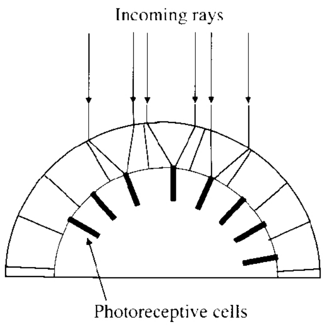

Figure 2.2: A sketch of the compound eye of a diurnal insect. Every facets has a photoreceptor associated.

Almost, all animal eyes that can be considered omnidirectional vision sensor are compound eye. The compound eye is composed of a set of optical elements apt to collect the light rays coming from different directions. These optical elements are densely packed to form the eye and are called *facets*.

For the purpose of this panorama on omnidirectional eye, we can broadly divide the animal compound eyes in three main categories. This division depends on the technique used to focus the light on the retina.

The first set is composed of eyes where at every facet is associated a photoreceptive cell, as sketched in Fig. 2.2. This kind of eye is frequent in diurnal insects.

The second group is composed of eyes with a single retina. The refraction

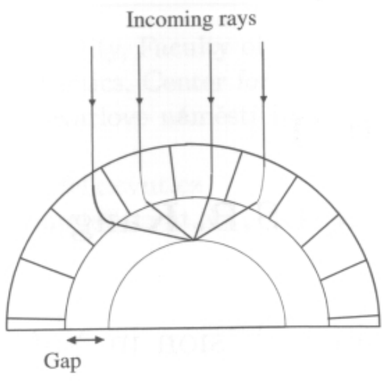

Figure 2.3: A sketch of the compound eye of a nocturnal insect. Note that rays of light entering at different facets are focused in the same point on the retina with a refraction.

index of every facet is graduated in order to progressively bend the path of the incoming light rays. The bending causes parallel rays coming from the same source to focus at the same point in the retina, Fig. 2.3. Such kind of eye is apt to work in conditions of very low lightening. This compound eye is found in nocturnal insects.

The third group is composed of eyes similar to the one of the night insects, but this group uses reflections instead of refractions in order to focus the light on the retina. At every facet is associated a lenticular element with a reflective lateral surface. Once the parallel rays of light coming from the same object enter the different facet, they are reflected at the lateral surface of the lenticular elements and focused on the retina. Fig. 2.4 shows a sketch of this kind of compound eye. This last type of eye can be found in crustaceans.

2.2 Omnidirectional Vision in Arts

At the beginning of the XV century, after the brilliant intuition of Giotto in the middle of the XIV century, Filippo Brunelleschi unrevealed the geometrical rules underlying the human visual perception and created the **perspec-**

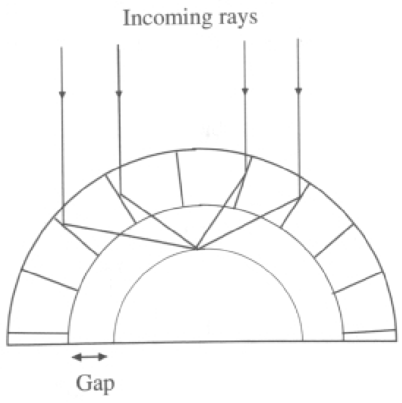

Figure 2.4: A sketch of the compound eye of a crustacean. Note that rays of light entering at different facets are focused in the same point on the retina with a reflection.

tive. The perspective enabled the artist to give a more realistic representation of reality by following some simple geometrical rules. At the same time, the artists discovered that they could play with these geometrical rules to alter the perception of reality. One of the first examples is the representation in paintings of hemispherical mirror called *witch mirror*[1] .

2.2.1 The extension of the perception

In the painting "*The Wedding of Giovanni Arnolfini*" of Jan van Eyck (Fig. 2.5) the witch mirror represents a scenical artifice to extend the perception of the spectator. The artist was bind to the classical representation of the bridal couple in the nuptial room. Introducing the witch mirror, he can expand our sensorial horizont behind the usual border and can represent the whole room, himself while observing the bridal couple from the door of a second room.

The same functionality of enlarging our sensorial experience perceiving a larger portion of the world and then having a better understanding of the

[1]The name of these mirrors come from the "*strange*" reality that is reflected by these mirrors, like if it was altered by a witch or some evil spirit.

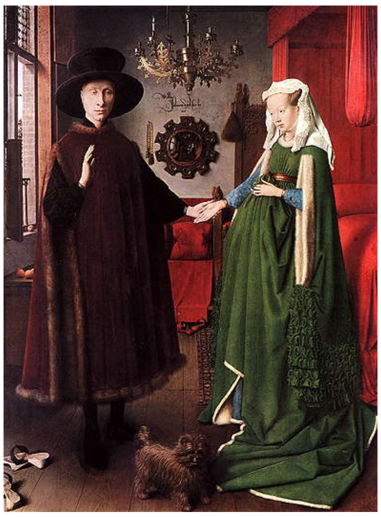

Figure 2.5: “*The Wedding of Giovanni Arnolfini*” of Jan van Eyck.

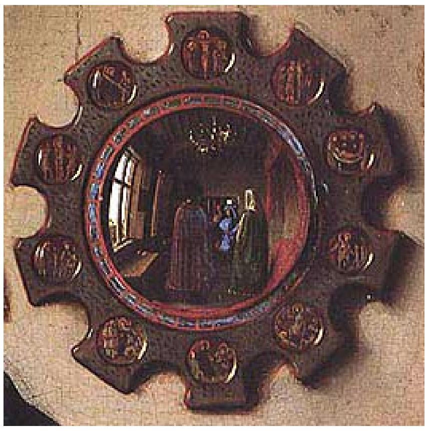

Figure 2.6: The zoom on the witch mirror on the wall behind the bridal couple showing the rest of the room and the painter.

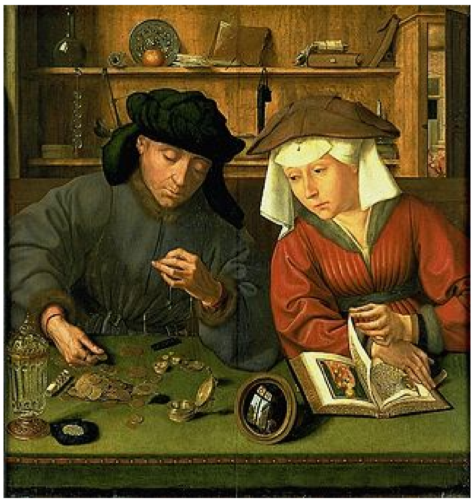

Figure 2.7: “*The praetor and his wife*” of Quentin Metsys.

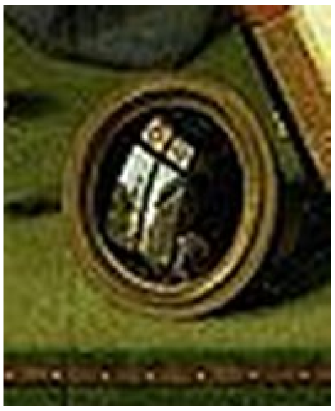

Figure 2.8: The zoom on the witch mirror on the table of the moneylender reflecting the window, the person waiting beside the window and the view out of the window.

reality is performed by the witch mirror in the "*The moneylender and his wife*" of Quentin Metsys (Fig. 2.7). Here, the scene illustrates the moneylender and his wife while they are counting some coins and looking at an object. The main scene does not tell the whole story, it is only the convex mirror that reveal the drama that is going on. Close to the window reflected in the mirror, there is a person waiting for the decision of the moneylender. This person is pawning his goods and he is waiting with impatience the decision of the moneylender.

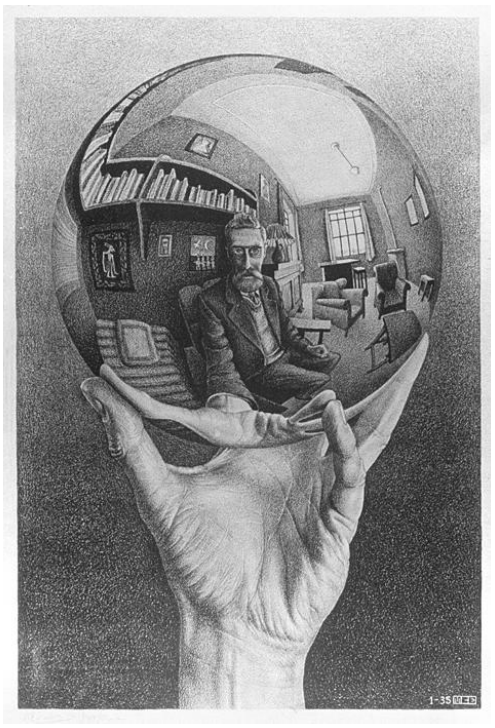

Figure 2.9: A litograph of Escher: Hand with Reflecting Sphere 1935.

The philosophycal meaning of extension of the reality and of the knowledge is reached in the famous printing of Escher *Hand with Reflecting Sphere* (1935) (Fig. 2.9). Here the painter is observing the spectator through the reflection on the sphere. The observer has a complete view of the world of the painter and he completely identify himself with the painter and with his mind.

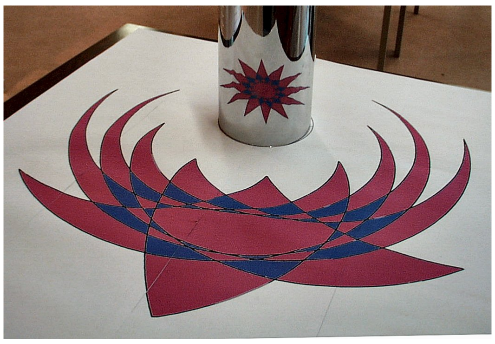

Figure 2.10: An example of anamorphosis. The correct perception of the star is perceived only after the reflection on the reflecting cilindrical surface.

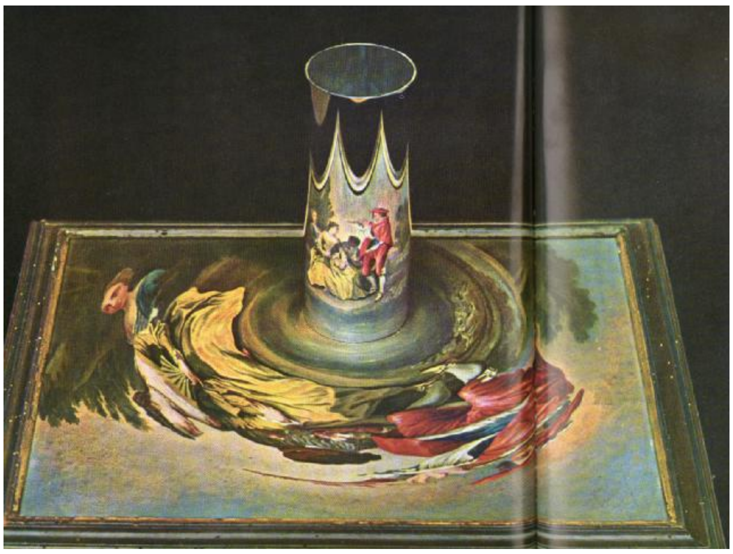

Figure 2.11: An second example of anamorphosis. The correct perception of the painted scene is perceived only after the reflection on the cilindrical surface.

Another example of how reflecting surface can enlarge and puzzle our sensorial experience is the case of anamorphosis. A simple example of anamorphosis is depicted in Fig. 2.10. In anamorphosis the object is not represented following the geometrical rule of perspective, but it is geometrically distorted at a grade where it is not recognisable. The geometrical distortion can be removed only with a reflecting surface with an appropriate shape and position. The image reflected by the mirror surface appear now to follow the perspective rules. A more complex example is represented in Fig. 2.11. As Benosman and Kang briliann tly say in their book "*Panoramic Vision*" [6]:

> *"...The catoptric anamorphosis is fascinating not only because it reveals what is hidden, but it also offers two contraddictory ways of perceiving reality. In fact, the eye perceives the distorted and its corrected version on the mirror, and simultaneously understands both the illusion and the mechanism of the illusion. ..."*

The distortion of the perspective, the witch mirrors, the anamorphosis, all toghether contributed to create the understanding that what we perceive through our eyes is just one of the possible representation of reality. If we can change the way we perceive the reality we can expand our knowledge or extract more information from the appearance of reality as we will show in the next chapters.

2.2.2 Capturing the horizon

In the first part of this section, we saw how artists played with the geometrical rules underlaying perception, in order to extend the sensorial horizont of the observer. In the second part, we will briefly report the efforts made by the artists to capture a complete view at 360° of a scene, in order to reproduce the apparence of the environemnt: the *panoramic art*.

The world *panorama* was introduced at the end of the XVIII Century and is the result of the union of the two greek words pan ($\pi\alpha\nu$ = "all") and horama ($\acute{o}\rho\alpha\mu\alpha$="sight"). For a person of the beginning of the XIX century, the meaning of the word "*panorama*" was very different from the current meaning. The initial meaning of this word refered to the invenction of the Scottish Robert Barker patented in 1767. The panorama was a format of

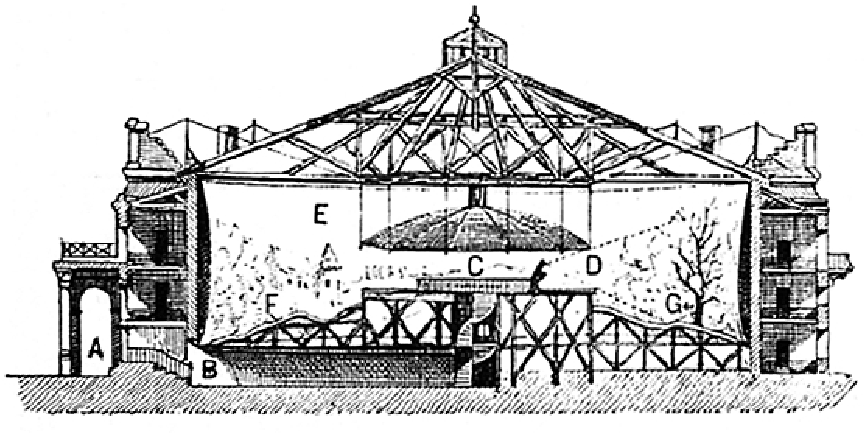

Figure 2.12: The panorama. A) Entrance, B) dark access corridor, C) spectator stage, D) field of view of the spectators, E) *vellum*: a reversed umbrella that limited the field of view of the spectators, G) painting, F) slope covered of grass.

painting at 360° that sourrounded the spectator. A scketch of the typical structure of a panorama is depicted in Fig. 2.12. The spectator was within a "*rotunda*" surrounded by the painting. The aim was to impress the spectator with a realistic representation of a natural or urban landscape. Everything was designed to convey this reality impression on spectators. The spectators entered the rotunda through a dark tunnel that brought them directly to the center of the panorama, a sort of mysterious trip. Once entered in the panorama the impression was really to be in the center of the depicted scenary. The lighting where shielded by the *vellum* (a kind of reversed umbrella that limited the field of view of the spectators), the slope between the stage and the painting was covered with grass (in order to convey the idea of a natural landscape). We could say it was one of the first attempt to realise an *immersive virtual reality.* Most of the paintings realised for the panorams have been lost. Few of them survided. In Fig. 2.13 is represented the cityscape of Edinburgh in Scottland as painted by Robert Barker in 1787.

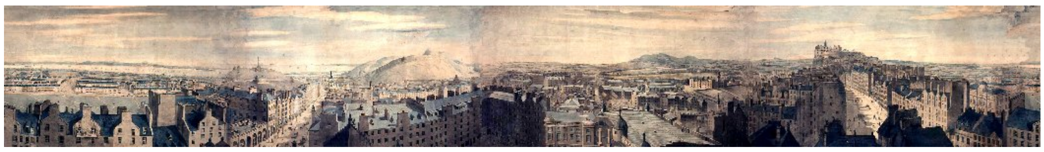

Figure 2.13: The panorama of Edinburgh - Scottland. R. Barker (1787)

Panoramas were build in all the major cities of Europe and of the United States of America. It was a great commercial success, but at the end of the XIX, the attractive of panoramas quickly declined. In the while,the photography was invented. The photography was used to recreate even more realistic landscapes, but it did not have a big success of public. Nevertheless, this was the born of the panoramic photography. The cameras used to grab these early panoramic pictures are the ancestors of modern panoramic cameras and panning cameras used by the scientists. In Fig. 2.14 is represented one of the most successful panoramic cameras, i.e. the Kodak Cirkut 10. This dates back to 1902 and it is still in use by lovers of panoramic photography. In Fig. 2.15 is depicted a modern panoramic picture of the Mount Mauna Kea Observatory

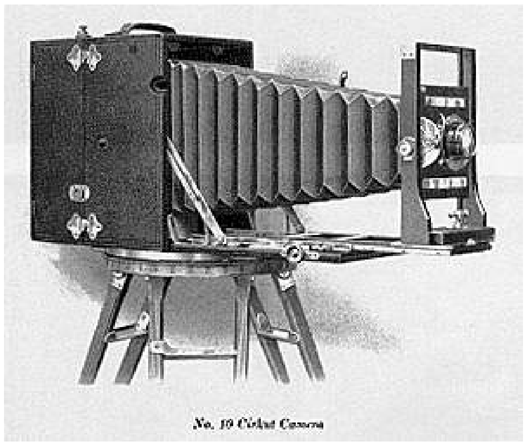

Figure 2.14: An ancian panoramic camera.

Figure 2.15: A panoramic picture at the Mauna Kea observatory.

2.3 Omnidirectional Vision in Science

The bending of the laws of perspective and the panoramic art inpired the machine vision community to explore new way of capturing pictures of the environment.

The modern omnidirectional sensors used in computer vision and robot vision can be devided in three big groups. This distinction arises from the different imaging technique[2] . The three goups are:

- the compound-eye cameras;
- the panoramic cameras;
- the omnidirectional cameras;

At this point, a brief note on terminology is needed. There is a mix-up in terminology in the scientific community. The adjectives *panoramic* and *omnidirectional* are used as synonims, with a sligtly more technical flavour for *omnidirectional.* In this dissertation we will use the term "**panoramic**" for imaging device able to generate a perspective image at 360° of the surrounding with a limited vertical field of view (tipically a panning perspective camera). The term "**omnidirectional** will be used for sensors that produces non-perspective images with a 360° horizontal fild of view and with a vertical field of view that can be bounded or not.

[2]For a more detailed survey on the different types of omnidirectional sensor, see the survey paper of Y. Yagi [88].

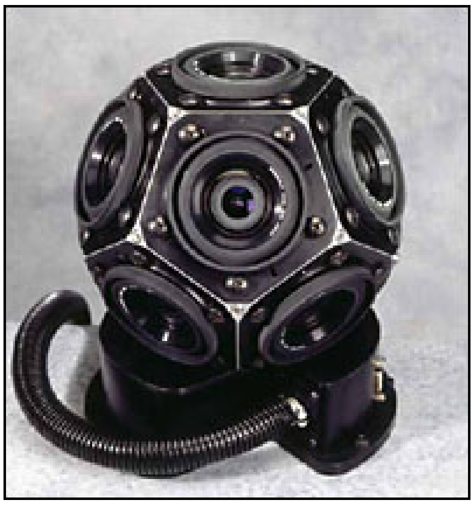

Figure 2.16: The DodecaTM 1000 Camera produced by Immersive Media.

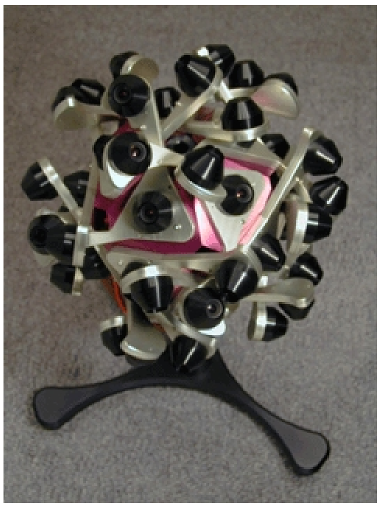

Figure 2.17: The S.O.S. sensor (Stereo Omnidirectional System) produced by ViewPLUS Inc.

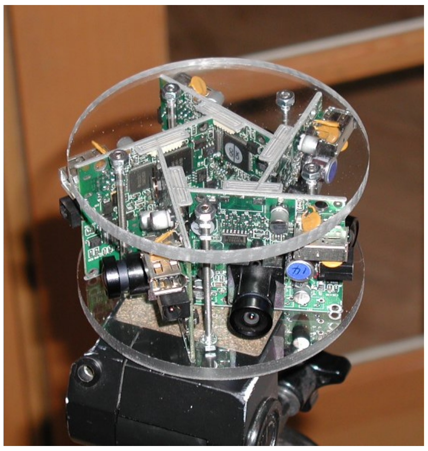

Figure 2.18: The RingCam realised in the Microsoft Laboratories.

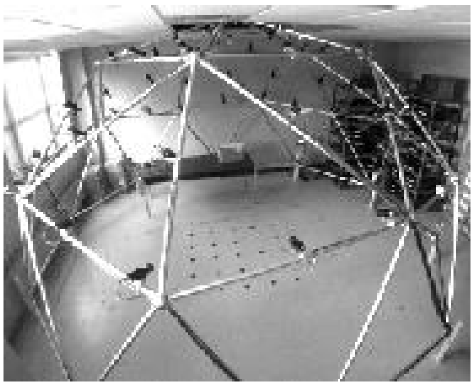

Figure 2.19: The dome for virtualising artistic or sport performance at Carnagie Mellon University.

2.3.1 Compound-eye cameras

We will not discuss in detail the compound-eye cameras. We will only mention it for sake of completeness in this overview. Compound-eye cameras uses multiple camera to grab pictures in different directions and then stich them one to the other in order to produce a global view of the environment. The advantages of these cameras are the high resolution these sensors can achieve and the possibility to grab the pictures in different direction at the same time. The disadvantage is the complexity of the system and the need of a accurate calibration process.

The DodecaTM 1000 Camera is composed of 11 cameras able to grab almost spherical image. DodecaTM 1000 Camera is produced by Immersive Media. The S.O.S. sensor (Stereo Omnidirectional System) has almost the same spherical field of view of the DodecaTM 1000 Camera, but it can perform stereo vision in this sphere of view. This is possible because the system is composed by 20 triplets of CMOS cameras looking at different directions. The S.O.S. sensor was realised by ViewPLUS Inc. Despite these two prototypes, the most commonly used compound-eye cameras are composed of few cameras looking at the horizon in different directions that shot at the same time, like the RingCam depicted in Fig 2.18 realised in the Microsoft Laboratories in U.K. The pictures from the different cameras are merged to produce a panoramic image, called also **panoramic cylinder** [40].

Out of curiosity, we present a fourth type of sensor that usually it is not considered an omnidirectional sensor, but it can be considered a peculiar kind of compound-eye camera. This sensor is not looking *around*, like the other sensor presented, it is looking *inside*, Fig. 2.19. It does not generate a unique omnidirectional image. It performs N-stereo vision and it is used to digitalize motion performances as dance or sportive events [42].

2.3.2 Panoramic cameras

As we said in the previous note, in this dissertation we use the term panoramic camera for sensors able to produce perspective panoramic views using a single camera. Usually this is achieved by panning a camera around the vertical axis passing through the focal point of the camera, see Fig. 2.20. This approach requires very fine calibration and synchronisation of the movements of the camera and provides high definition panoramic images. If the camera does not rotate about its vertical axis, but around a vertical axis at a certain distance from its focal point, it is possible to obtain rough range panoramic images by matching the views of an object from different positions [13] [40]. This technique is very slow and it is not suited for dynamic environment. In dynamic environment, we need cameras able to capture a global view in one shot in order to have at any time in the field of view all the moving objects. These cameras are omnidirectional cameras.

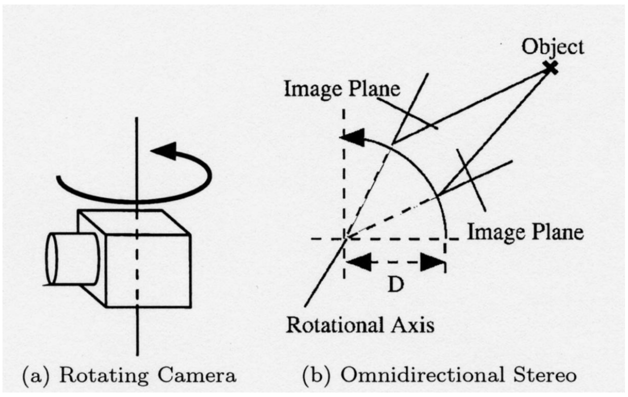

Figure 2.20: The panning camera (left) and the range technique (right).(Courtesy of Prof. Y. Yagi at Osaka University)

2.3.3 Omnidirectional cameras

Even if omnidirectional camera have been realised with different techniques, the basic idea is always the same, i.e to gather the light coming from the objects in the surrounding of the sensor and convey it into the sensor by changing the path of the rays of light. Cameras that use only the refractive effect of lens to bend the light are called **dioptric cameras** (from dioptrics the science of refracting elements). Cameras that use the combined effects of reflection from a mirror and of refraction from a lens are called **catadioptric cameras** (from catoptrics, i.e. the science of reflecting surfaces and dioptrics).

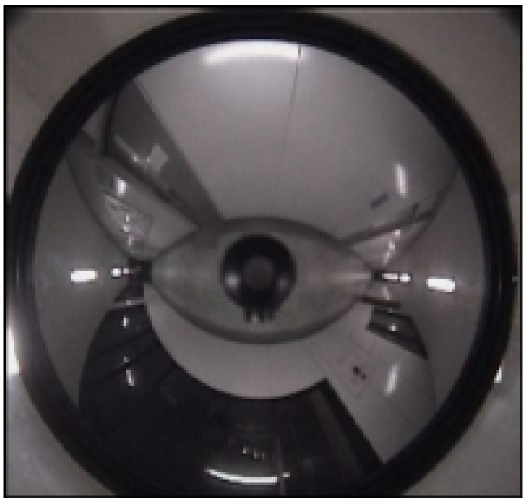

Figure 2.21: An Omnidirectional image.

The omnidirectional camera mostly used by the machine vision community can be groupped in three cathegories: cameras that uses special lens, camera that uses a convex mirror and a set of lens, and cameras that uses two mirrors and a set of lens.

2.3.4 Special lens cameras

Cameras with the use of fish-eye lens can acquire almost a hemispherical view. The drawback is that the resolution of the images is good at the centre but very low at the periphery. This is not good for robot navigation, where the objects to locate lie on the floor and they appear at the horizon or below.

Figure 2.22: A camera mounting a PAL lens.

Figure 2.23: A cameras mounting convex mirrors of Accowle Co. Ltd.

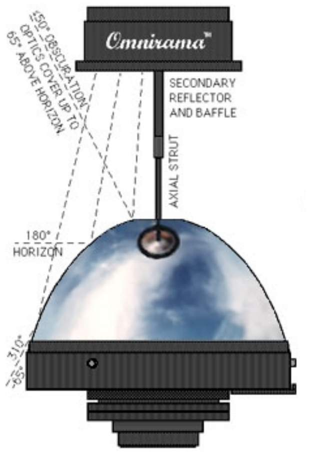

Figure 2.24: An example of folded catadioptric camera.

In other words, the resolution is very good looking at the ceiling but poor at the horizon. Greguss proposed an optical lens called Panoramic Annular Lens (PAL) composed of three reflective and two refractive planes [31]. See Figure 2.25. This does not need alignment and can be easily miniaturised.

2.3.5 Convex mirror cameras

Convex mirror cameras are the most widely used in robotics to obtain omnidirectional images. The sensor is composed by a perspective camera pointed upward to the vertex of a convex mirror. The optical axis of the camera and the geometrical axis of the mirror are aligned. This system is usually fixed on top of a mobile robot like in Figure 5.1. Different shapes of the mirror have been used. The most common are conical mirrors, hemispherical mirrors, hyperboloidal mirrors and paraboloidal mirrors; see Figure 3.2. Every shape presents different properties that one has to take in account when choosing the mirror for a particular task. In Chapter 3, we will compare three possible

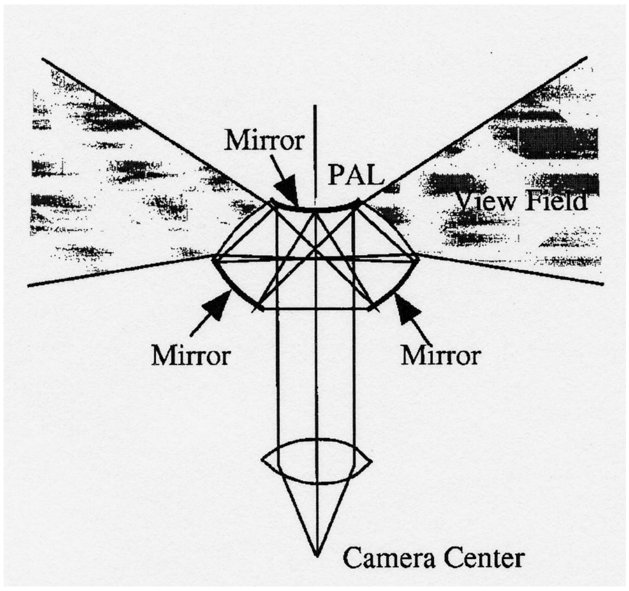

Figure 2.25: A sketch of a basic optics of PAL. (Courtesy of Prof. Y. Yagi at Osaka University)

different profiles for the mirrors.

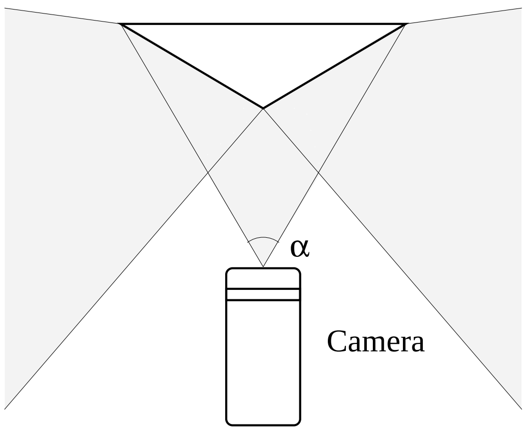

Figure 2.26: A sketch of a basic optics of a convex mirror camera.

To produce these mirrors out of glass would be very expensive and for some particular shape would not be possible. Fortunately, they can be realized from a cylinder of stainless steel shaped with a numeric control lathe. The surface of these mirror is smooth enough and reflective enough for the purposes of omnidirectional vision.

The catadioptric omnidirectional cameras with a single convex mirror will be the sensor we will discuss in the rest of the dissertation, but before moving on in the next chapter, where we will explain how to build a convex mirror with a custom profile, let us discuss the third type of omnidirectional camera.

2.3.6 Folded catadioptric cameras

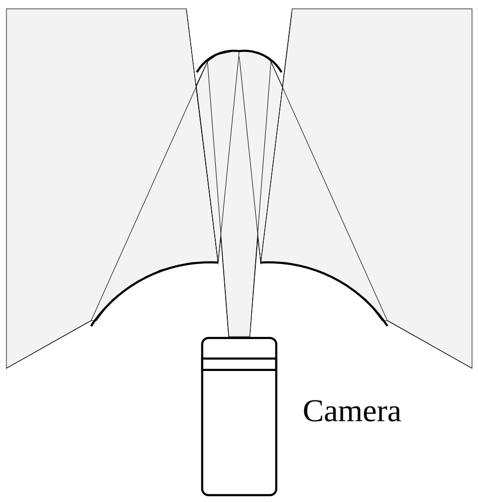

Figure 2.27: A sketch of a basic optics of a folded catadioptric camera.

Usually catadioptric cameras tend to have big dimensions compared to conventional cameras, because a minimal distance is required between the camera and the convex mirror. To overcome this limitation, folded catadioptric cameras were developped [74]. They use the optical folding method to fold the optical path between the curved mirror and the lens system. Folding with a curved mirror creates a 180° fold and can reduce undesidered optical effects. An example is like the Omnirama of Versacorp in Fig. 2.24.

2.4 Conclusions

In this chapter, we saw the different ways used by animals, artists and scientists to capture omnidirectional images. The lesson we learned from panoramic are is that reality depends on the way we observe it. The lesson we learned from the vision of animals is that "the way we observe" depends on what we are looking for. Again animals tell us that our perspective sight is just one of the possible way of vision.

In summary, when we design an artificial vision system for a robot we should take into account the task of the robot. From this analysis we could conclude that maybe the robot does not need a high resolution image, but a wide image with different resolutions in different regions of the image. Therefore, we should design an omnidirectional vision sensor customised on these requirements.

In the next chapter, we will see a technique to build omnidirectional vision sensor tailored on the task of the mobile robot.

Chapter 3

Omnidirectional Mirror Design

In the previous chapter, we gave an overview on the variety of panoramic and omnidirectional sensors. As we said, the catadioptric sensors are the most successful omnidirectional vision sensor. Their popularity is due to: *the low cost* (compared to PAL[1] sensors); *the high-speed* in collecting the data (compared to the panoramic cameras) and *the flexibility*.

The flexibility of the catadioptric systems derives from the possibility to easily change the transfer function of the sensor. The transfer function of the sensor describes how points in the three dimensional *world* are mapped into points in the two dimensional *image*. In a catadioptric system, the shape of the mirror determines the transfer function of the sensor.

In this chapter, we will show how a desired mapping between *world points* and *image points* can be obtained with a customised profile of the omnidirectional mirror. The design of a custom mirror profile enables to overcome the limitations of classical omnidirectional sensors and to expand their range of applications. In other words, the design of omnidirectional sensors with a custom profile is a key issue in simplifing or developping new applications. In the second part of the chapter, we will present the actual design of three

[1]PAL = Panoramic Annular Lens.

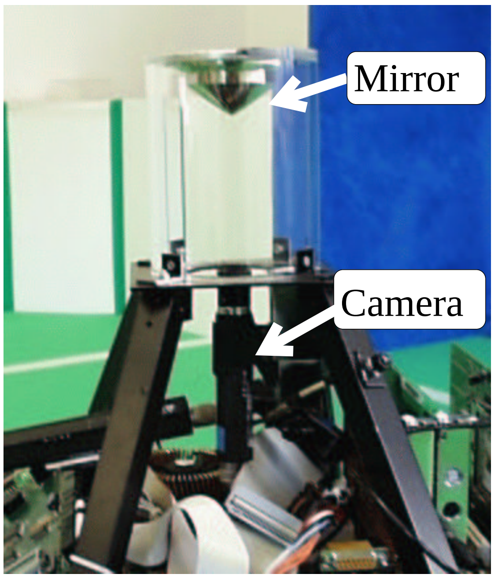

Figure 3.1: The omnidirectional vision system. The camera is the vertical black stick and it is pointed upward to the omnidirectional mirror. Note the custom profile of the mirror.

mirrors tailored for different applications.

3.1 Classical Mirror Shapes

Before describing in detail how is possible to create a custom profile for an omnidirectional mirror, we will give a brief overview on the most used types of omnidirectional mirror. These shapes has been so widely used in mobile robotics that they can be called *classical mirror shapes*. In Fig. 3.2, some of the most used mirror shapes are presented. As we said, every one of these mirror shapes realises a different mapping between the world points and the image points. These mappings determine the resolution and the field of view (FOV) of the different sensors. Let us discuss briefly the properties of each shape:

- (a) **conical mirrors** have good resolution in the peripheral, but they produce a singularity at the cone tip.

- (b) **hemispherical mirrors** they have good resolution in the centre area but poor resolution at the peripheral region. These mirrors present the widest view angle among convex mirrors.
- (c) **hyperboloidal mirrors** have good resolution both in the centre and in periphery. The view angle is almost as wide as that of the hemispherical mirror, but the most important advantage is the presence of an "*effective view point*" located at the focus of the hyperbole . The presence of a single viewpont enables the reconstruction of distortion free images. As it is depicted in Figure 3.3, from the image of a hyperboloidal mirror it is possible to reconstruct a panoramic cylinder or a perspective images at the desired angles.
- (d) **paraboloidal mirrors** have the same resolution as hyperboloidal mirrors even if with smaller angle of view. They present a single viewpoint when used with a orthographic projection camera.

These typologies can be mixed to exploit the benefits of the different classes. For instance, Bonarini used a mirror composed by a sphere intersecting a reverse cone in order to avoid the excessive distortion introduced by the cone tip and have the good resolution of the hemispherical mirror in the centre of the image [9]. Another example is the mirror of Sorrenti, he proposed a multi-part mirror for the specific task of the Robocup competitions (www.robocup.org). In this mirror, each part is devoted to the observation of a different area of the play ground [52].

The two major drawbacks of the systems that acquire a single omnidirectional image in a snapshot are the low resolution and the typical distortion of the omnidirectional images. The low resolution combined with the geometrical distortion produces images hardly intelligible by a human. This can be a problem for applications like video–conferencing or tasks that require to display images to a human operator. If the application requires to display

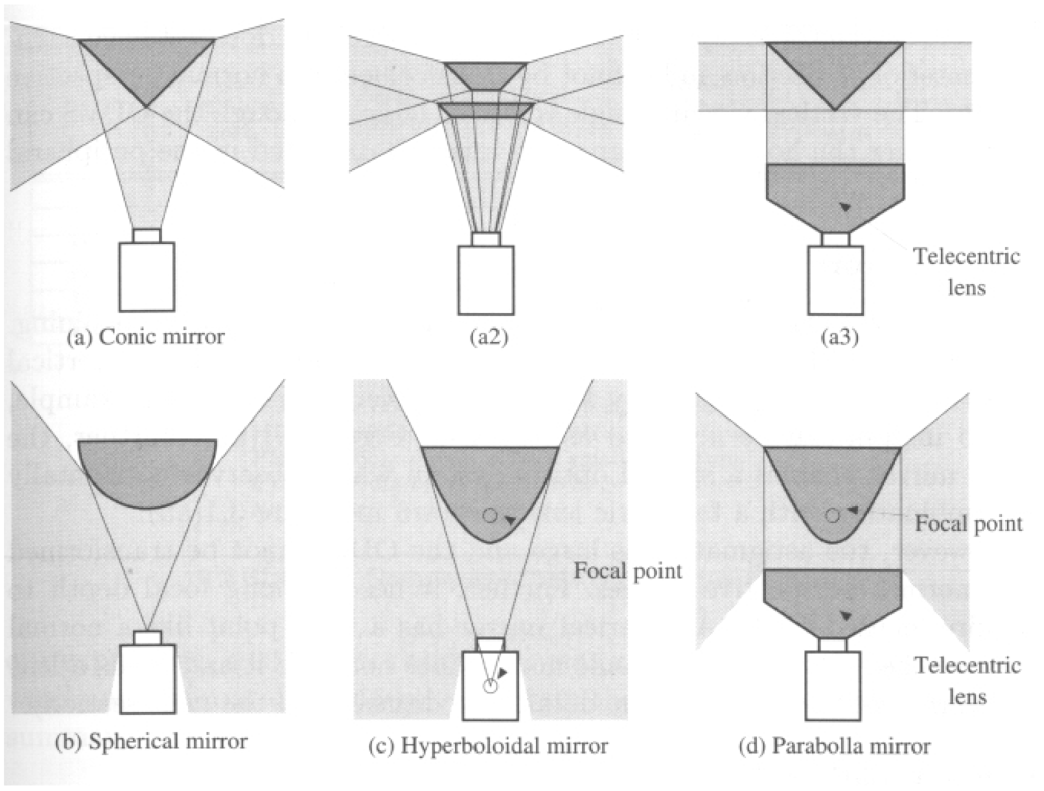

Figure 3.2: The different mirror profiles. (Courtesy of Prof. H. Ishiguro at Osaka University)

a final image to a human operator, it is possible to reconstruct perspective images from omnidirectional images [78]. This type of reconstruction is limited by the resolution of the sensor, but mainly by the geometry of the omnidirectional vision sensor. In fact, only sensors with a *unique effective viewpoint* enable an exact geometrical reconstruction of perspective images (for a detailed theory on omnidirectional catadioptric systems with a single–viewpoint, please refer to the work of Nayar [3]).

The *single viewpoint constraint* can be relaxed if we are not interested in an *exact* reconstruction of the perspective image (the work of Derrien and Konolige reports how is possible to approximate the single viewpoint condition even in catadioptric system without this geometrical property [26]).

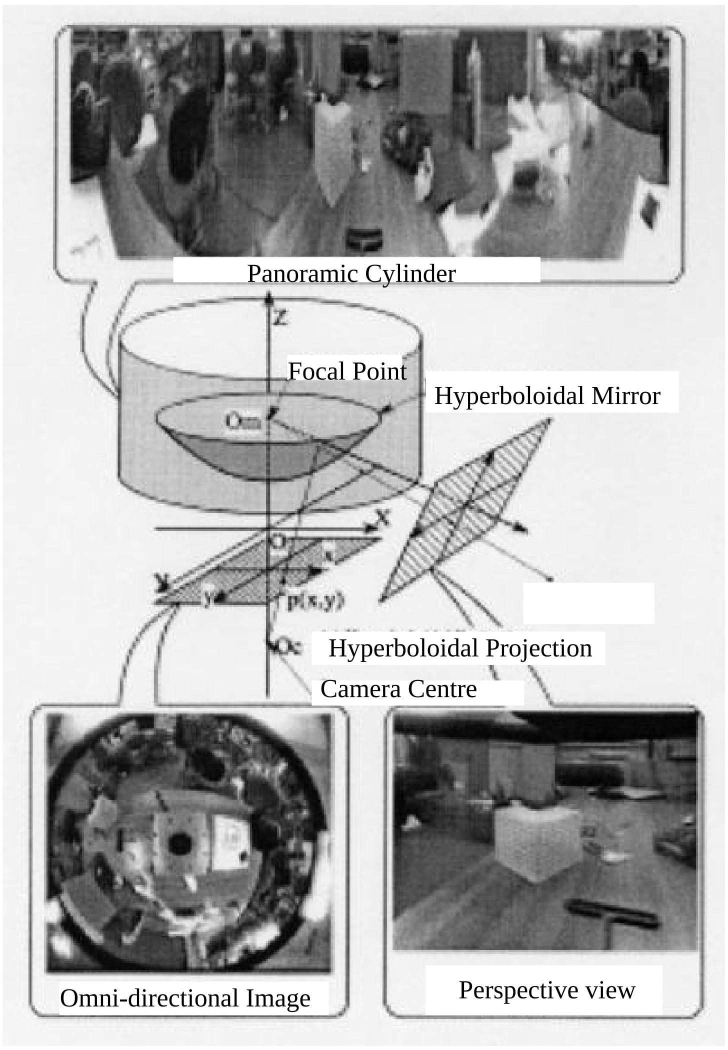

Figure 3.3: Hyperboloidal projection and examples of transformed images. (Courtesy of Prof. Y. Yagi at Osaka University)

On the other hand, the human readability is not always essential. In lots of applications the final step of the image processing is not the presentation of an image to a human operator, but is to extract features to be used in successive processes. A typical example is a vision system for navigating a mobile robot . Here the distortion is not a problem, because we can design the algorithm to take in account the geometrical distortion. Neither is the low resolution, because we are more interested in the positions of the objects rather than in the details on their surfaces. An extreme example of this is the work of Franz [27].

Abandoning the single viewpoint constraint permits a greater flexibility in the design of the omnidirectional vision sensor because we are no longer limited by geometrical constraints. In particular, it is possible to *consider the geometry of the mirror as a variable in the design of the vision system.* In the past, most of the catadioptric omnidirectional vision systems used convex mirrors with simple geometrical revolution surfaces: hemi-spheres, cones, hyperboles and parabolas. All these shapes have nice geometrical properties that have been diffusely studied [4] [37], but they strongly limit the flexibility of the sensor. Lately, researchers started to use more complex surfaces in order to realise custom mapping functions between the world points and the point on the imaging sensor. The mirror can be shaped in order to have a mapping function that simplifies the image processing [33] [28]. An example is the work of Lima that used an omnidirectional mirror designed to give a bird's eye view of the RoboCup field of play [53] [33]. This choice preserves the field geometry in the image, permitting a straightforward exploitation of the natural landmarks of the soccer field, goals and fields lines, for a reliable self-localisation. Another example is the work of Bonarini, that introduced the idea of multi-part mirrors to obtain different image resolutions in specific areas around the robot [10]. The work of Marchese and Sorrenti combines the two ideas proposing a mirror composed by three parts [52]. The works of these authors have been the starting points to develop our work also presented in [59] and in [58].

In this chapter, we present our approach to the design of a mirror with a custom profile and three examples of mirrors designed for different applications. Our approach showed to be successful also in the map building task (as documented in [70]) and not only in the RoboCup community (where our work [59] was selected as a candidate for the Best Paper Award of the

RoboCup Symposium of 2001 in Seattle – USA). Our design technique raised interest in other research groups, like the GMD Robocup Team of the **Fraunhofer Institut** of Bonn that committed us the design and production of the omnidirectional mirror for their goalkeeper, the CS Friburgh Robocup Team of the **University of Freiburg** that is testing one of our three parts mirrors and the **University of Catania** that wanted us to design a new omnidirectional sensor for one of their new robot.

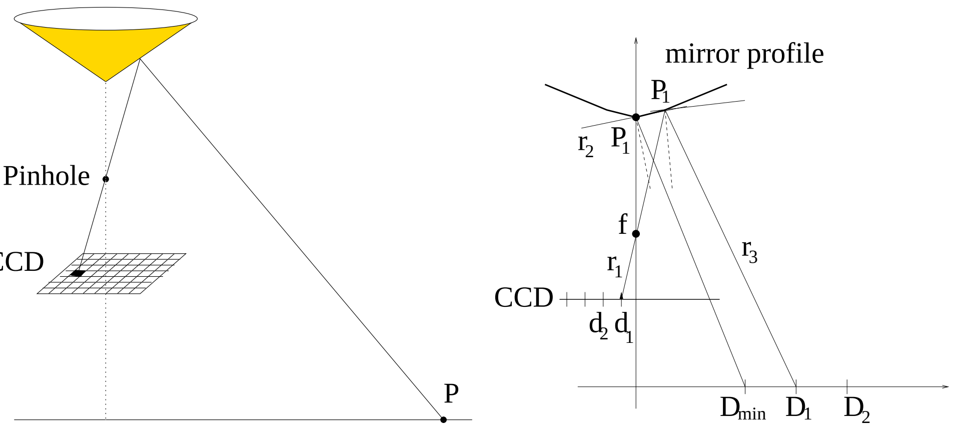

Figure 3.4: (Left) Image formation sketch (Right) The geometrical construction of the custom mirror

3.2 The design of the mirror

In this section we delineate an algorithm for the design of a custom mirror profile. The algorithm is a modification of the one presented in [52]. To understand the algorithm, we have to understand first the image formation mechanism.

In Fig. 3.4, we sketch the image formation mechanism in a catadioptric omnidirectional vision sensor. Consider the point P laying on the floor. Using the pin-hole camera model and the optical laws, for every point at distance

d_{OP} from the sensor, it is possible to calculate the coordinates (x, y) of the corresponding image point P' on the CCD.

Vice versa, knowing the coordinate (x, y) of a point in the image plane, we can calculate the distance d_{OP} of the corresponding point in the world[2]. Because of the finite size of the sensitive element of the CCD, we do not have access to the actual coordinates (x, y) of the image point, but to the discrete corresponding pair (x_d, y_d) (i.e. the location of the corresponding pixel of the CCD). So, if we calculate the distance d_{OP} from (x_d, y_d), this will be discrete. The discrete distance deviates from the actual distance with an error that depends on the geometry of the mirror. In the next section, we will see how the amount of error we decide to tolerate impinges on the profile of the mirror.

The main point in the design of a custom profile is the identification of the function that maps the desired points of the world into the desired points of the CCD. This is a function $f : R^3 \rightarrow R^2$ that transform world point (X',Y',Z') into image points (x,y).

Actually, what we want is a simpler function. We want a function that maps points laying on the plane Y=0 (the ground) around the sensor from a distance D_{MIN} up to a distance D_{MAX}. Therefore, exploiting the rotational symmetry of the system, the problem can be reduced to find a one-dimensional function f^* where d_{MAX} is the maximum distance on the CCD:

$$f^* : [D_{MIN}, D_{MAX}] \rightarrow [0, d_{MAX}] \tag{3.1}$$

The exact solution of this problem can be found with a quite complex differential equation. In [33] a solution to this equation is reported for the simple case $d = f^*(D) = KD$, i.e. the distance, from the centre of the CCD, of the image of a world point is proportional to the distance of the world point from the sensor's axis. In [52] is reported an approximated solution. In [59]

[2]For a detailed theory of catadioptric image formation, refer to the homonym paper of Nayar [3]

we presented this algorithm applied to the design of a mirror to be used in the RoboCup domain, but this technique can be applied to design mirrors for any application.

3.2.1 The algorithm

The solution we use is similar to the one presented in [52], consisting in a local linear approximation of the mirror's profile with its tangent. This solution is completely general and permits to choose a arbitrary set of world points and map them in an arbitrary set of CCD points. Let us see in the detail the algorithm:

1. transform the interval $[D_{MIN}, D_{MAX}]$ in a discrete set of points in the world $[D_0, D_1, D_2..., D_N]$ that will be mapped by f^* in the discrete set of points on the CCD $[0, d_1, d_2, ..., d_N]$ (remember these two sets can be arbitrarily chosen);

2. the tip of the mirror is in $P_0 = (0, Y_0)$ and the tangent to the mirror is $tan(arctan(D_{MIN}/y_0)/2)$. With this choice the point at distance $D = D_{MIN}$ is mapped into d=0. Let us call r_2 the line passing by P_0 whose derivative is $tan(arctan(D_{MIN}/y0)/2)$;

3. r_1 is the line passing by the pin hole (0, f) and the point $(-d_1, h)$ on the CCD, where h is the height of the CCD on the ground. The intersection between r_1 and r_2 determines the point P_1. The line r_3 will be created as the line passing by the point P_1 and the point $(D_1, 0)$. Now the line r_3 and r_1 constitute the path the light has to follows if we want to map the world point $(D_1, 0)$ into CCD point $(-d_1, h)$. Therefore the tangent to the profile of the mirror in the point P_1 must be perpendicular to the bisector formed by r_3 and r_1. And so on, until all the points in the set $[D_0, D_1, D_2..., D_N]$ are mapped in the set $[0, d_1, d_2..., d_N]$;

4. The mirror profile is obtained by the envelope of all the previously calculated tangents at the points P_i, i=0, 1, 2, ..., N;

Another variable in the design of the mirror is its radial dimension. If we want that the omnidirectional view will be maximised in the camera image, we have to choose the radial dimension of the mirror depending on the camera–mirror distance. Consider Fig. 3.7(left), α is the angular aperture of the camera. If the border of the mirror is tangent to the solid angle α, the omnidirectional image will be exactly circumscribed by the camera image frame. The closer we position the mirror to the camera, the smaller the radial dimensions of the mirror will be. If we want that the system can grab focused images, the minimum distance between the mirror and the camera (D_{min}) is limited by the *closest subject distance* of the camera[3] [37]. On the other hand, if we can tolerate a certain amount of defocus on the images, we can place the mirror closer and make it smaller and lighter.

3.2.2 The making of the mirror

In order to test the mirror profile obtained with this algorithm, before machining the actual mirror, we can test its performances in a simulated environment. The set of points describing the mirror profile can be used to create a virtual model of the mirror in a virtual world created with a ray-tracing program. In our work we chose the open-source program POV-Ray[4] . In Fig. 3.5(a) the virtual model of a mirror is depicted and in Fig. 3.5(b) is presented a simulated omnidirectional image obtained with the virtual mirror in a virtual reconstruction of the RoboCup field of play. Using the synthetic images generated with PovRay the final design of the mirror profile is assessed. If this is satisfactory, the set of points describing the mirror profile

[3]In fact, the virtual image of reflected objects forms behind the mirror surface, as detailed by Ishiguro in [37]. Also the focal depth (Δ_{min}) is important if we want to have the whole image in focus and not just a slide of the mirror's reflection.

[4]Information and downloads at www.povray.org

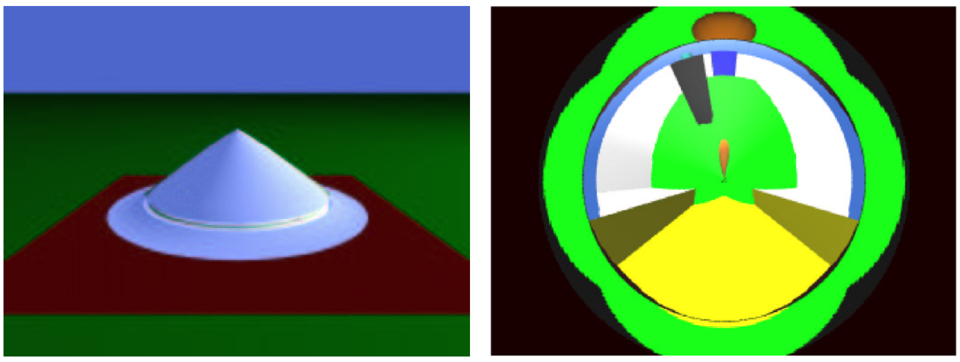

Figure 3.5: (Left) The virtual model of a custom profile mirror. (Right) A virtual omnidirectional image of the virtual reconstruction of the RoboCup field of play.

is passed to a numerically controlled lathe, that machines a cylinder of an aluminium alloy to obtain the final mirror. To decrease the weight of the final mirror it is possible to unload the mirror by scooping a concave hollow in the back side of the mirror. In Fig. 3.6(a) you can see the actual mirror produced and in Fig. 3.6(b) you can see an omnidirectional image captured in the RoboCup field of play.

3.3 The task commits the design

As we tried to stress in the previous sections, the mirror's profile should be designed according to the task performed by the robot. As an example, we will consider the design of mirrors for similar tasks and for very different tasks. In this paper, we report the differences in the design of the mirrors for two of our soccer player robots and for a robot whose task is to explore an unknown environment and to build a map of it using the Spatial Semantic Hierarchy [70] [46].

The task of the goalkeeper is to prevent the ball from rolling into its own goal, by stopping the ball with its own body and kicking the ball away with

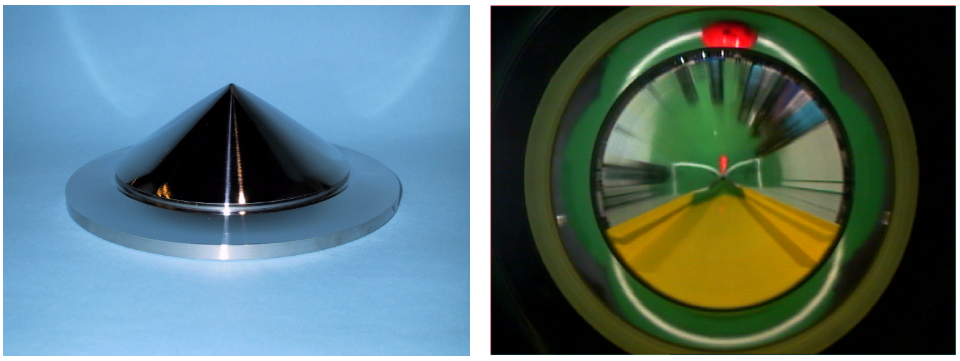
Figure 3.6: (Left) The actual mirror produced for the goalkeeper. (Right) An omnidirectional image acquired with the omnidirectional sensor of the goalkeeper.

its pneumatic kicker.

The task of the attacker is to kick the ball in the opponent goal and to catch the ball when this is still or to win the ball when this is carried by an opponent.

The task of the mapping robot is to locate the objects in the environment, to track the vertical edges of the objects and to follow the baseline of the objects.

The tasks of the two soccer robots are quite similar, but nevertheless we will see how a mirror tailored for each robot can improve the performances of the robots. On the other hand, we will see that the mirror designed for the mapping robot will have a totally different profile. Let us consider first the requirements for the soccer robots and then for the mapping robot.

3.3.1 Requirements for the soccer robots

Similarities: The described tasks implies that the vision systems of the two robot should have the following capabilities:

All these requirements corresponds to the following **requirements** on the vision sensor:

Num.	**Capabilities**
A	to spot the ball in the field of play, even when it is far away
B	to precisely locate the ball when it is near the robot's body
C	to identify the team's markers carried by the other robots

Table 3.1: The capabilities required to the vision system of the soccer robots

Num.	**Constraints**
A	to have a large field of view with a good resolution for looking at the field of play
B	to present a high resolution area around the robot
C	to have a very wide field of view that extends from the ground up to above the horizontal, the resolution is not important

Table 3.2: The constraints on the vision system of the soccer robots

These constraints require to have three different zones of the sensor with very different optical properties. So, we decided to design a multi-part mirror composed of three parts: a inner part and two circular rings, that we called respectively: the **measurement mirror** that observes the wider area of the field of play with a good resolution; the **proximity mirror** that observes the area around the robot's body with a high resolution; the **marker mirror** with a large field of view, but with very low resolution.

Differences: There are small differences in the tasks performed by the two robots. For instance,

So, we obtain two additional **requirements** for the vision sensor of the attacker:

Also the mechanical construction of the two robots influences the design of the tailored mirrors. The bodies of the two robots have different sizes and heights, so the regions of low, good and high resolution around the robots should have different dimensions.

Num.	**Requirements**
D	the goalkeeper should observe precisely **its own goal** in order to be able to shield it effectively and to locate it-self with respect to it. The attacker robot should be able to see **both goals** from any points of the field of play, in order to always know where are its own goal and the opponent goal
E	the attacker moves much more in the field of play and so it should be lighter than the goalie

Table 3.3: The constraints on the vision system of the soccer robots

Num.	**Constraints**
D	to have a wider vertical field of view (to view both goals from anywhere)
E	be more compact (in order to be lighter)

Table 3.4: The constraints on the vision system of the soccer robots

3.3.2 Requirements for the mapping robot

As will be diffusely explained in Chapter refchpt:omniMapping detailed in [70], in order to build a topological map of an unknown environment using the Spatial Semantic Hierarchy proposed by Kuipers, the robot should be able to spot the *distinct places* along its path and to navigate using the pre-defined *control laws* between two distinct places. As detailed in [71], the robot uses the vertical edges to detect meaningful topological situations and to pose new distinct places and uses the baseline of the objects to navigate between two distinct places. Therefore the vision system should be able to:

All these requirements corresponds to the following constraints on the vision sensor:

A) to have a vertical field of view spanning from the ground close to the robot to some degrees over the horizon (every vertical in the environ-

Num.	**Requirements**
A	to robustly detect the vertical edges present in the environment
B	to precisely locate the baseline of the objects close to the robot

Table 3.5: The requirements on the vision system of the mapping robot

Num.	**Constraints**
A	to have a vertical field of view spanning from the ground close to the robot to some degrees over the horizon (every vertical in the environment will be in the field of view)
B	to present a high resolution area around the robot

Table 3.6: The constraints on the vision system of the mapping robot

ment will be in the field of view);

B) to present a high resolution area around the robot;

These requirements are satisfied with a mirror composed by two parts with different profiles. The inner part of the mirror occupies most of the image and generates a highly distorted image in order to stretch the vertical edges (longer lines are recognised more robustly) and distorts non-vertical lines into curves that cannot be confused with radial lines. The outer part of the mirror presents high resolution and low distortion to easily detect, using a Hough transform, the position and directions of the base lines of the objects.

3.4 The final design

The relative radial dimensions of the different parts of the mirror depends both on the proportion of the image we want to dedicate to the rays reflected by each part and by the resolution we want in each area.

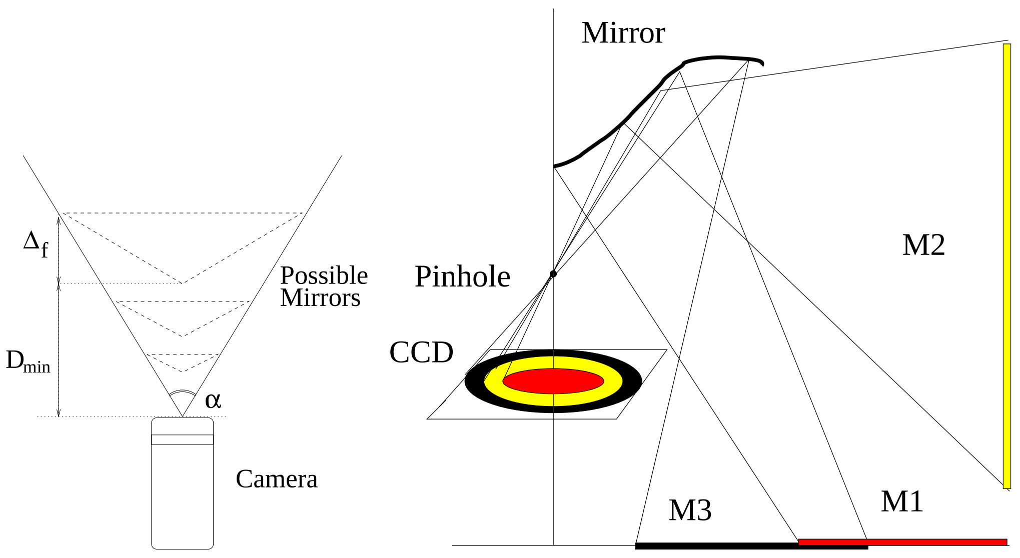

Figure 3.7: (Left) The radial dimension of the mirror if we want the omnidirectional view to occupy the widest portion of the image. (Right) A sketch of the multi-part mirror profile.

In the general structure of the three mirrors, we can identify two similar regions: the inner part and the outer part. We will discuss first the inner part and the outer part common to all mirrors and then the annular ring introduced only for the soccer robots. These three parts are called respectively: **measurement mirror**, **proximity mirror** and **marker mirror**. In Section 3.4.2, we will detail the differences between the mirrors explaining the differences in the geometrical dimensions of the mirrors and in the different curvatures of their parts.

3.4.1 The common structure

Let us consider first the inner part of the mirror, called the *measurement mirror*. This part has the wider field of view. For the tip of the *measurement mirror* we have two possibility: a mirror with a continuous curvature, like the Bonarini's and Sorrenti's mirrors, or a mirror with a discontinuity in the vertex, like conical mirrors. The latter has been our choice. In fact, in a multi-part mirror is possible to eliminate the disadvantages presented by a conic mirror, exploiting other sections of the mirror. The first disadvantage is the low resolution close to the sensor. This is overcome by the outer part of the mirror: the *proximity mirror*, that permits to have a very good resolution near the body of the robot. The second disadvantage (in the case of soccer robots), the limited field of view, is eliminated by the middle circular ring of the mirror, i.e the *marker mirror*, that permits a long range field of view. Therefore, considering the whole structure of the mirror we have no drawbacks to the advantages introduced by a mirror with a discontinuity in the vertex and thus this will be our choice.

The measurement mirror

We chose to design a mirror that maps world points on the CCD with a constant *relative error* α, i.e. a relative error that does not depend on the distance from the sensor. So, the position of an object close to the sensor will be determined with good precision while an object far away from the robot will have a sensible absolute error. This choice is sensible both for the soccer robots and for the mapping robot. The constant relative error is obtained dividing the space between the minimum and the maximum visible distance in a set of intervals of increasing size, each one mapped in one pixel.

The resulting profile is the first part of the mirror profile sketched in Fig. 3.7 and it maps the world points into the area I_1 of the CCD.

The proximity mirror

The *measurement mirror* produces low resolution images close to the sensor. To clearly see objects close to the body of the robot we designed the *proximity mirror*. The proximity mirror is the outer part of the multi-part mirror, so it has the most convenient position to observe objects close to the body of the robot. This part is designed with a low curvature and a quite large portion of the image is dedicated to the light it gathers. Thus, objects close to the robot have quite big apparent dimensions. To enhance this effect we made this latter part concave, so points closer to the robot are mapped in outer points of the image, Fig. 3.7 (right). Fig. 3.7 (right) presents a sketch showing how the different areas of the world are mapped on the image. Note that there is an overlapping region that is seen by both the measurement mirror and the proximity mirror. This is not a problem, on the contrary, it can be used to perform more precise measures.

As we said before, these two parts are enough for the mirror dedicated to the mapping task, while for the soccer robots we need an additional portion with very low resolution and very wide field of view called marker mirror.

The marker mirror

In the RoboCup competitions every robot has to wear a coloured marker that identifies the team the robot belongs to. The marker must be positioned at a maximum height of 60cm. Therefore, we need a part of the mirror pointing to objects over the field of play. This implies to see objects out of the game arena. The vision of object out of the field of play causes troubles to the vision systems of the robots that are designed for the highly structured RoboCup environment. In order to reduce the bad influence caused by seeing many unknown objects, we dedicated just a small portion of the image to the vision of the markers. The light reflected by the *marker mirror* will be mapped in a low resolution annular ring: area I_2 in Fig. 3.7 (right). In this area we do not care about precision of the measurements, we want only to be able to detect the markers and to associate them to the robots localised with the *measurement mirror*.

Robot	Low Resolution	Good Resolution	High Resolution
Goalkeeper	$2\,^\circ$	70 cm– 6m	40 – 80 cm
Attacker	$20\,^\circ$	60 cm– 7m	30 – 100 cm
Mapping	−−	100 cm – $10\,^\circ$	30 – 120 cm

Table 3.7: The areas at different resolution of the three omnidirectional vision sensors

3.4.2 The mirrors' parameters

In this section we will see how the separate design of the three mirrors fulfilled the different requirements of each mirror. Let us first discuss the parameters of the soccer robots. In order to fulfil requirement D the attacker's mirror has a vertical field of view of $110\,^\circ$, while the goalkeeper's mirror has a vertical field of view of $92\,^\circ$. In order to fulfil requirement D the radial dimension of the attacker's mirror is 4 cm, while the one of the goalie is 7 cm. The resulting weights are 75 gr. for the attacker's mirror and 150 gr. for the goalie's mirror. For the mapping robot, we chose a vertical field of view of $100\,^\circ$ and a radius of 5cm with a weight of 100 gr.

The extensions of the different resolution areas are reported in Table 3.7. Note that for the low resolution areas a angular value is given, because the field of view of this area extends over the horizon and so it is meaningless to speak of an area for it. The angular value represents the filed of view over the horizon. The mapping robot does not have the low resolution area, but its good resolution areas extends $10\,^\circ$ over the horizon, as reported in Table 3.7

The resulting profiles are shown in Fig.3.8 note the different scales in the three plots. For a comparison of the true dimensions of the three mirrors refer to Fig. 3.9

270

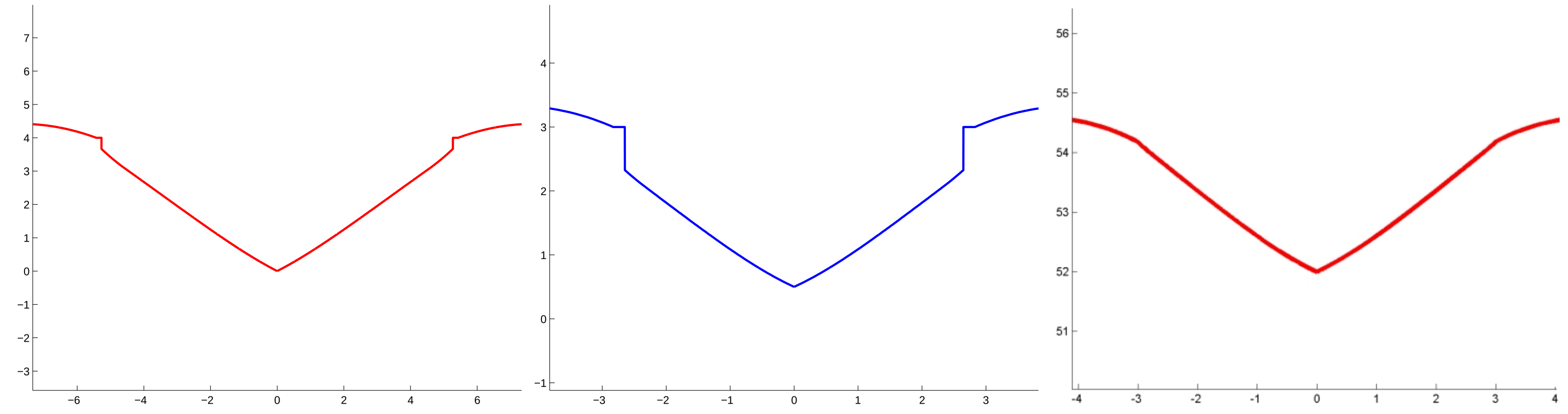

(1) (2) (3)

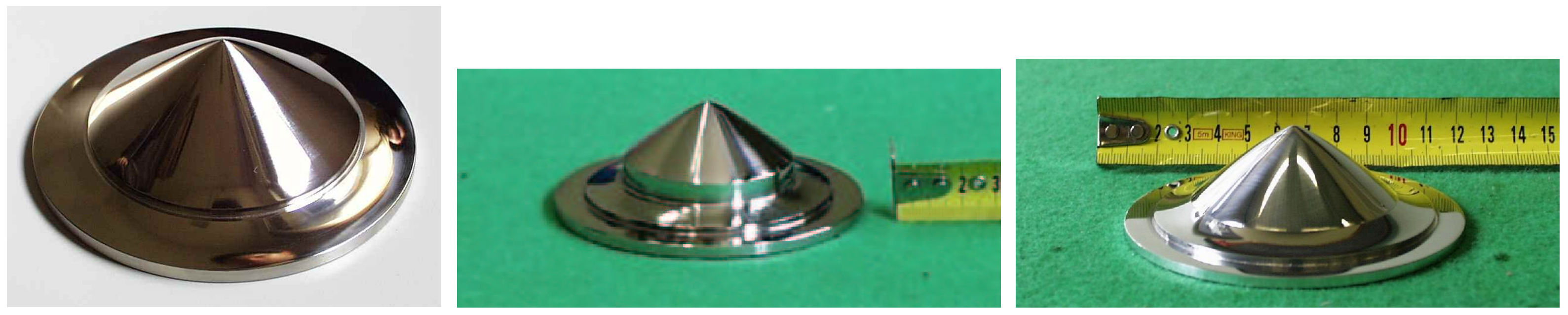

(1) (2) (3)

Figure 3.8: (Left) The profile of the mirror of the attacker robot. (Center) The profile of the mirror of the goalkeeper robot. (Right) the profile of the mirror of the mapping robot.

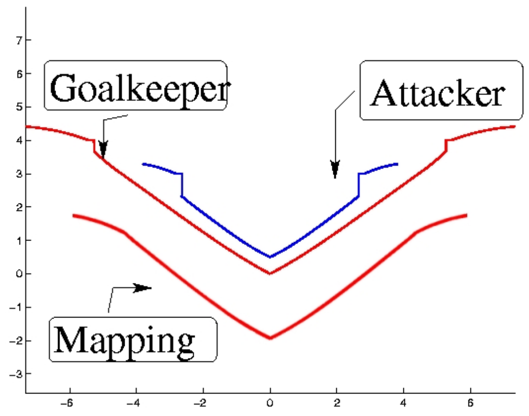

Figure 3.9: A comparation of the attacker's, the goalie's and the mapping's mirror profiles. Note that not only the sizes of the three mirrors, but also the slopes of the different segments are different.

3.5 Conclusions

In the first part of this chapter we detailed the design and production steps to realise a mirror with a custom profile for an omnidirectional sensor. We detailed all the phases of the process: the design, the simulations and the actual machining of the mirror. In the second part of the chapter we focused on showing how the task assigned to the robot commits the design of the omnidirectional mirror. We highlighted how different tasks produces different requirements for the vision sensor. We gave an example of this, detailing the design choices for three different mirrors. We showed the three mirrors produced for the mapping robot, the attacker robot and the goalkeeper robot, discussing the similarities and the differences.

This chapter is the result of several works presented in [59] [64] [62] [66] [70].

Chapter 4

Omnidirectional Vision for Robot Localisation

In the previous chapter, we understood in detail how the omnidirectional vision system works and how is possible to build a custom sensor. In this chapter, we will apply this sensor to the robot localisation problem. We will present two original results in the localisation problem: the hierarchical localisation and a solution to the perceptual aliasing. The hierarchical localisation is the possibility to have different accuracies in the robot localisation depending on the environment structure. The problem of the perceptual aliasing is the problem to be able to discriminate between two different location that have the same appearance. The two solution have been proposed within the image-based localisation approach. This work sprouted from a collaboration with prof. H. Ishiguro of the University of Osaka (Japan), so the approach we used in the image-based localisation is the one proposed by Ishiguro in [39].

4.1 Robot Localisation

A mobile robot, that moves from place to place in a large scale environment, needs to know its position in the environment to successfully plan its path and its movements. The general approach to this problem is to provide the robot with a detailed description of the environment (usually a geometrical map) and use some kind of sensors mounted on the robot to locate it in its world representation. Unfortunately, the sensors used by the robots are noisy and they are easily mislead by the complexity of the environment. Nevertheless, several works successfully addressed this solution using high precision sensors like laser range scanners combined with very robust uncertainty management systems [84] [16]. Another solution, very popular in real-life robot applications, is the engineering of the environment. Artificial landmarks, as stripes or reflecting dots, are added to the environment. The robot can use these objects, easy to spot and to locate, to calculate its position. An example of successful application is the work of Hu [35].

Unfortunately, this two approaches are not always feasible. First of all because there are situations in which an exact map of the environment either is not available, like old buildings or unexplored environment, or is not useful, like in dynamics environments in which the configuration of the objects in the space frequently changes. So, the robot needs to built its own representations of the world. This internal representation of the world can be something different from a metrical map, for instance a topological map. Topological maps are representations of the environment that capture the topology of the environment and that have been successfully used for tasks like robot navigation or map building [22] [50] [81].

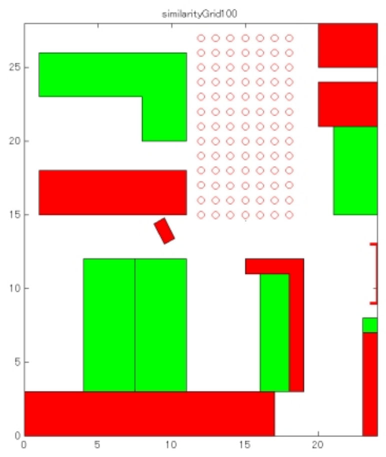

Figure 4.1: Image based localisation. The map of a test environment. The red circles represent the reference locations.

4.2 Image-based Localisation

If we shift our attention from robots to humans, it is proved that, in addition to the capability of reasoning about the environment topology and geometry, humans show the capability of recalling memorised scenes that help themselves to navigate. This implies that humans have a sort of *visual memory* that can help them to locate themselves in a large environment. There are experimental evidences that also very simple animals like bees and ants use the visual memory to move in very large environments [23].

In order to mimic this approach the robotics researchers proposed a new approach to the robot navigation, i.e. the **image-based navigation** [1] [41] [29] [45] [39]. In the image based navigation approach, the robotic agent is provided with a set of *views* of the environment taken at several locations in the environment. These locations are called **reference locations** because the robot will refer to them to locate itself in the environment. The corresponding images are called **reference images**. In Fig. 4.1 is sketched the map of the test environment we will use in the reminder of the chapter. The red circles represent the reference locations, i.e. the locations where the reference images were grabbed . When the robot moves in the environment, it can compare the current view with the reference images stored in the visual memory. When the robot finds which one of the reference images is more similar to the current view, it can infer its position in the environment. In fact, it is closer to the corresponding reference location more than to any other reference location. This give a topological localisation of the robot. If the reference positions are organised in a metrical map, an approximate geometrical localisation can be derived.

With this technique, the problem of finding the position of the robot in the environment is reduced to the problem of finding the best match for the current image among the reference images. The problem now is how to store and to compare the reference images, that for a wide environment can be a large number. As we will see in Section 4.2.1, different methods have been proposed.

As we said, this work started from a collaboration with prof. H. Ishiguro. Therefore, we adopted the image-based approach proposed by Ishiguro in [39]. This method is different from the ones of the other authors because it uses peculiar properties of the omnidirectional images. Let us see how this method works. The robot is equipped with an omnidirectional camera and takes a set of omnidirectional images at the reference location, then it compares the current omnidirectional image with the reference images. In order to store and match efficiently a large number of images, we transform each omnidirectional view into a compact representation by expanding it into Fourier series. The agent memorises each view by storing the Fourier coefficients of the low frequency components. This drastically reduces the amount of memory required to store a view at a reference location. With this approach also the matching of the current view against the visual memory is computationally inexpensive. Details on how to calculate the image signature from the original image are given in Section 4.2.1. In Section 4.2.2, we will describe the process of matching the current view against the visual memory. This process is based on the calculation of the degree of similarity between two omnidirectional images using the signature associated to them.

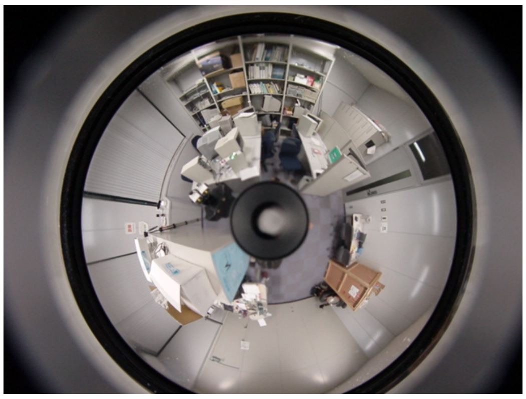

Figure 4.2: An omnidirectional image taken at a reference location.

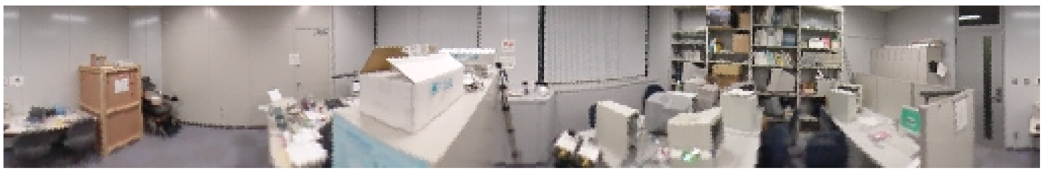

Figure 4.3: The panoramic cylinder created by the omnidirectional image of Fig. 4.2.

Through the rest of the chapter, we will show why this method should be preferred with respect to other methods proposed and we will illustrate several benefits this method carries with it. In particular, we will focus on the possibility of calculating a **hierarchical localisation** for the robot and how the similarity between the images can be used as weights of the samples in a Monte Carlo localisation process.

In Section 4.3, we will show experimental evidence of the hierarchical localisation in a complex real-world environment in which many objects are present and we will give some hints on how it will be possible to create a **hierarchical description** of the environment.

In this first section, we introduced the problem of image-based localisation and navigation, we outlined the solution adopted in this work, we highlighted the advantages of our method with respect of the approaches of other authors. In the next section, we will explain the technique we used to reduce the dimensionality of the input data and how the signature associated to each image is calculated.

4.2.1 Image signature

As we pointed out in the introduction, the first problem to tackle when building an image-based localisation system is to find a manageable way of storing and compare the reference image. The aim is to have a data set that fully describes the environment and permits to reliably associate the current view with the reference view taken at a nearby location, all this while keeping the dataset small enough to be easily stored and fast processed.

The first step, in order to lower the number of required reference image, is to use an omnidirectional camera [37]. An omnidirectional camera can store in a single image a 360° view of the environment from a certain location, see Fig. 4.2. Conversely, if the robot is fitted just with a standard perspective camera, the view of the environment from a certain location changes with the direction of gaze. In order to be able to recognise this point regardless of the instantaneous heading, the robot needs to take several pictures in the different directions. The amount of memory required to store and retrieve such a big number of images can rapidly grow to an unmanageable size. A solution can be to constraint the movements of the robot in order to have the camera pointing always at the same location [21], but this strongly limits the motion of the robot. Another solution can be to extract from the images some features that reduce the amount of required memory while retaining a unambiguous description of the image. A good example of this is reported in [87], where 936 images where store in less than 4MB. Nonetheless, to collect such a big number of images is tedious and time consuming. Moreover, high resolution images are not needed for tasks like navigation and localisation.

Let us come to the second step, the comparison of the current image with the reference images. The simplest approach might appear some sort of direct comparison of two images pixel by pixel, but this is not robust at all and will force us to store the whole image using a lot of memory storage.

Ishiguro proposed to use the Fourier transform of the omnidirectional image and to use a subset of its Fourier coefficients as signature for the image [39]. He did not apply the 2-D Fourier transform to the original omnidirectional image, Fig. 4.2, but he calculated the 1-D Fourier transform of every line of the corresponding panoramic cylinder. The **panoramic cylinder** is a new image obtained unwarping the original omnidirectional image, as depicted in Fig. 4.3 .

The use of the panoramic cylinder brings great simplifications in the solution of the matching problem. First of all, the panoramic cylinder is a periodic function along the x-axis and this simplify the calculation of the Fourier transform and second it is the natural representation for implementing a *rotational invariance*. As we said, the robot must be able to match the current view with the corresponding reference image regardless of the current heading. So, we need to introduce a sort of *rotational invariance* in the calculation of the *similarity* between two images. Using the Fourier coefficients as signature for the images, this come for free. Let us explain how this works.

If the robot grabs two omnidirectional images at the same location but with different headings, these two images are actually the same omnidirectional image rotated about its centre. The amount of rotation correspond exactly at the number of degrees the robot rotated. This means the two panoramic cylinders created by unwarping the omnidirectional image are actually the same image just shifted along the x-axis. Let see how this consideration affects the Fourier transform of the two images. If $f(x)$ is one row of the the first panoramic cylinder, $f(x-a)$ is the corresponding row of the shifted panoramic cylinder and we applying the **Shift Theorem**, we can write:

$$\mathcal{F}\{f(x-a)\} = e^{-j2\pi as}\mathcal{F}\{f(x)\} \tag{4.1}$$

where $\mathcal{F}\{f(x)\}$ is the Fourier transform of $f(x)$. In other words, the Fourier transform of a shifted signal is equal to the Fourier transform of the original signal, multiplied by the unit magnitude complex coefficient $e^{-j2\pi as}$. This properties states for every row of the panoramic cylinder. This means that the amplitude of the Fourier transform of the shifted image is not changed and there is only a phase change, proportional to the amount of shift a.

Coming back to our panoramic images, we can then associate the magnitude of the Fourier transform to the appearance of the environment from a particular place and the phase of the Fourier transform to the heading of the robot. In such a way, when the robot is turning on the spot and the apparency of the environment is not changing, the magnitude of the Fourier transform does not change. What is changing is the phase of the Fourier transform and the amount of change is proportional to the change in the heading.

Associating the apparency of the environment, and then the position of the robot, to the magnitude of the Fourier transform and the heading of the robot to the phase of the Fourier transform, we obtained both the desired *rotational invariance* and a way to calculate the difference between

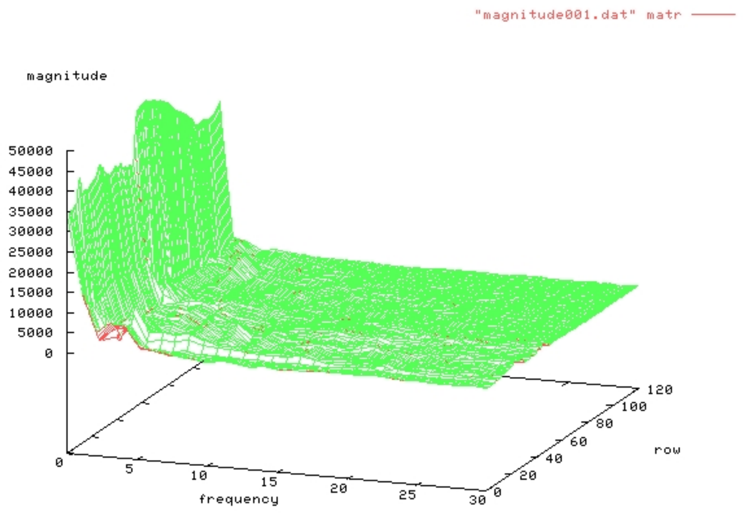

Figure 4.4: The power spectrum of the Fourier transform of the image in Fig. 4.3. Note that only the first 30 components are shown and components after the 15th have very small values and so can be neglected in the calculation of the similarity function.

the current heading and the heading associated to the reference image. On the rotational invariance using the Fourier transform, see also [77].

Other authors used different approaches for reducing the memory requirement of the omnidirectional images. The most used technique is to extract a set of eigenimages from the set of reference images and to project the images into eigenspaces. The drawback of such systems is that they need to preprocess the panorama images they created from the omnidirectional image in order to obtain the rotational invariance like in [1], in [41] and in [29] or to constrain the heading of the sensor like in [45].

The reduction on the memory requirement with our method is large, Table 4.1. Figure 4.2 shows a 640×480 pixels omnidirectional image at 24 bit per pixel. Figure 4.3 is shown the 512×80 pixels panorama cylinder at 24 bit

Image	Memory Required (in bit)	Memory Required
omnidirectional	$640 \times 480 \times 24$	7.3 Mbit
panoramic cylinder	$512 \times 80 \times 24$	980 Kbit
Fourier signature	$80 \times 15 \times 2 \times 8$	19 Kbit

Table 4.1: The different memory requirements illustrating the impressive memory saving introduced by the Fourier signature.

per pixel, created from the omnidirectional image. Figure 4.4 shows a plot of its magnitude coefficients of the Fourier series. As the figure shows, dominant powers exist in the frequencies before the 15th. As a result, we can represent the omnidirectional image just with the values of the first 15th Fourier components. In summary, the signature associated to each omnidirectional image is a three dimensional array composed of 80 rows (corresponding to the rows of the panoramic image), 15 columns (corresponding to the first 15 Fourier components) and two values for each element (corresponding to the module and the phase of the Fourier component).

In the next section, we will describe how these 15 values are used to assess the degree of similarity between the images.

4.2.2 Similarity computation

To compute the similarity between two omnidirectional images we define a **similarity function** that takes as arguments the two sets of m values representing the magnitude of the first m Fourier components associated with two omnidirectional images. First of all, we transform the two omnidirectional images in the two corresponding panoramic cylinders. Suppose each panorama image is composed by l row. We transform every row into Fourier series and we take only the first m frequency components, the first m components with non neglectable magnitude. We define the similarity $Sim(O_i, O_j)$ between two omnidirectional images O_i and O_j as

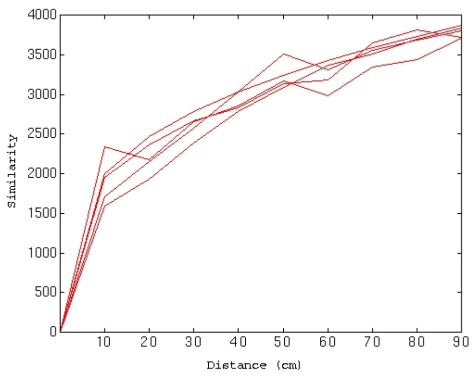

Figure 4.5: The plot of the similarity function values versus the distance between the reference image and the current image. The different lines in the plot represent different pairs of reference image - current image.

$$Sim(O_i, O_j) = \sum_{y=0}^{l-1} \sum_{k=0}^{m-1} |F_{iy}(k) - F_{jy}(k)| \tag{4.2}$$

where $F_{iy}(k)$ and $F_{jy}(k)$ are the Fourier coefficients of the k-th frequency of y-th row of O_i and O_j, respectively. In other words, as a measure of similarity between two omnidirectional images, we are using the L1 *norm* between the Fourier coefficient of the corresponding panoramic cylinders.

The plot in Fig. 4.5 depicts how the value of the similarity function changes depending on the distance between the current image and the reference image. The different lines in the plot represent five different pairs of *reference image-current image* taken in an cluttered office environment. The similarity linearly decreases with the distance within a short range and it is related, somehow, even for a long distance. In fact, as you can see from the plot in Fig. 4.5, the value of the similarity function steadily grows when the distance between the two images increases, but after a certain distance it will saturate. This happens because when the two images are taken at points far apart one from the other there is no correlation at all between the two

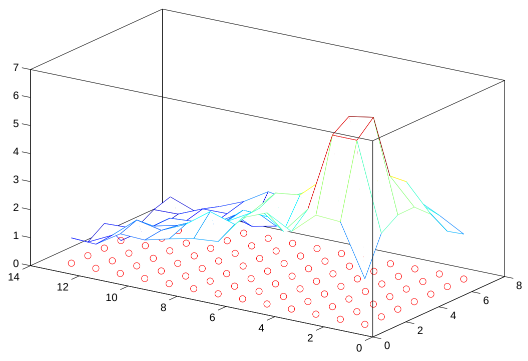

Figure 4.6: The values of the similarity functions calculated at every reference point for the current image. The empty circles on the xy plane represent the reference images. The full circle represents the actual position of the current image. The hight of the surface at every reference location is proportional to the degree of similarity of the reference image with the current image.

images[1] . The absolute value of the similarity function is unimportant, it depends on the environment layout, what is important is the relative values obtained for the current image against all the reference images. The reference image that matches best the current image is the one with the lowest value for the similarity function. So this give us a topological localisation for the robot. In other words we do not know where the robot is, but we know that it is closer to the location of the matched reference image than to any other reference location.

However, most of the time a precise geometrical localisation is not necessary for tasks like navigation. For the robot is enough to have a topological localisation and in most situations the robot can effectively navigate with a broad topological localisation. In fact, the localisation accuracy the robot needs to navigate depends on the environment and on the current action the robot is performing. If the robot is crossing a wide open space, it does not need to know where it is down to the centimetre, but if it has to enter a

[1]This is exploited in the practical implementation of the algorithm to speed up computation: when the partial sum of Eq. 4.2 exceeds a predetermined threshold the computation of the similarity function is stopped and a *no-matching* value is returned.

door the accuracy must be high. This is similar to the behaviour we experience walking in a street of an unknown town using a map. When we are following the high-street we do not need to know our exact position on the map, but when we have to take a detour or to enter a building we need to shrink down the uncertainty about our position, maybe looking for additional environmental clues. We called this process **hierarchical localisation**.

In this section we proposed a quantitative measure of the amount of similarity between two omnidirectional images. In the next section we will introduce the concept of the hierarchical memory-based localisation and how this can be easily calculated from the signature associated to the omnidirectional images.

4.3 Hierarchical Memory-based Localisation

As we hinted in the previous section, when navigating in large environments the robot needs to know its position with different accuracies depending if it is travelling in a clear area or if its manoeuvring in a cluttered area. This can be achieved with *hierarchical localisation*.

Also other authors spotted the need for different localisation accuracy depending on the kind of motion required to the robot. The work in [29] is an example of a vision-based navigation system that uses different localisation accuracies for different tasks. This system uses two different vision-based navigation strategy: a *topological* navigation and a *visual-path following* navigation. The system switches between these two alternatives depending on the situation. The drawback of this solution is that visual path following requires handmade design and an accurate control systems. We solved the requirement of a different localisation accuracy within the frame of topological image-based navigation using the same technique described in Section 4.2, actually simplifying this technique.

To explain how this work, we need to give some insight on the meaning of the Fourier coefficients we can calculate from the panoramic cylinders.

When we calculate the Fourier transform of a brightness signal, like one row of the panoramic cylinder, we are actually decomposing this signal in its component on a set of basis functions:

$$\{sin(2\pi\omega x), cos(2\pi\omega x), \omega \in \mathbb{R}\}$$

This basis functions are related to the spatial brightness variation. The first basis function, the one with zero frequency, is the constant brightness signal and the coefficient associated to it is giving the level of brightness. Basis functions with higher frequencies are related to brightness patterns with higher spatial frequencies. The relation between the Fourier components and the brightness pattern present in the image can be easily understood with the example of Fig. 4.7, kindly provided by Marco Foracchia. The test image presents a continuum of brightness patterns at different frequencies Fig. 4.7 (a). In Fig. 4.7 (b) is represented the Fourier transform of the test image. Now, we apply a pass-band filter to the Fourier transform and we keep only the middle frequencies, i.e. those components that are with in the filter, Fig. 4.7 (c). In the last stage, we calculate the Fourier antitrasformation of the filtered components and we will obtain Fig. 4.7 (d). As you can see, this is just the test image with the spatial frequency of the brightness signal filtered if out of the the pass band filter.

When we are calculating the similarity function for two images we are summing up all the contribution from the different frequency components, the low frequency values give the biggest contribution to the final value of the similarity function.

When looking for the similarity between two images we can see that the average brightness of the images changes very slowly when increasing the distance between the two images. While the distribution and the presence of

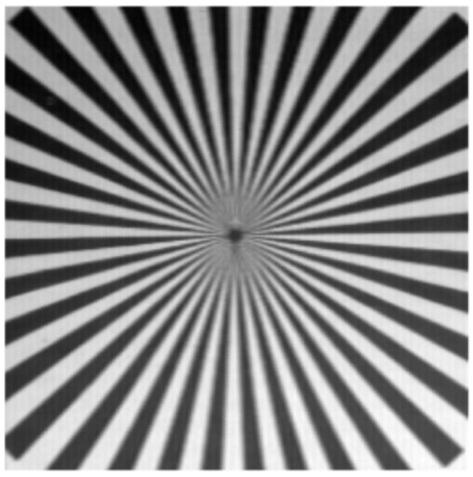
(a)

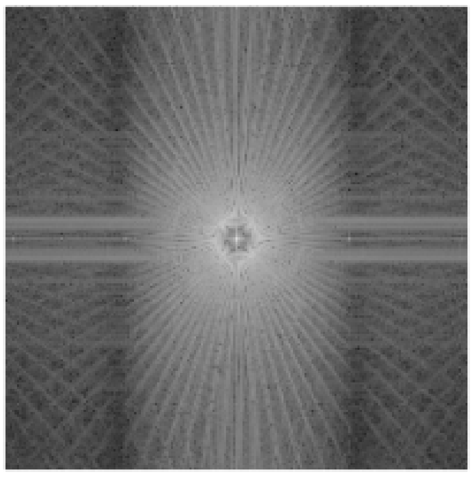
(b)

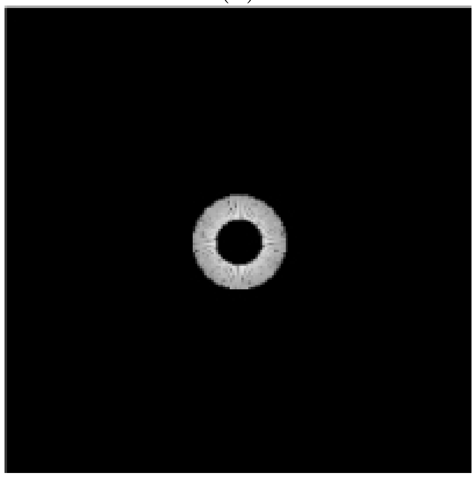
(c)

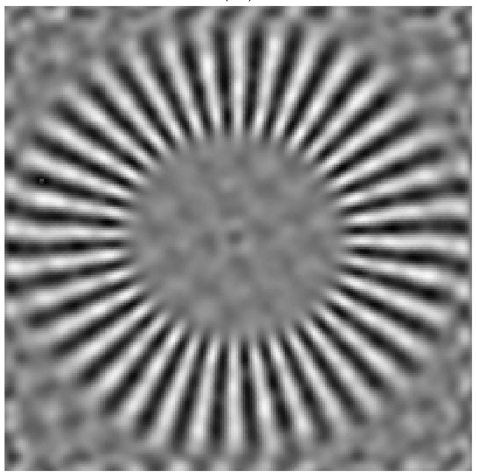
(d)

Figure 4.7: The relation between brightness pattern and spatial frequency. (a) The test image presenting a continuum of brightness patterns at different frequencies. (b) the Fourier transform of the test image. (c) A pass-band filter applied to the Fourier transform. (d) The Fourier antitrasformation of (c)

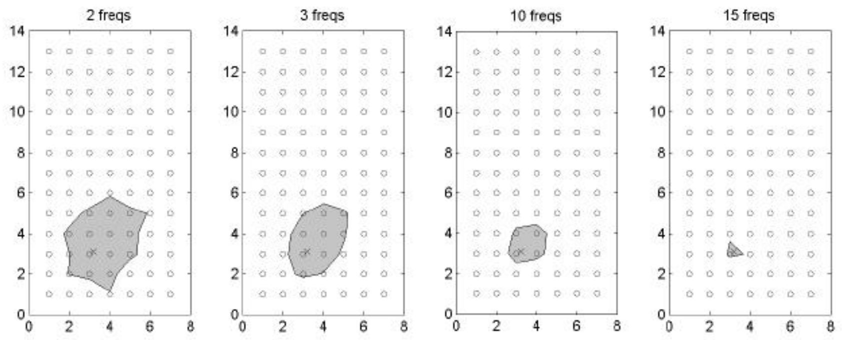

Figure 4.8: An example of hierarchical localisation. The number of Fourier components used to calculate the similarity function is increasing from the left to the right. The empty circles represent the reference images. The full circle represents the actual position of the current image and the gray area represent the calculated possible locations of the robot.

brightness patterns (that represent the objects in the environment) changes much faster. Therefore, we can expect that the low frequency components of the Fourier transform of the two images are similar in a larger interval of distances than the higher frequency components. This means that if in the calculation of the similarity function we stop the calculation of the sum in Eq. 4.2 to the first N Fourier components (with $N < 15$) our current image will match not only the closest reference image, but also a larger number of reference images distributed in the surroundings of the current position.

As a result, we can have an hierarchical localisation just by choosing the number of Fourier components to compare with the similarity function. In other words, within the technique used in this work, the hierarchical localisation comes for free from the calculation of the similarity function and actually save some computational power as well. In fact, if the robot needs only a broad localisation it does not need to calculate the inner sum in Eq. 4.2 for every value of k, it can just stop at the very first values. The result is to match the current view not only with the closest view but also with other reference views close to it. When a more precise localisation is needed, like in situation in which the robot has to manoeuvre in a cluttered environment, the sum can be extended to higher values of N in order to have a more strict matching against only one reference images. So Eq. 4.2 becomes Eq. 4.3

$$Sim(O_i, O_j) = \sum_{y=0}^{l-1} \sum_{k=0}^{N} |F_{iy}(k) - F_{jy}(k)| \qquad \text{where } N < 15 \tag{4.3}$$

In Fig. 4.8 is depicted a graphical representation of the hierarchical localisation achieved with our system. The empty circles represent the reference images. The full circle represents the actual position of the current image. The possible position of the robot, as calculated by the system, is represented by the gray area. From the left to the right the number of Fourier components used to calculate the similarity function is increasing, consequently the gray area showing the possible localisation of the robot is shrinking. In this test the reference image were taken on a 25 cm grid in a office environment cluttered with many pieces of furniture, as you can see from pictures in Fig. 4.2 and Fig. 4.3.

In Fig. 4.9, we present the hierarchical localisation obtained at different locations in the same environment. In the figure is sketched also a rough map of the test environment. In which the objects present in the environment are sketched as boxes of different colour. Lighter boxes represent lower objects

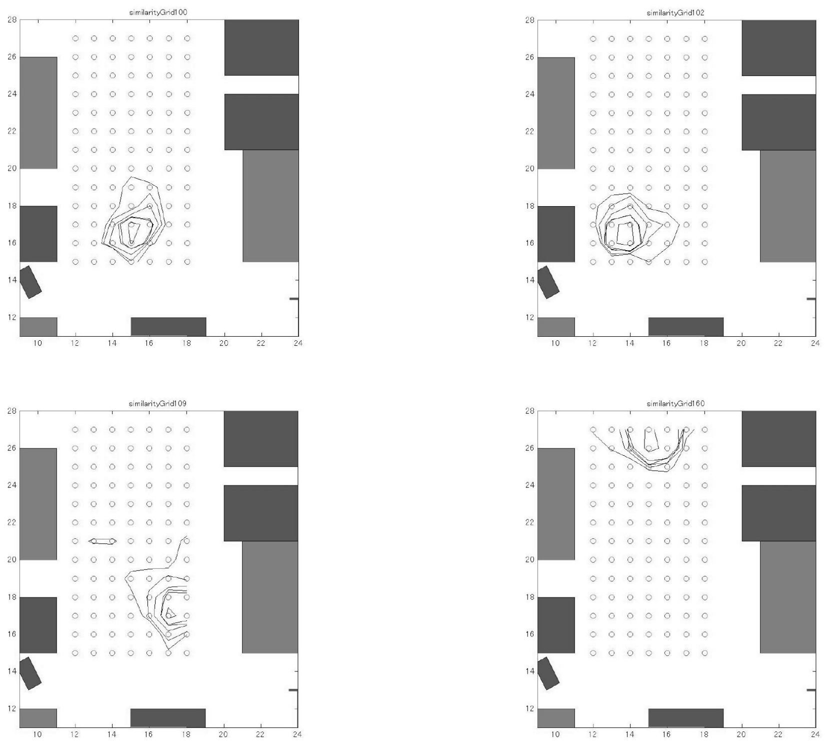

Figure 4.9: Several examples of hierarchical localisation at different places in the environment. The layout of the room in which experiments were performed is shown and the boxes represent the objects in the environment. Lighter boxes represent lower objects, darker boxes represent taller objects.

(like desks or chairs), darker boxes represent taller objects (like filers or shelves). At the moment of writing, we are investigating the relation between the shape of the localisation areas and the disposition of the objects in the environment.

In summary, our method provide a direct way of calculating the hierarchical localisation for the robot by comparing the frequency spectrum of the current image with the frequency spectrum of the set of reference images. Broad localisation is provided at minimal computational cost, just comparing very few frequency components. When higher accuracy in the localisation is needed, the system will use a little extra computational power.

4.4 Monte-Carlo Localisation

As we stated in the introduction, the image-based navigation is mislead in situation in which the appearance of the environment is the same in two different points. For this reason, we used a Markov particle filter to represent the belief about the robot position and how this belief can be updated everytime the robot grabs a new image.

The approach we used is inspired by the one proposed by Burgard in [87]. Every time the robot moves, it grabs a new image. The grabbed image is compared with the reference images in the memory of the robot and a similarity value is calculated for every reference image. These similarity values are used to assign a weight to the sample used in the Monte-Carlo localisation process.

There are two main differences with respect to Burgard's work. The first is that we used an omnidirectional vision sensor, so that at every position in the environment is associated one and only one image (with a drastic reduction of the number of required images). The second is that we do not associate any *visibility region* to the reference images in the memory database.

The pose of the robot l_t is estimated with Monte-Carlo localisation, a variant of the Markov localisation [2, 87, 19]. The Monte-Carlo localisation algorithm is composed of the following steps:

Algorithm 4.1 Monte-Carlo Localisation algorithm

```
1: ${s'_t} = \texttt{Predict}({s_{t-1}}, \texttt{odometry}(a_{t-1}))$
2: ${w'_t} = \texttt{Weight}({s_{t-1}}, \texttt{similarity-grid})$
3: ${s'_t, w''_t} = \texttt{Normalise}({s_{t-1}, w'_t})$
4: ${s_t} = \texttt{Re-sample}({s_{t-1}, w''_t})$
5: $l_t = \texttt{Estimate}({s_t})$
```

Let us discuss in detail the single steps.

1. the step `Predict` predicts the position of the new sample s'_t from the current sample s_{t-1} using the odometry information.

2. the step `Weight` assigns to each sample s'_t obtained in step 1 a weight. The weight is proportional to the degree of similarity of the current image with the reference images in the neighbours of the sample. Every weight is calculated as the weighted mean of the similarity values S_j associated to the closest reference images g_j (i.e. $g_i \in C$). The closer is a sample to a reference image and the higher is the contribution of the corresponding similarity value to the final value of the weight, as can be inferred from Eq. 4.4

$$w'^i_t = \sum_{g_i \in C} S_j(D - ||s'^i_t - g_j||) \tag{4.4}$$

where D is the distance threshold.

3. the step `Normalise` simply normalises the samples before the re-sampling;

4. the step `Re-sample` eliminates the sample with lower weights (i.e. the sample with a low similarity to the current image) in order to focus

the elaboration on the samples with higher similarity. The re-sampling algorithm is the one proposed in [19];

5. the step `Estimate` returns as estimation of the robot position the average position of all the samples present at the moment;

In Fig. 4.10 are presented two examples of Monte-Carlo localisation based on the similarity between the current image and the reference images. The estimated position of the robot is calculated as the average position of the samples and is marked with a black square. The **upper series** presents the *position tracking* problem. In the position tracking task the robot knows its initial position (left) and the belief distribution is update with the new observation at every step the robot takes (middle and right). The **lower series** presents *global localisation* problem. The initial position is unknown to the robot (the samples are uniformly distributed in the environment) (left) and the robot has to infer its position in the environment. During the motion of the robot the belief distribution is updated and converges to the actual position of the robot (middle and right).

4.5 Conclusions

In this chapter, we presented two steps we took toward a robust vision-based localisation system that can operate in every type of environment. We presented our approach to the problem of lowering the computational and memory requirements posed by the image-based localisation. This solution uses the Fourier transforms of the omnidirectional images grabbed by the robot. We discussed the advantages of this solution with respect to the solutions devised by other authors. We focused on the possibility offered by this representation to implement a **hierarchical localisation** of the robot. To overcome the limitation of the vision-based localisation systems, i.e. the

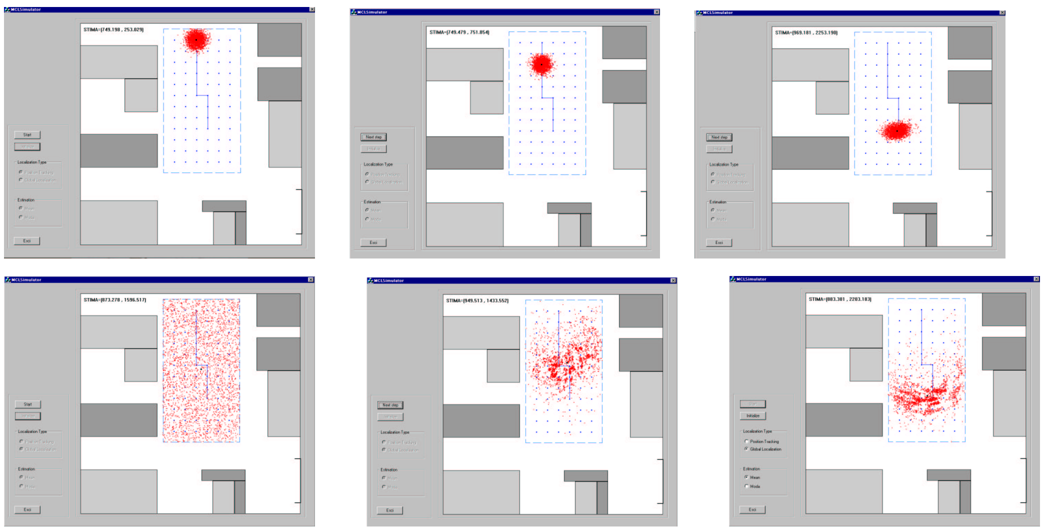

Figure 4.10: Two examples of Monte-Carlo localisation are presented. These are some snapshot of our system while tracking the robot position, in the upper sequence, and while performing a global localisation, in the lower sequence.

lack of robustness in case of perceptual aliasing, we introduced a **Monte-Carlo localisation technique**. We showed that this system is able to track the position of the robot while moving and it is able to estimate the position of the robot without any prior knowledge on the real position. This work has been described in [57] and [68]. At the moment of writing, we are testing robustness of our system to occlusion, kidnapping and odometric noise. The final step of this project will be to test this system in large outdoor environment and in indoor environment with high perceptual aliasing like a long corridor with several identical doors and junctions. The feeling is that because the current system does not make any assumption on the structure of the environment, it should work on outdoor images without any modification.

The natural extension of the **hierarchical localisation** is a **hierarchical description** of the environment in which the density of the reference images in the space is no longer constant but depends on the structure of the environment. In fact, consider an empty space where the reference images are very similar, we can represent this space just with a single reference image representative of all close reference image.

Chapter 5

Omnidirectional Vision for Mapping

In the previous chapter, we saw how the robot can calculate its position with respect to a set of reference images. The image-based localisation is feasible in environments with a limited extensions. In very large environments, we need a more compact representation of the *world*. In this chapter we will see how this compact representation could be a topological map of the environment. We will explain how a robot fitted with an omnidirectional vision sensor can extract the topology of the environment using the theory of the *Spatial Semantic Hierarchy* (SSH) proposed by Kuipers. This work demonstrated that an omnidirectional vision sensor has properties that enables to simplify the implementation of the SSH (Spatial Semantic Hierarchy).

5.1 Mobile Robot Navigation

Often, a mobile robot does not need a map to perform a simple displacement, especially if the environment is very simple or highly engineered. But, if the robot's task requires an *understanding of the world*, the robot has to answer the three questions posed by Levitt and Lawton [51]: "Where am I?", "How do I get to other places from here?", "Where are other places relative to me?".

In other words, it needs a map of its *world*. There is a wide range of different maps a robot can use. Different kinds of maps answer the three basic questions using different properties of the environment. We have to keep in mind that the distance which separates two objects is only one of the properties of the space in which the two objects are embedded. The choice of which property to exploit and therefore which kind of map to use depends on the task the robot will be required to perform.

Two examples that are poles apart are metric and qualitative maps. In metric maps the space is represented in a single global coordinate system. The relation between different places is a metrical relation composed of measure of distances and angles. In qualitative maps, the environment is represented as a set of *places* connected by *paths*. There is no metric or geometric information, such as distances, angles, etc. but only the notion of proximity and order [43].

What if there is no map? Can the robot be induced to build its own map? This idea opens another stream of research: the map building task. In this case, the robot has to travel through an unknown and unexplored environment and to construct a map of it. Again, depending on the task these maps can be very different [7] [27]. One of the most effective representations of an environment is the so called *topological map*. This is a qualitative map which extracts from the environment the topological relationships between the different places and paths. The advantages of such a representation are its compactness, because it represents only interesting places and not the whole space, and its intrinsic solution to the problem of movement uncertainty. This is because when a robot goes to places, its position is known with a certain error and this error accumulates while it moves. Because topological maps do not rely on a global coordinate system, the error in position is reset whenever the robot reaches one of the distinct places identified within the space. One of the key issues in the generation of topological maps is the abstraction of a discrete set of distinct places from the continuous sensorial experience. Topological maps can be upgraded to metric maps by adding metric information to the places and to the relationship between paths and places. Therefore, a map can be seen as a hierarchal structure built layer by layer. Benjamin Kuipers created a formalisation of this intuition: the Spatial Semantic Hierarchy (**SSH**).

The purpose of this chapter is to show the effectiveness of omnidirectional vision as sole sensor for a robot building a topological map of a man-made environment[1] , using the Spatial Semantic Hierarchy. So far, the SSH was only implemented on either simulated robots or real robots with very simple sensors, as sonars. No attempt to use a vision sensor has been made.

In Section 5.2, the basic concepts of the Spatial Semantic Hierarchy are introduced. In Section 5.4, we present the simulations run in a virtual environment to generate simulated omnidirectional image sequence. We performed a qualitative analysis of the simulated images. From this analysis, we identified transitions in the image sequence and features in the images themself, strictly related to the SSH representation. In Section 5.5.1 We present the algorithms designed to extract the desired information from the image sequences. Finally, in Section 5.6, we present the results of simulated experiments and in Section 5.7 we present the results of experiments performed with the real robot of Fig. 5.1, in a test environment. The robot depicted in the picture is the goal keeper of the Artisti Veneti Team[2] .

[1]like an office or a building

[2]Artisti Veneti Team is the team of The University of Padua at Robocup Championship, the robot football competition.

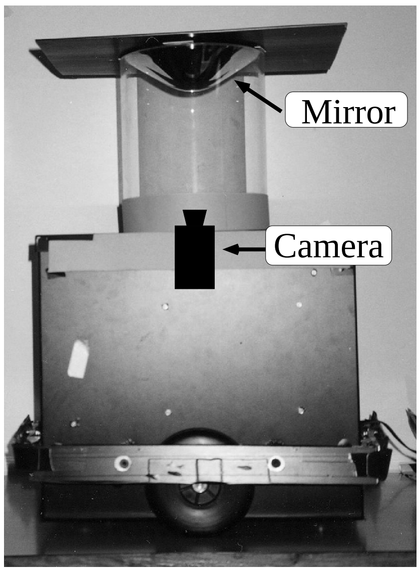

Figure 5.1: The robot with its omnidirectional vision sensor.

5.2 The Spatial Semantic Hierarchy

The SSH (Spatial Semantic Hierarchy) is a model of the way humans organise their knowledge of a large environment that extends beyond their sensorial horizon, i.e. an environment with section not directly perceptible. In other words, the SSH is a model of the knowledge of large-scale spaces of humans, intended to serve as a "method for robot exploration and map building" [46]. This model was proposed by Benjamin Kuipers [49] [47] [48] [79]. The SSH is made up of several layers: the sensory level, the control level, the causal level, the topological and the metrical level. Each layer can be implemented independently, even if they strongly interact. Let us see in details what each layer is about:

The Sensory Level

The sensory level is the interface with the agent's sensory system. It extracts the useful environmental clues from the continuous flux of information it receives from the robots' sensors.

The Control Level

The control level describes the world in terms of continuous actions called control laws. A control law is a function which relates the sensory input with the motor output. Each control law has conditions for its appropriateness and termination. A selected control law is retained until a transition of state is detected. These transitions can be detected with a function called a *distinctiveness measure*. The distinctiveness function must be identified depending on the sensor used and the features which are to be extracted from the environment.

The Causal Level

The causal level abstracts a discrete model of the environment from the continuous world. This discrete model is composed of *views*[3] , *actions*[4] and the causal relations between them. At this stage causal maps and planning are possible using these three basics elements. For this purpose, it is convenient to classify actions into two categories: *travels* and *turns*. "A **turn** is an action that leaves the agent at the same place. A **travel** takes the agent from one place to another" [79].

The Topological Level

The topological level represents the environments as places, paths and regions, with details of how they are connected or contained one in the other. To use Kuipers words:

> *The topological model of the environment is constructed by the non monotonic process of* ***abduction****, positing the minimal set*

[3]A view is defined as the sensor's reading at a place where a transition of state is detected.

[4]An action is defined as the application of a sequence of control laws.

of places and paths needed to explain the regularities observed among views and actions at the causal level.

The Metrical Level

The metrical level augments the topological representation of the environment by including metric properties such as distance, direction, shape, etc. At this stage, it is possible to build a global geometric map of the environment in a single frame of reference. This may be useful, but is seldom essential.

5.3 Omnidirectional vision and map building

omnidirectional vision produces images with a wide angle of view but with low resolution. This is not a problem, because most of the task which require an understanding of what is happening in the surroundings do not need high resolution images. It is better to gather the biggest amount of information from the highest number of directions than to have a detailed analysis of a small area.

In the case of a map building robot, the advantages of omnidirectional vision are clear. For this task a vision sensor with high acuity is useless, it is not necessary to capture the details of objects and surfaces, but only to estimate their positions and dimensions. An omnidirectional image captures at once all the objects visible from the robot location. This image has a strict connection with the *views* introduced in the causal level of the SSH, i.e. with the sensor reading at a distinct place. With an omnidirectional sensor, the robot does not need several shots to understand the surroundings. It does not need to turn and take a look around. It does not need to be fitted with moving parts (camera or mirrors) to increment its field of view. These are just implementational considerations, there are deeper aspects supporting the use of an omnidirectional sensor in the process of building a map with the SSH.

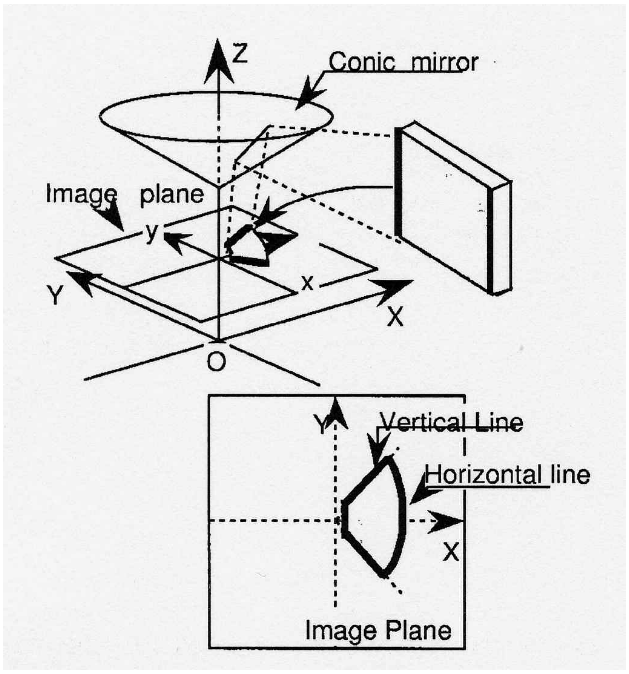

Figure 5.2: The conic projection. (Courtesy of Prof. Y. Yagi at Osaka University)

To understand these considerations we have to take a look at how a omnidirectional sensor maps the scene into the image plane. Consider Figure 5.2. In this figure a conical mirror is represented, but the properties which are illustrated apply to any kind of omnidirectional sensor.

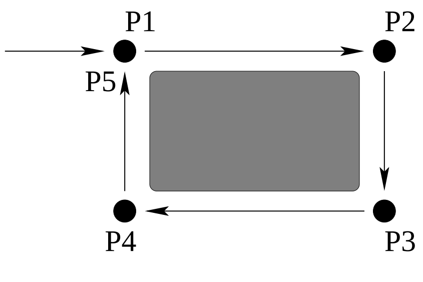

Figure 5.3: The "exploring around the block" problem. The problem of recognising the same place under different state labels.

The vertical edges in the scene are mapped in the image plane as radial lines originating from the point corresponding to the tip of the mirror. Therefore, to extract the vertical edges from the images, the image is searched for radial lines. The azimuth of a radial line in the image corresponds to the azimuth of the vertical edge in the scene, as viewed from the optical axis of the camera. The vertical lines in the environment provide an optimal clue to divide the environment into topologically different places and they can be used to generate a *distinctiveness measure* needed to distinguish transition of state in the robot ontology. Another advantage of the omnidirectional vision is its rotational invariance. If the robot rotates of a certain angle about the optical axis of the camera, the relative position of the objects in the image does not change. The image is only rotated and the objects appear to have experienced an azimuthal shift equal to the angle of rotation. This permits a straightforward solution to the problem of *exploring around the block*, i.e. of recognising the same place under different state labels. See Figure 5.3. Using the SSH terminology, it is easy to spot whether the current **view** is the same as has been experienced before and therefore to consider this view not as a different **place** but as the same place reached from a different direction.

Another problem which is easily solved by omnidirectional vision is to discriminate the type of movement the robot is performing at a given time. Using optical flow techniques, Svoboda showed that with an omnidirectional vision system it is very easy to discriminate between a small rotational movement and a small translational movement [82]. This task is very difficult for a vision system fitted with a perspective camera. Moreover, using active vision on an omnidirectional vision system it is possible to estimate precisely the motion of a robot. See again [82] for a literature review.

The main disadvantage of omnidirectional vision with respect to perspective vision is the already mentioned poor resolution. This is because with an omnidirectional sensor light is gathered from a much wider area than with a perspective camera. Therefore, if the sensitive surface of the CCDs is the same, more points have to be mapped into the same pixel. The shape and size of the mirror influences the resolution of the sensor. Within certain limits, it is possible to design mirrors that maximise the image resolution in the most interesting regions of the scene.

Other disadvantages of the omnidirectional images are the high distortion introduced into the image and the poor human readability. A mirror with a single focal point, like a hyperboloidal mirror, overcomes these difficulties. In fact the geometry of such a mirror permits transformation of portions of interest of the omnidirectional image into a perspective image. See Figure 3.3.

5.3.1 The assumptions

In the image analysis, we make use of some assumptions. It is worth to make them explicit here.

- The robot is moving in a indoor environment. This is a man-made environment like an office or a building;
- The lighting in the environment does not change during the motion of the robot;
- The objects present in the scene are static: they do not change their positions;
- The floor is almost flat and horizontal;
- The walls and the object present in the scene have vertical edges and surfaces;
- The axis of the camera and the mirror are vertical;
- The robot can only turn on the spot or move on a straight line. It cannot make more complex movements;

The last assumption is strong but permits to greatly simplify the image sequence interpretation. Several constraints on the edge movements are based on this last assumption.

5.4 The Simulations

As reported in the previous chapter, omnidirectional images are not easy to understand. They present a point of view (and a field of view) we are not used to. So we used a simulator to generate omnidirectional images of a virtual environment. The aim of this simulator was to gain an intuitive understanding of the dynamic of the sensor (i.e. how the image changes when the robot moves), and of the proprieties of omnidirectional images. The qualitative analysis of the images permitted us to extract clues about the distinctiveness measure and features we should use in the process of building the map of the environment.

To generate simulation of omnidirectional images we used a ray-tracing program called **POV-Ray**[5] .

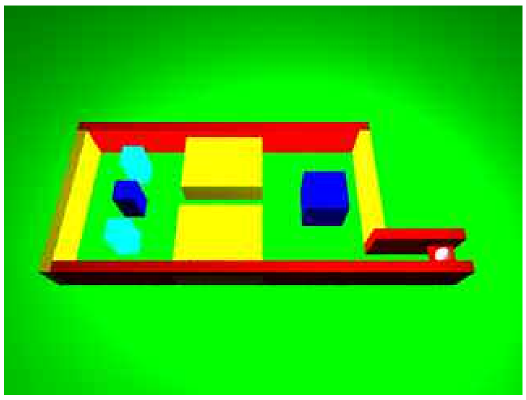

Figure 5.4: The virtual environment generated for the simulations of the vision system. The robot is the red square with the white sphere on top of it.

[5]POV-Ray is a free software for creating three-dimensional graphics. It is downloadable at the web site **www.povray.org**.

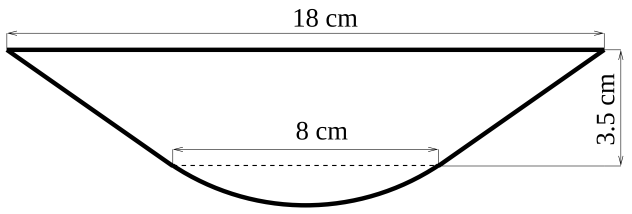

Figure 5.5: The Mirror Profile.

Using POV-Ray we created a virtual environment in which to carry out the simulations. A simulated robot moves in this environment taking snapshots with its omnidirectional viewer. The environment is designed to present to the robot typical views of an indoor space. The environment is a basic model of a man-made environment like an office. See Figure 5.4. Typical views are corners, doors, corridors and convex objects (like cabinets or boxes). The robot is represented as a red square with a white sphere on top of it. The robot moves through the maze along a predefined path. We generated a sequence of simulated images captured by the omnidirectional sensor while the robot moves in the maze.

To simulate the omnidirectional sensor we built a model of the omnidirectional sensor mounted on the real robot. The mirror of the real sensor is a multipart-mirror composed of a cone intersecting a sphere. It has a hybrid shape with respect the ones reviewed in Subsection 2.3.5. The dimension of the cone, the radius of the sphere and the position of the point of intersection are calculated such that the cone and the sphere are tangential at the intersection point. If they were not tangential, a discontinuity would be present in the image. Figure 5.5 depicts a sketch of the mirror profile with its dimensions.

We reproduced a model of this mirror in POV-Ray. The multi-part mirror is defined as the intersection of two primitives: a sphere and a cone. The surfaces of the two primitives are defined as totally reflective, so they behave like mirrors on which the image of the surrounding world reflects. This reflection is the image captured by a perspective camera placed under the mirror and pointing upward to the mirror.

In Figure 5.6.a we show a perspective view of the simulated environment and in Figure 5.6.b how the same scene is seen by the omnidirectional viewer. Note that the body of the robot does not appear in the simulated images. We simulated only the viewer not the whole body. In the next paragraph, we will explain which kind of feature we extracted from the omnidirectional images to understand the surrounding environment.

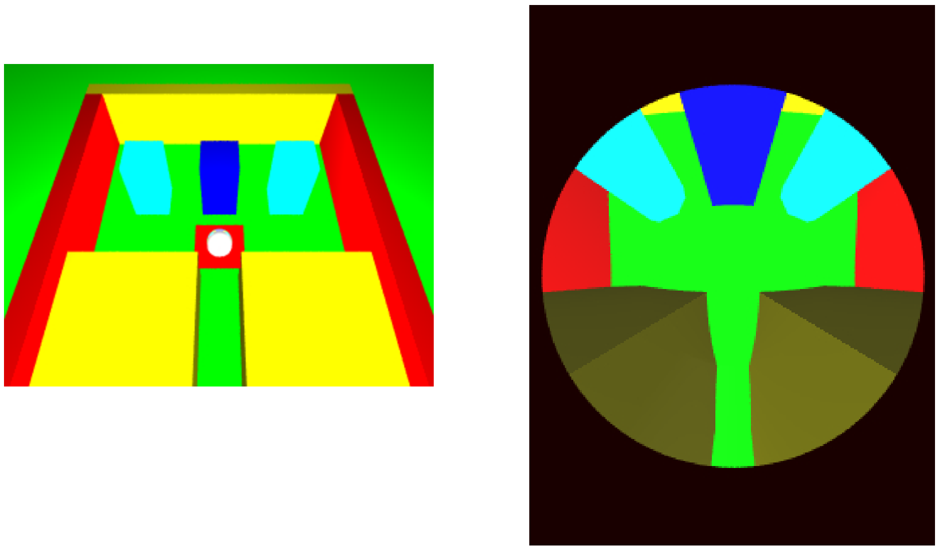

(a) (b)

Figure 5.6: (a) The perspective view of the virtual environment. The robot is the red square with the white sphere on top of it. (b) How the same scene is seen from the simulated omnidirectional viewer. Note that the body of the robot does not appear in the image.

5.4.1 The feature selection

To extract from the images the information about where are the objects in the environment and where the robot is going, we need to select a feature, or a set of features, to search for. These features must be present in the environment or in the pictures of the environment and must be reliably, and possibly easily, detectable. First, we have to decide if we want to search for features naturally present in the scene or if we want to exploit the use of artificial landmarks. The task for which this robot is designed: map building, presumes the existence of an unknown and unexplored environment. Therefore, we have to discard the use of artificial landmarks. Several author selected features that strictly speaking are not present in the environment but only in the pictures of the environment, like brightness pattern or other features only loosely related to the objects in the world. Usually, these features are extracted from the pictures with the use of heavy mathematical tools [44] [86] [27]. We decided not to follow this approach, but to select features that humans can easily understand and that are strictly binded to the objects in the real world. The features we selected are the vertical edges present in the world. The vertical edges are diffusely present in the environment the robot is designed for: an indoor man-made environment like an office or a building. Examples of vertical edges are doors, the sides of a cabinet, the legs of a chair, etc. As we said, vertical edges are mapped by the omnidirectional mirror as radial lines. Therefore, we search the images for radial lines. When the robot moves, the edges appear to move in the image. Analysing this movement it is possible to extract information both on the topology of the environment and on the robot's movements.

5.4.2 Qualitative Analysis

We decided to move the robot in the maze with two basic movements: translations and rotation on the spot. This was done to mimic the distinction made by the SSH between the two type of actions: travel and turns. If we force the robot to move only in straight lines and to turn on the spot to change the heading direction, it is possible to identify two separate sets of constraints on the apparent movements of the edges. The apparent motion of the edges depends on the movements of the robot and on the topology of the environment.

The topological events for translations

In Figure 5.7 is presented a simulation of the translation of the robot. For a better understanding of the scene two frame sequences are presented: the perspective view of the environment in which the robot is moving and the corresponding sequence acquired by the omnidirectional camera of the robot. The situation depicted in the sequence is a typical situation faced by the robot: it exits a corridor and it aims for an object. In this sequence several thing happen. Focus your attention on the following:

- The robot approaches some objects and it moves away from others;
- Objects in the heading directions appear to expand;
- Objects in the escaping directions appear to contract;
- The vertical edges of the scene appear as radial lines that move changing their azimuth;
- There is an optical flow of radial lines with respect to the heading direction;

It is possible to identify some topological events in the frame sequence. These events happen at a single point in the space, therefore they can be used to identify distinct points in the space. This is the key idea that permits us

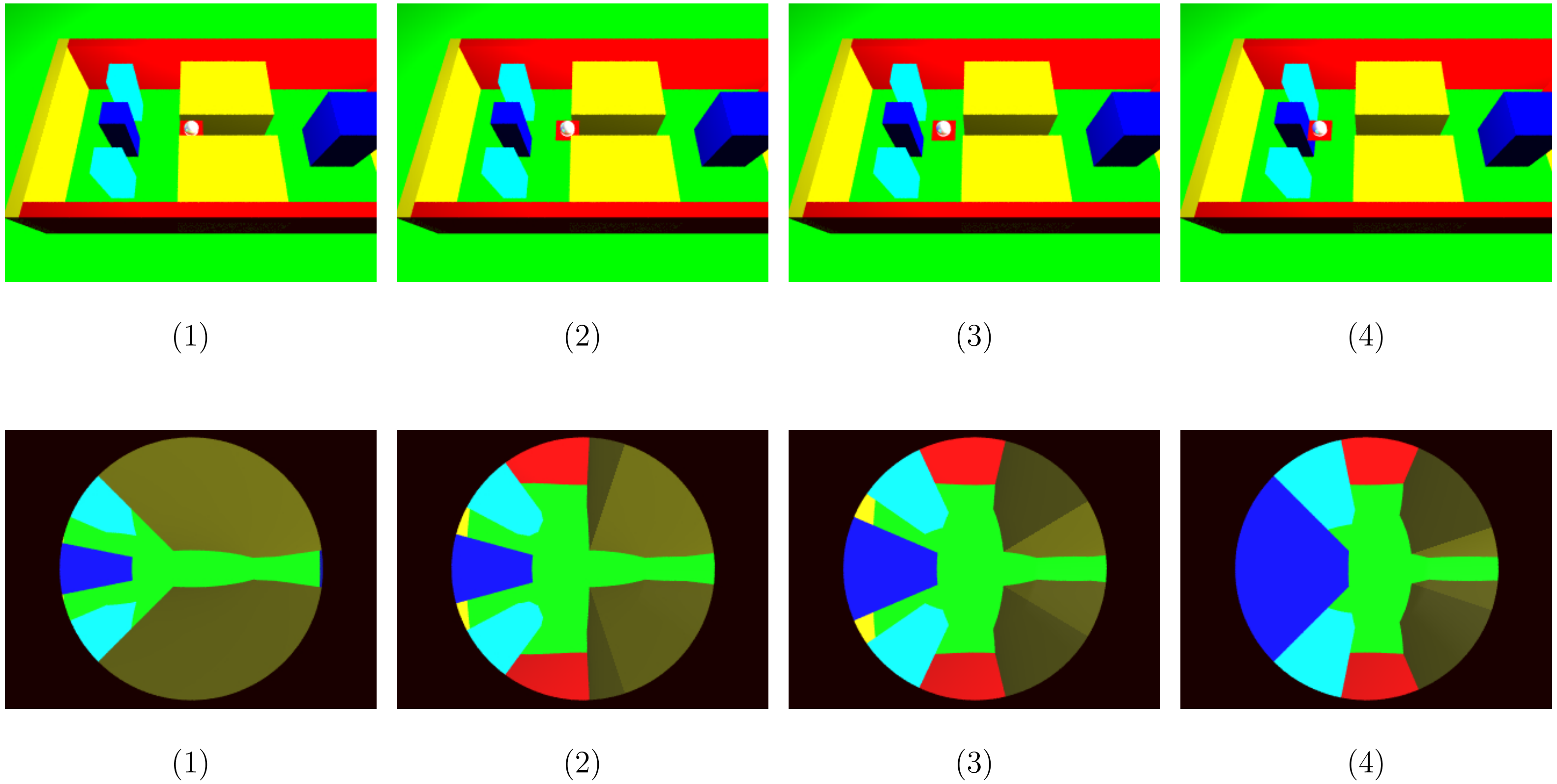

Figure 5.7: (Top) Perspective view of the robot moving along a corridor. The robot is the red square with the white sphere on top of it. (Bottom) The corresponding sequence acquired by the omnidirectional camera of the robot

to extract from the continuous world a set of distinct places as required by the Spatial Semantic Hierarchy.

- A new edge exits from occlusion, Figure 5.8;
- An edge disappear because occluded by another object, Figure 5.9;
- The two vertical edges are 180° apart in the vision sensor, Figure 5.10;
- The robots sees two pairs of vertical edges 180° apart, Figure 5.11. This identify a single point in the space. This point is the crossing point of the imaginary lines connecting opposites edges, as shown in the bird's eye view in Figure 5.12;

The movements of the edges in the frame sequence are subject to the following constraints. These constraints will be used by the algorithm that track the edges in the frame sequence.

- New edges exit from occlusion at a smaller[6] angle than the occluding edge;
- When an edge is occluded by another, the one that survives is the one with the smaller azimuth in the previous frame;
- The edges closer to the robot have a bigger azimuthal speed;
- Given a certain speed of the robot there is a maximum displacement an edge can experience from a frame to the next;
- The colours on the side of the edges change only slightly from a frame to the next one;

New edges exit from occlusion at a smaller angle than the occluding edge, referring to the absolute value of the angles. It is possible to look at it as if one edge splits in two when a new edge exits from occlusion, Figure 5.8.

[6]We define an angle as "smaller" than another, when it is closer to the robot's heading direction

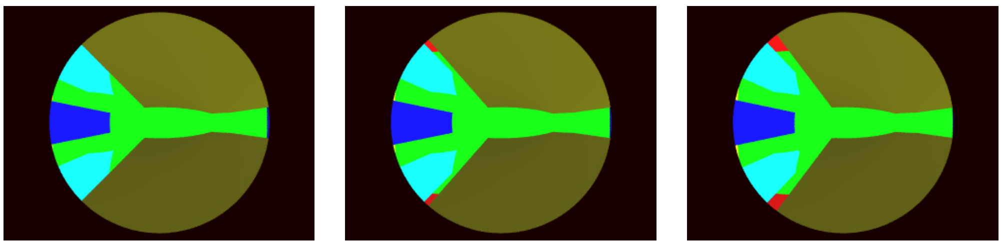

(1) (2) (3)

Figure 5.8: The simulation of an edge exiting from occlusion. Note that in the first frame a part of the two cyan boxes is occluded by the corridor walls. In the second frame all the edges of the cyan box are visible. In the third the cyan boxes are clearly visible.

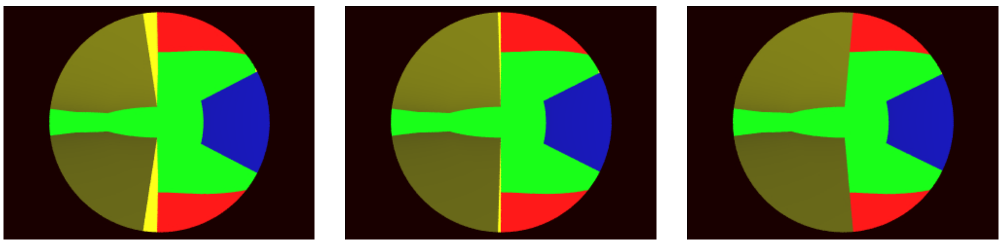

(1) (2) (3)

Figure 5.9: The simulation of an edge going to be occluded. In the first frame, the edge between the yellow corridor boxes and the red walls are clearly visible. In the second frame, they are just visible. In the third frame, they disappeared.

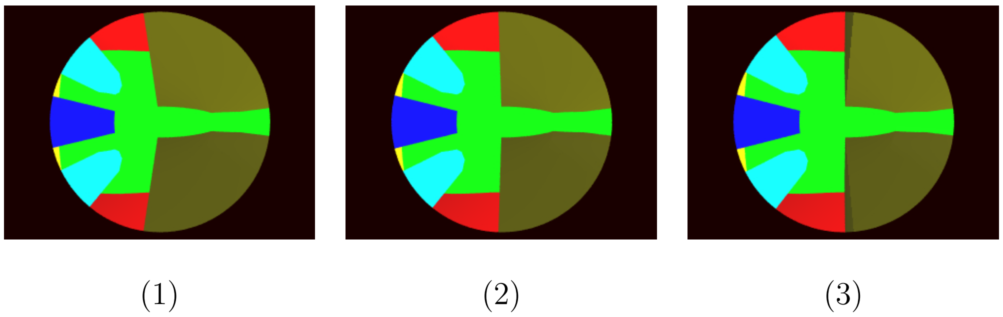

Figure 5.10: The simulation of the robot passing through a door. In the first frame, the edges of the yellow corridor boxes are not yet at 180° . In the second frame, they are at 180° . In the third, they are not longer at 180° .

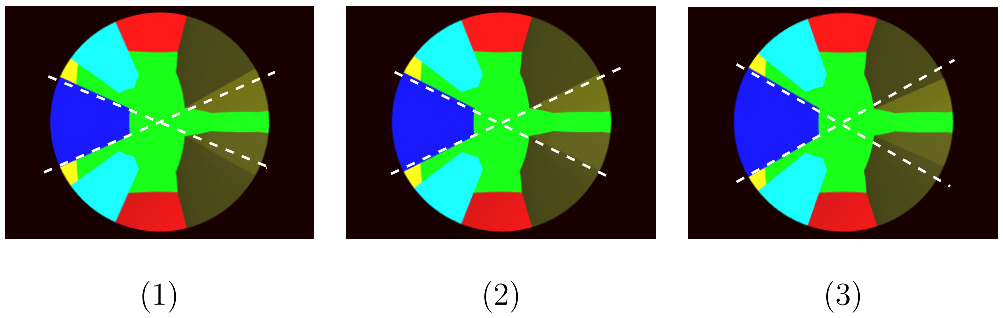

Figure 5.11: The simulation of the crossing point of the imaginary lines connecting opposites edges. In the first and third frame, the edges of the blue box and the corridor are not exactly 180° apart. In the second they are.

When an edge is occluded by another, the one that survives is the one with the smaller azimuth in the previous frame (always referring to the absolute value of the azimuth). It is possible to look at it as two edges merge when one edge disappear because occluded by the other, Figure 5.9.

The two vertical parts of a door frame are 180° apart in the vision sensor when the robot is passing through a door, Figure 5.10;

The robots sees two pairs of vertical edges 180° apart, Figure 5.11. This identify a single point in the space. This point is the crossing point of the imaginary lines connecting opposites edges, as shown in the bird's eye view in Figure 5.12.

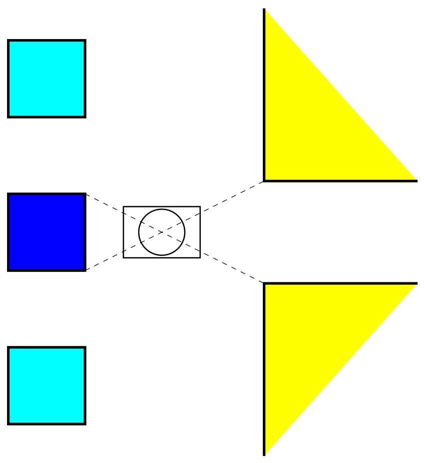

Figure 5.12: The bird's eye view of the crossing point of the imaginary lines connecting opposites edges.

The topological events for rotations

Refer to Figure 5.13, in this sequence the robot is turning on the spot in front of the blue box where it stopped in the sequence of Figure 5.7. As before we draw from these pictures the considerations and the constraints that apply to the movement of the vertical edges in the image. Focus your attention on the following events:

- The robot turns on the spot;
- The distance of the robot from the objects does not change;
- Objects do not change their shape;
- The vertical edges of the scene appear as radial lines that move only by changing their azimuth;
- The number of visible edges is constant: no edges appear or disappear;

The last consideration comes from the fact that there is no relative displacement between the robot and the objects. Therefore, the occlusions do not change. In other words, the image does not change, it appears only rotated around its centre.

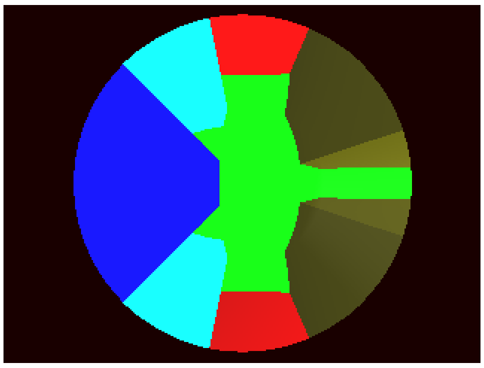

(1)

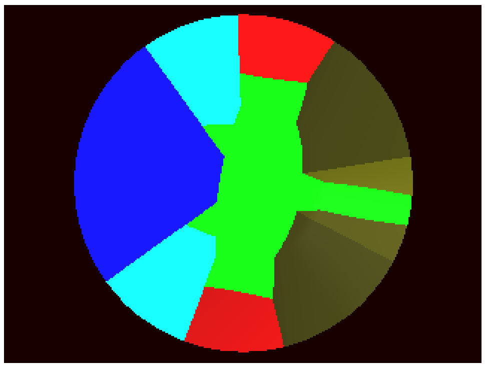

(2)

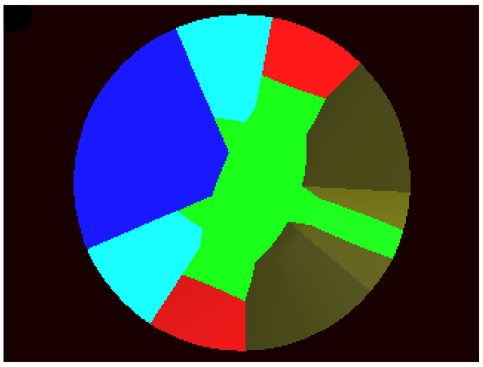

(3)

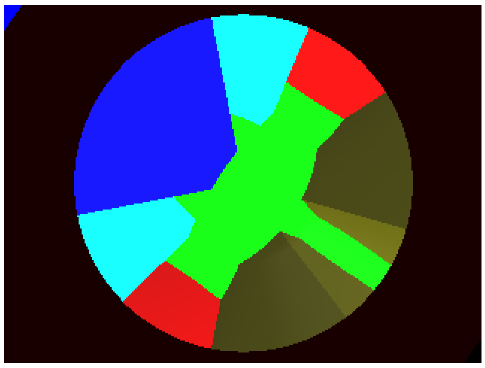

(4)

Figure 5.13: The simulation of a sequence acquired by the omnidirectional camera of the robot while it turns on the spot

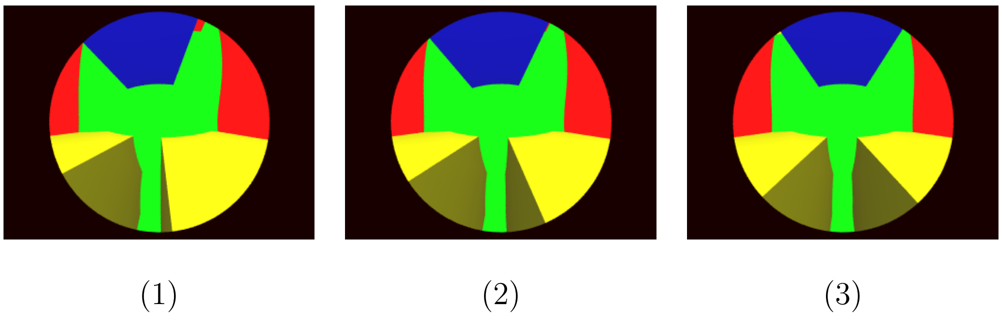

Figure 5.14: The simulation showing that not all radial lines are vertical edges. Notice how the baseline of the right yellow corridor box appears to be radial only in the first frame and in the others frame it is not.

The only topological consideration we can draw from the rotation sequence is that nothing changes and all the views the robot experiences are related to the same physical place. Therefore, in the implementation of the SSH all the *views* that differ only for a rotation around the centre of the image must be correlated to the same *place*.

We can extract the following constraints for the edges:

- All the edges experience the same azimuthal shift;
- The colours on the sides of the edges change only slightly from a frame to the next one;

All the vertical edges in the scene are mapped into radial lines in the image, but the converse is not always true. It is not true that all the radial lines in the image correspond to vertical edges in the scene. There could be some radial lines in the image that are actually radial to the vision sensor. For an example see Figure 5.14. There, the right baseline of the corridor happens to be radial in the first frame. In fact, if the robot is moving on a straight line, an accidentally radial line will appear as radial only for few frames, unless the line lies in the direction of the motion. If the robot is turning on the spot, the accidentally radial line will not disappear until the robot moves away from that spot. This suggests that it is not enough to match the edges in two consecutive frames, but that we need a check over a longer period of time: a memory, as to say. For instance, we could require a minimum life time before confirming a candidate radial line as a vertical edge.

5.5 The Vision System

The vision system has to perform two tasks necessary for the navigation of the robot: to detect and locate the objects in the surroundings of the robot and to give information about the movements of the robot it-self. Because the robot does not have direct access to information on its position or on its movements, the autonomous behaviours that will control the robot must come from the mix of these two sources of information.

The vision software is thought to work in real time while the robot moves from point to point. Its work can be ideally divided into two parts: to extract the selected features from the single frame and to use the information in the frames sequence to understand the environment. From a single frame the robot extracts the vertical edges and from the frame sequence it understands how the edges moves in the image. From the apparent motion of the edges we can draw conclusions about the topology of the surroundings. For instance, if an object occludes a second one, it must be closer to the robot than the second one. The robot takes a snapshot at a certain location, Figure 5.15. While it moves to the next location, it processes the image. First, it performs an edge detection to extract the edges from the picture, generating a black and white image, Figure 5.16. Second, the black and white image, containing only the detected edges, is processed with a Hough transform to identify the radial lines, see Figure 5.17 where the detected radial lines are marked with a black dot. Lastly, the most delicate task is performed: the edge matching. The robot has to recognise an edge from frame to frame. Therefore every edge has to be matched with its corresponding edge in the previous frame. The matching process exploit the colours in the image. The average of the colours in small areas around the detected edge is used as a signature of the edge. By comparing these signatures in consecutive frames we solve the correspondence problem. Figure 5.18 shows the output image of our program after the edge matching. The coloured dots are used to label the edges, every edge is associated to a unique colour. The black star-like dots beside each edge are the regions where we calculate the average of the colours to calculate the edge signature.

The approach used has been inspired by the paper of Yagi [89] Nevertheless, the novel matching algorithm is designed by the author.

5.5.1 The algorithm

In this paragraph, we present the algorithm that tracks the edges throughout the image sequence. This can be divided into three main parts: an edge detector, the Hough transform and the matching algorithm. The program we developed in this project is not real time as in the design specification. This is because in the project we focused more in the problem-understanding and in the accuracy of the results than in the optimisation of the software. For this reason in the design and choice of the software the speed was not an issue.

The edge detector

The edge detector used is the Canny edge detector [18]. This edge detector is computationally intensive, but it works well and compared with other edge detectors, like the Sobel's one, it produces thinner lines. The Canny edge detector does not produce a shift of the edge position with respect to their position in the original image. There is a problem: the Canny edge detector

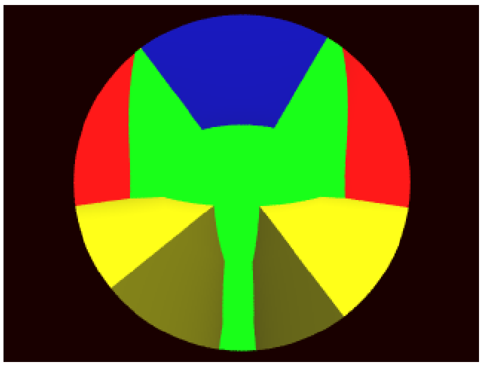
Figure 5.15: The unprocessed image as view from the robot's camera.

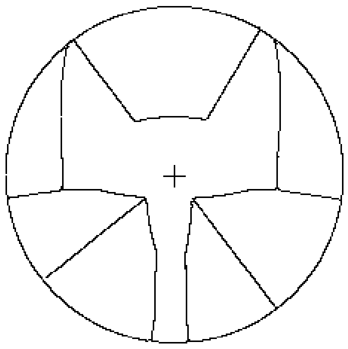
Figure 5.16: The image after the Canny edge detection.

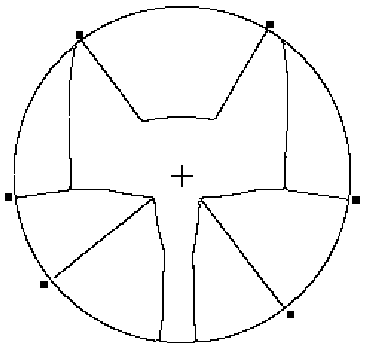
Figure 5.17: The edge image after the Hough transform.

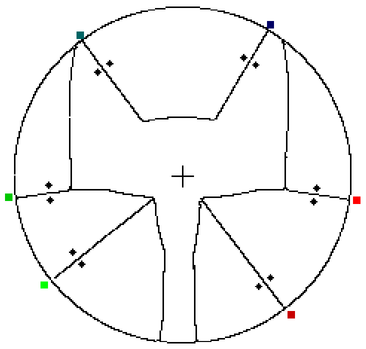
Figure 5.18: The final result showing the edge matching.

works with monochromatic images and we have RGB colour images[7] . To overcome this problem two approaches are possible. We can transform the colour image into a grey level one and use this as input for the Canny edge detector. Otherwise, we split the colour image in three images, one for each colour channel and we apply the Canny edge detector separately to each channel image. In the end, we combine the three resulting images by applying the logical OR operator. In other words, each pixel reported as an edge pixel at least in one of the three edge detections is an edge pixel of the final image. The two possibilities are displayed in Figure 5.19. The latter process is computationally intensive but it is very accurate. Simulations showed that working with the grey level image obtained from the colour image can result in a loss of information. As you can see in Figure 5.19 working with the grey scale image we lost the two vertical edges on the left of the image.

The Hough transform

Once we have extracted the edges in the image, we have to select only the edges corresponding to the vertical edges in the scene. Therefore, we need a process to identify the radial edge in the picture. The Hough transform is such a process [34]. For this task a new parametrisation of the image was found by the author which greatly simplifies the complexity of the transform. The new parameters are the angular coordinate and the radial coordinate of the pixels in a polar coordinate system with the origin in the centre of the image. In such a polar coordinate system, a radial line is described as a sequence of pixels with the same angular coordinate and varying radial coordinate. See Figure 5.20 a). To find out where the radial lines are in the image we apply the following algorithm: for each edge pixel we calculate its angular coordinate, we round it down to the unit of degree and we incre-

[7]An RGB colour image is a colour image where each pixel is represented as a triplet of values: one value for the amount of red in the pixel, one for the amount of green and one for the amount of blue

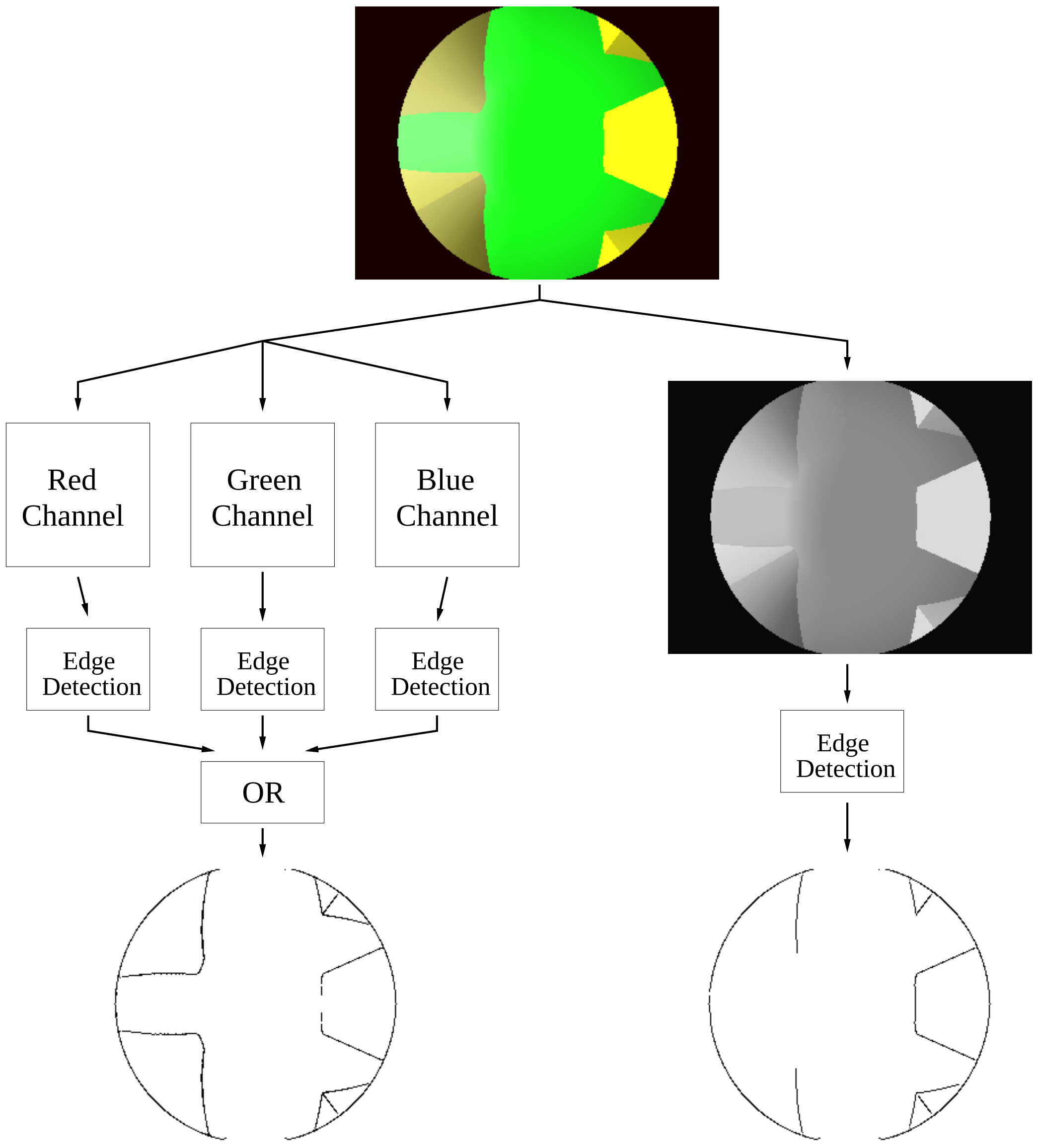

Figure 5.19: The two possible processes for a Canny colour edge detection.

ment a counter corresponding to this number. When all the edge pixels are processed, we look at the histogram of the counters values. The counters that show a value over a certain threshold correspond to the position of the radial edges in the image. See Figure 5.20 a). The threshold corresponds to the minimal length (in pixels) of the radial lines that we consider as vertical edges. The choice of the threshold to set for the minimal length of a vertical edge must be well assessed. A threshold set too low can detect as composing a radial line also pixels that have the same angular coordinate but not belong to the same line or lines that occur to be radial just for a small bit. On the other hand, a threshold set too high does not identify some vertical edges, especially when they just appeared in the field of view and they are like small segments in the periphery of the image.

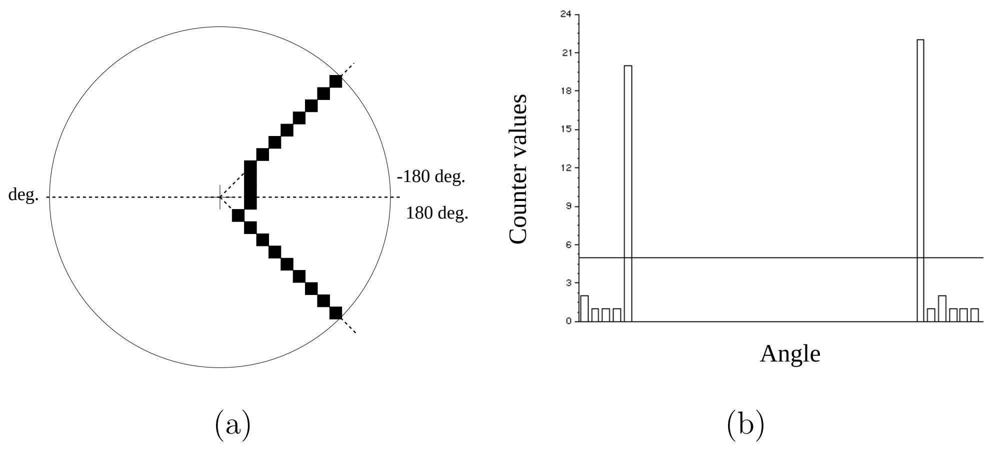

Figure 5.20: A the Hough transform.
(a) The black squares are enlarged pixel. Notice they all have the same angular coordinate. (b) The histogram for the Hough transform.

The matching algorithm

Once we have identified the vertical edges in the pictures, we have to track them along the frame sequence, i.e. we have to be able to recognise an edge in different frames. To identify an edge, we use the colours on the left and the right side of the detected edge. To extract colour information, robust to the noise of the picture, we calculate the colour as the average colour over a window positioned across the edge. In Figure 5.21 is presented a close up of a processed image showing the averaging windows. Each window is composed of two sub-windows. These are the star-like dots on the sides of each edge.

The colour of a pixel in the image is represented by a RGB triplet. The average colour calculated over the pixels of each sub-windows is represented by a RGB triplet, as well. Each component of the triplet is the average of the values of the corresponding colour channel over the pixels of the sub-windows. The windows are placed on a circumference that intersect all the significant edges, Figure 5.22. The windows are designed to follow the edge as it moves around in the circle. To understand how this is done, think of the two sub-windows connected by a rod. The rod is kept always tangential to the ideal circle shown in red in Figure 5.22. The length of the rod is enough to keep the sub-windows at a certain distance from the edge, this permits us to avoid eventual border effects caused by the edge, but short enough not to overlap with another edge detected nearby. The shape of the sub-windows has been chosen to be approximately circular for two reasons. First, because in this way the minimum distance between the edge and the sub-windows is approximately constant and second because while the sub-windows moves around with the edge, it spans always over the same pixels. The former assures us that the sub-windows never goes too close to the edge. The latter that we calculate the average colours around the edge always on the same pixels.

At this stage, the program is able to assign to each edge its colour signature. To track the edges along the whole frame, the program tries to match the edges in the current frame against the edges on the previous frame and so on for the whole length of the sequence. The matching is done with the colour signature, but this could be not enough to correctly identify an edge in the previous frame. In fact, there could be other edges in the image that have similar colours signatures. Using the two sets of constraints drawn in the previous subsection for the edge motion, it is possible to avoid mismatches by shrinking the area where to look for the corresponding edge. In the case of linear motion, the first constraint is that the absolute value of the azimuthal

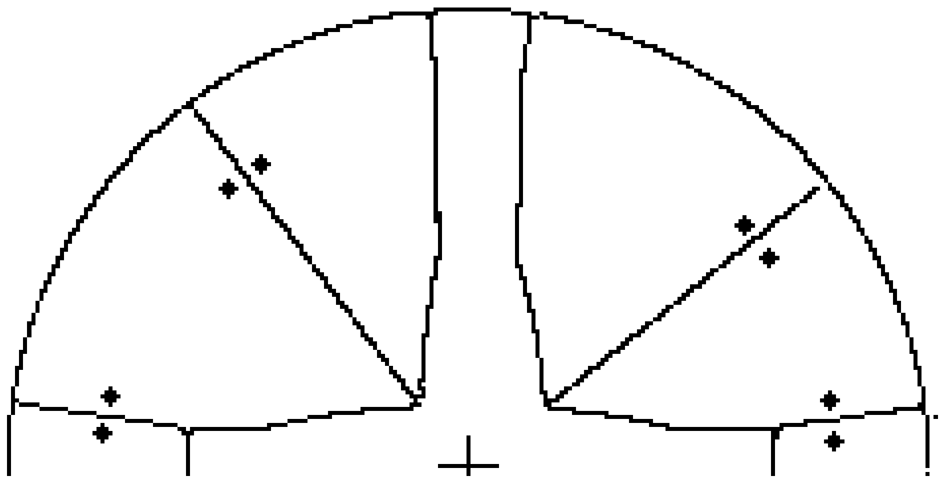

Figure 5.21: A close up of a processed image showing the averaging windows. They are the star-like dots around the radial edges.

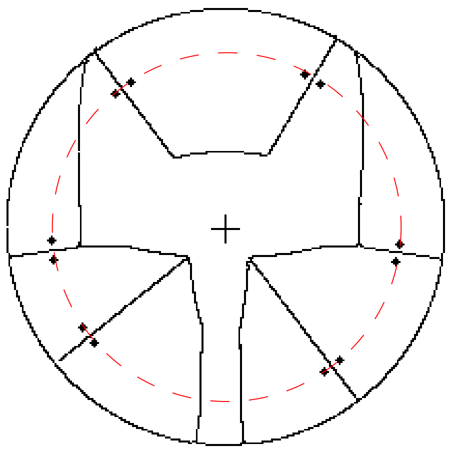

Figure 5.22: The disposition of the averaging windows in the 360° .

coordinate of the edge can only increase from one frame to the next, the second is that this increment is bounded to a maximum step. The size of this step depends on the maximum speed of the robot. In the case of rotation, the displacement of the single edge cannot be bounded: we do not know a priori what the turn will be and there is not a maximum turn the robot can take[8] . There is only a loose bound given by the maximum rotational velocity, but this is not such a constraint. Therefore, an edge can match anyone of the edges in the image with a similar signature. The only constraint we can use is that every edge has to experience the same azimuthal shift. Therefore, we implemented a backtracking algorithm that finds a matching for every edge checking that all edges experienced the same azimuthal shift. The backtracking is necessary to search completely the space of all possible edge matching.

There is a problem: we have these two different sets of constraints for the two different type of motion and the robot does not have access to any information to decide which set should be used. To overcome this, the matching algorithm tries to match the edges assuming the robot performed a rotation. If this does not results in a *good matching*, it assume a translation and applies the appropriate rules. A **good matching** is defined as a matching where more than half of the edges present in the image are correctly identified. If neither of the two set of rules is able to match more than half of the edges, the match that correctly labelled more edges is returned.

We defined a *good match* as requiring the match of more than half of the edges present in the image, because we cannot require that every edge in the current frame is matched with an edge of the previous frame. In fact, if a new edge exited from occlusion in this frame it cannot be matched with anything. On the other hand, it is very unlikely that a wrong matching could identify more than half of the edges.

In all the tests performed by the matching algorithm we introduced a certain amount of tolerance. We have tolerance on the colour signature, on the azimuthal shift and on the azimuthal increase. Let us consider them in detail. The tolerance on the colour signature states that two colour signatures

[8]Remember the robot does not have any direct access to informations about its movements

are considered the same if the values of each colour component differs by less than a certain threshold. The tolerance on the azimuth shift states that two azimuthal shifts are equal if the shift angle differ less than a certain threshold. The tolerance on the azimuthal increase allows an edge to pass this check even if its actual azimuthal coordinate is slightly smaller than in the previous frame. The tolerances reported have been tuned during the experiments on simulated and real sequences in order to have a matching algorithm flexible enough to cope with the noise but not so loose to produce mismatches.

After the matching process is completed, the program writes in a log file the information about the edges in the current frame: the unique label of the edge, its azimuthal position and the values of its left and right averaging windows. This file is useful for debugging purpose and can be used off-line for the reconstruction of the topology of the environment. So far, only the first two of the types of topological transition we saw in Subsection 5.4 are detected on the fly. In fact, the software is able to detect the topological event if the number of edges changes from one frame to the next.

To test the software we wrote, we performed first an experiment with a simulated sequence of frames and then we implemented the system on the actual robot.

5.6 The Simulated Experiment

To perform the simulated experiments, we generated a sequence of images captured by the camera under the mirror while the robot moves in the maze. This sequence of images were used as input for the vision system. Unfortunately, in POV-Ray it is possible to create only off-line simulations. It is only possible to generate a sequence of images, it is not possible to introduce an interaction between the vision system software and the rendering program. In other words, it is not possible to create an interaction between the robot

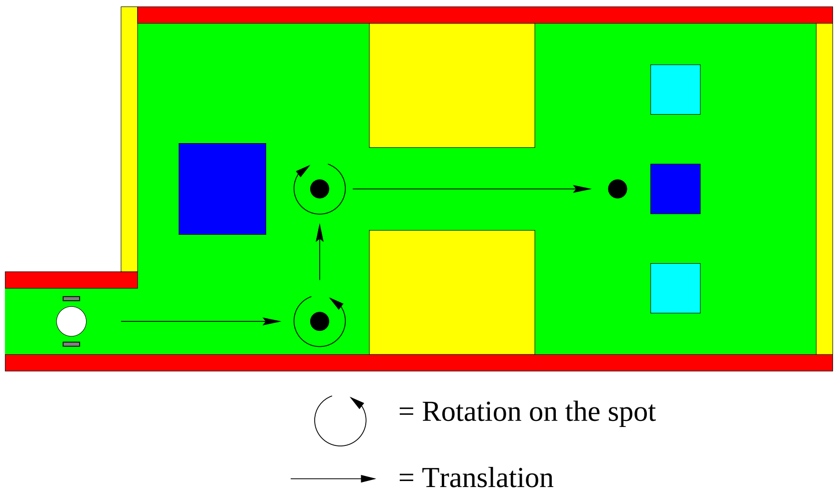

Figure 5.23: The path of the robot through the virtual environment.

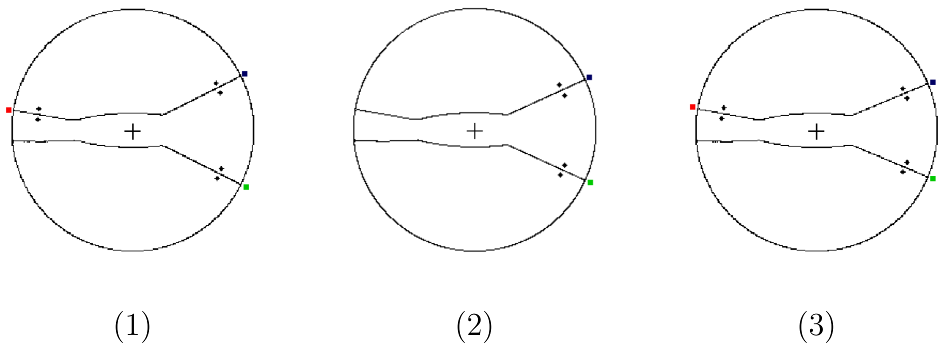

Figure 5.24: The simulation of an *ephemeral* edge. Notice that the edge on the left marked with the red dot is not present in the second frame.

and the virtual environment. So the robot followed the pre-planned path of Fig. 5.23.

Two problems sensitive to the choice of the threshold are the *ephemeral edges* and the *false edges*. These cannot be eliminated just tuning the threshold but their effects can be lowered.

We called **ephemeral edges**, those edges whose presence in the frame sequence is not detected for some frames and after a few frames is detected again. An example is the left edge in Figure 5.24. This happens because the value of the edge counters are under the threshold just for few frames. The

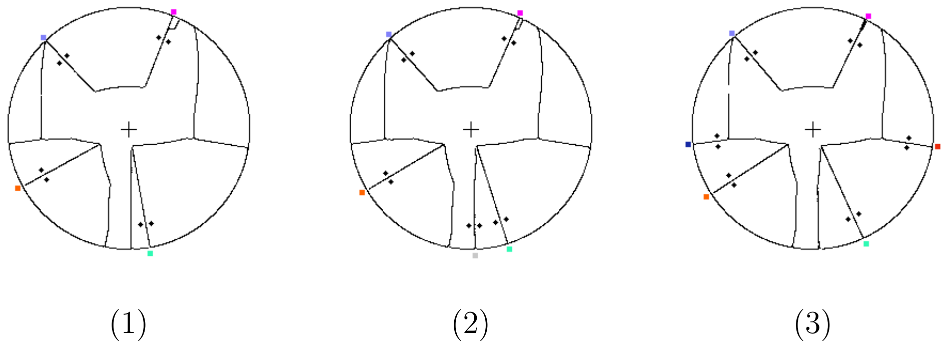

Figure 5.25: The simulation of a *false* edge. Notice that in the second frame the right baseline of the corridor is detected as a radial line. This does not happen neither in the previous frame or in the next.

reason can be either that the pixels of the edge spread in the neighbourhood in such a way that none of their counter is over the threshold or that there is a variation on the number of the edge pixels introduced by the Canny edge detector. So far, the program is not able to handle correctly the ephemeral edges. It does not realise that the new edge that appeared is actually the same that disappeared a few frames before. This is because the matching process uses only two frames: the current one and the previous one. This problem suggests the need of implementing a memory that spans over more frames causing a persistence of the edges for a certain number of frames after they disappeared. In this way, when an ephemeral edge reappears, it can be matched with this persistent image of the edge.

The **false edges** are the accidentally radial lines in the image. In other words, these are lines that are radial in the omnidirectional image, but that does not correspond to vertical edges in the environment as we discuss at the end of Section 5.4. In Figure 5.25 is presented the same sequence of Figure 5.14. The right base line of the corridor is detected just for one frame as a new vertical edge. This suggests the need of a confidence measure on the confirmation of an edge. An edge should be confirmed only if it is present in a minimum number of frames.

Despite these problems, the vision system software showed to be able to correctly track the edges all along the path followed by the robot in these simulations. See sequence in Figure 5.26 and Figure 5.27

The problems of the ephemeral edge and of the false edges could probably be solved off-line from the software that exploits the information on the edge to build the topological map. In other words, the memory of the system could be implemented at a higher level than the sensory level. Probably, it would be easy for this program to analyse the log file of the vision system and spot the presence of an ephemeral or false edge, easier than for the vision system to spot them on the fly.

5.7 The Real Experiment

As we said in the introduction, the environment chosen for carrying out the experiments was the robot football playground at the Intelligent Autonomous Systems Laboratory at the University of Padova. The room has white walls and a floor covering of green carpet. In this room we built a simple corridor with a turn. In the corridor were two boxes to reproduce a door-like view. See Picture 5.28. All the vertical surfaces were painted with uniform colours, except the two boxes. This was done to avoid textures that could fool the edge detector. During the experiments, also the boxes where covered with a uniform colour fabric, because of the noise they introduced. Like for the virtual environment, the colours chosen for the surfaces are vivid and they stand out one against the other to facilitate the recognition of the edge signatures.

When we described the omnidirectional vision system we said that the optical axis of the camera and the geometrical axis of the mirror are aligned. On the real robot this calibration is not an issue. It can be done roughly by hand and then we can find in the image where the tip of the mirror is

270

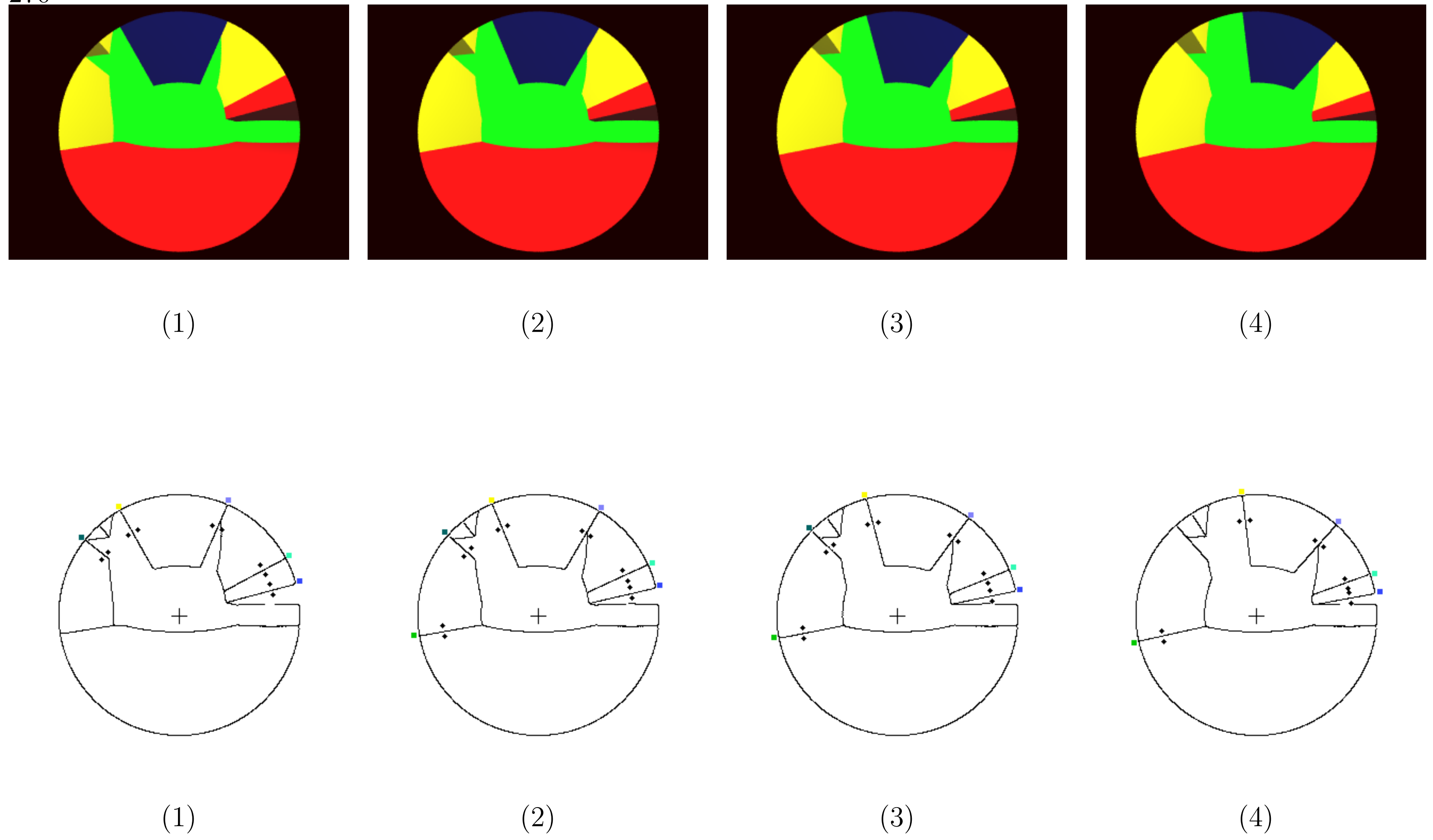

Figure 5.26: (Top) The camera view of a simulated image sequence for a translation of the robot. (Bottom) The tracking of the edges in this sequence.

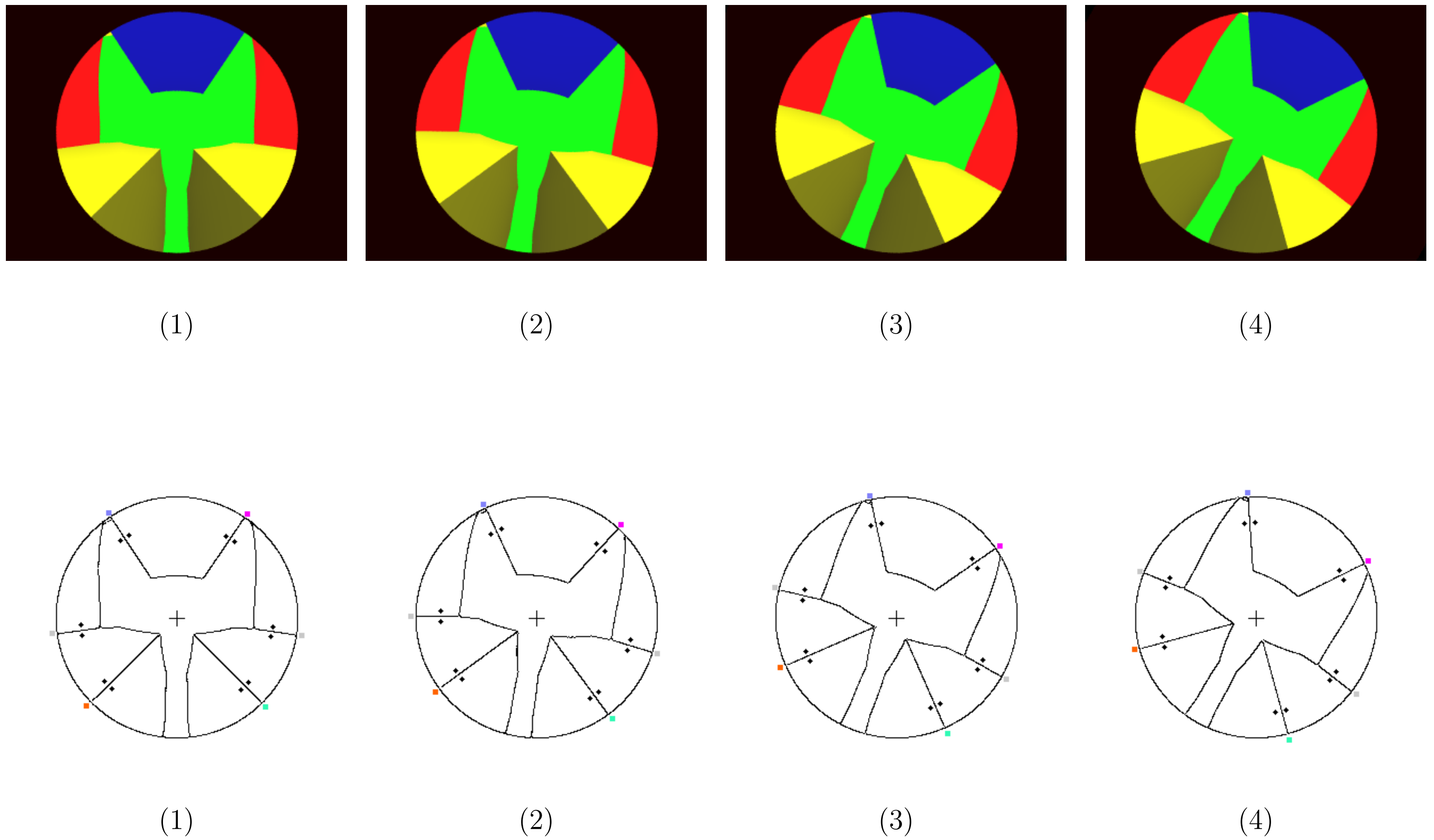

Figure 5.27: (Top) The camera view of a simulated image sequence for a rotation of the robot. (Bottom) The tracking of the edges in this sequence.

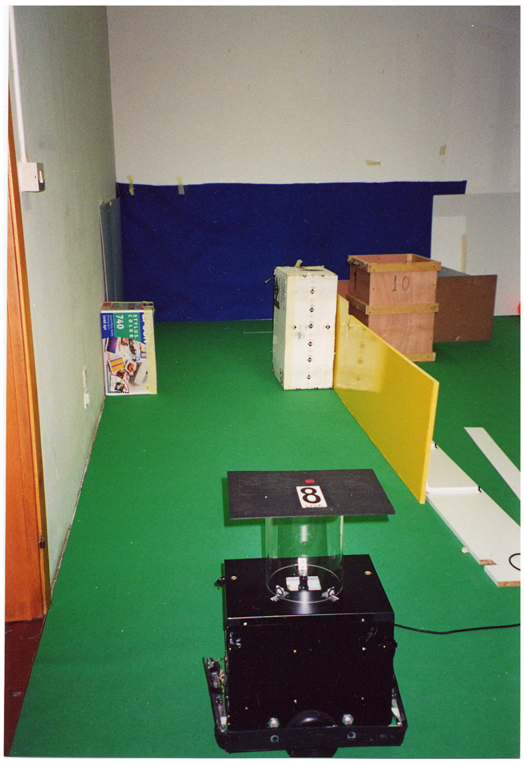

Figure 5.28: The experimental set-up. This is the *corridor* where the experiments were conducted. The two box represent a door. On the right, behind the wood box there is the turn of the corridor.

mapped. We need this information, because this is the point from where all the radial edges sprout and where we have to centre the polar reference system. The performance of the Hough transform depends on the accuracy of this estimation. In Figure 5.29 is represented how we found the real centre of the image. We prolonged the radial edges present in the picture, the crossing point of all the edges is the image centre. This estimations is simple and accurate enough for our purposes.

The results

All the thresholds set in the previous chapter had to be reset when working with the real images. The images are much noisier now. In Figure 5.30 an

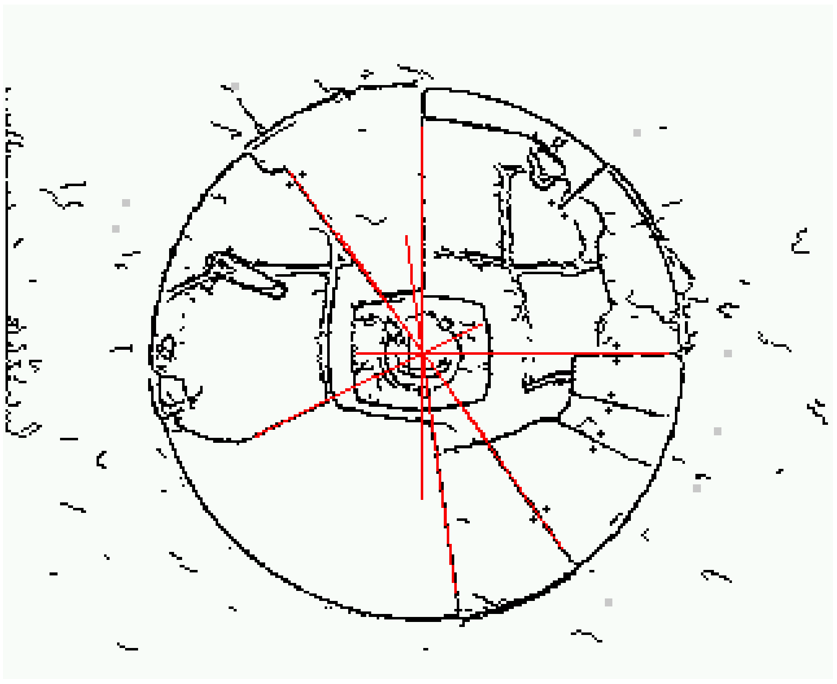

Figure 5.29: The centre of a real image. In red the prolongations of the vertical edges to find out where is mapped the vertex of the mirror.

example of the image process stages for a real image. The noise in the picture propagates down to all stages of the image process. The edge detection result is noisy, Figure 5.30 a). Several noise edgelets are detected, some edges are broken and noise spots are present. This makes it more difficult to reliably detect the radial lines and the radial lines only. In fact, in the Hough transform the pixels of the noise sums over the edge pixels and sometimes the noisy pixels can trigger a false detection of a radial line. An example is shown in Figure 5.31. The arrow shows a marker of a detected edge but the edge does not exists in the picture. It is just the effect of several noisy pixels accidentally having the same angular coordinate. This cannot be avoided setting the threshold higher, because we would have to set it so high to loose significant edges. These false edges do not last for more than two frames and then they could be easily filtered out by the software in charge of reconstructing the topology of the environment, if this is fitted with a

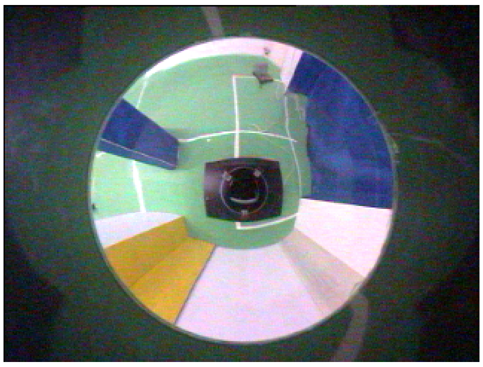
(a) The unprocessed image as view from the robot's camera.

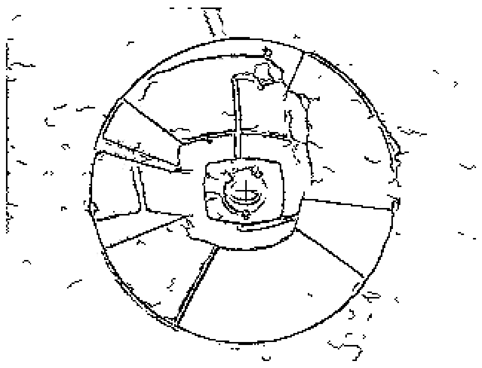
(b) The image after the Canny edge detection.

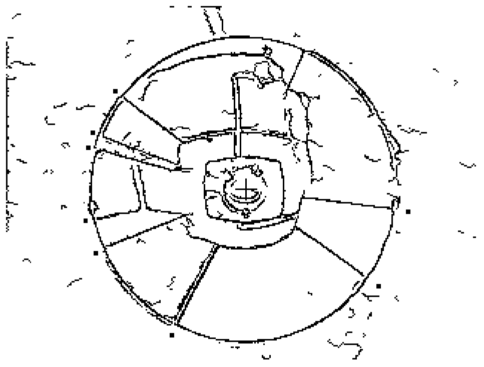
(c) The edge image after the Hough transform.

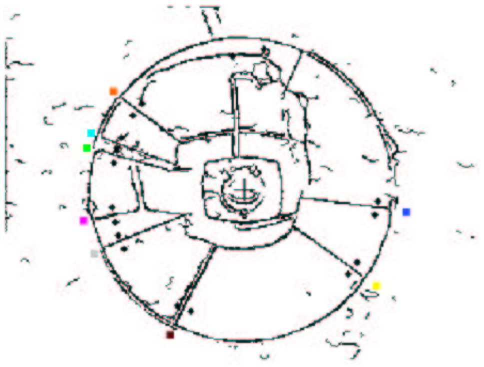
(d) The final result showing the edge matching.

Figure 5.30: An example of the image process stages for a real image.

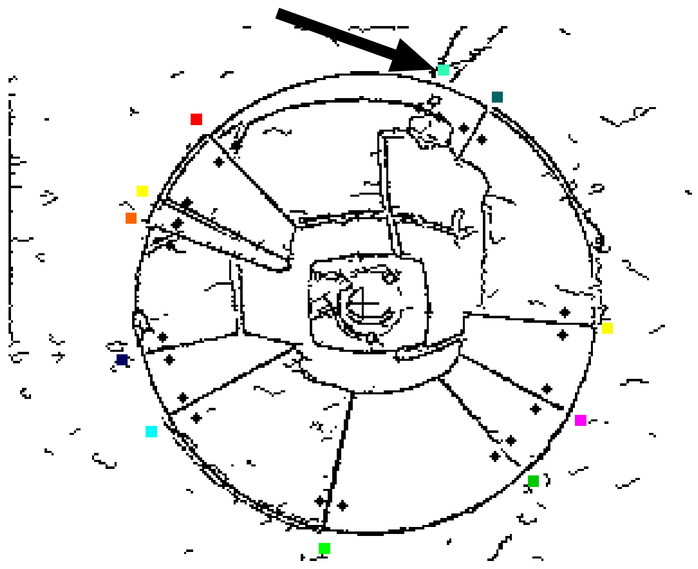

Figure 5.31: An example of false edge produced by the noise in the image. The arrow points the wrong marker.

temporal memory.

The problem of the ephemeral edges exists also in the real image sequences. The noise of the images worsens the problem compared to the simulated images. It happens more often, that an edge disappear and then reappear after some frame. Again this could be solved by introducing a temporal memory of the edges.

The undermining problem in the real image is the noise introduced by the CCD sensor of the camera. This noise affects mostly the colour of the pixels. The noise is so high that even if the robot is steady in the same position, the edge signatures of the same edge in two consecutive frame are different. This problem has been solved with two changes in the vision system software: the tolerance within two colours are considered the same has been increased and the windows over which the mean colour is calculated have been doubled. See Figure 5.32. Doubling the size of the averaging window, we use more pixels to calculate the mean colour and then the edge signature values are

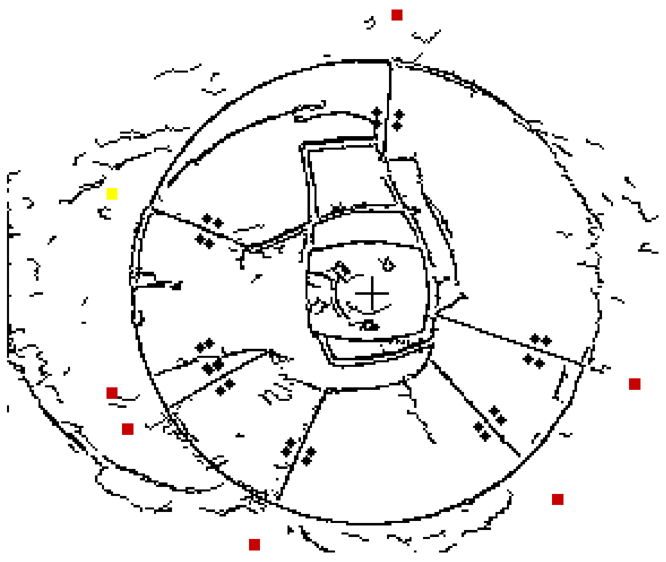

Figure 5.32: The averaging windows used in the real experiments. Notice that the averaging windows are doubled.

more stable.

When the robot moves, the colours around the edges change slightly because of different shadows and different reflections on the surfaces of the objects. To cope with this change we had to relax further the colour tolerance. Remember that the colour of every pixels of the image and the edge signature are represented as a RGB triplet. The new criterion we used is: two edge signatures are considered the same when at least two elements of their triplets are equal within a certain interval. This is enough to cope with the noise present when the robot moves in straight lines, but does not work when the robot turns.

Analysing the images taken from the robot when it rotates, we discovered that the robot failed to recognise the edges because the colours on the sides of the edges in different images are actually different. Consider that the view of the scene does not change and even the shadows and the reflections on the objects' surfaces are the same, this should not happen, and the image should be exactly the same, only rotated by the angle the robot rotated. If the explanation of this change of the colours is not in the scene, it must be in the vision system. The software of the vision system cannot be held responsible for that: it works fine in the simulation. The only candidate is the hardware of the vision system. Remember the camera sees the world through the Perspex cylinder that support the mirror. The explanation of the change of colours can be found in the changes of the light reflection on the Perspex cylinder. These reflections change because the robot's body does not have a cylindrical symmetry. As you can see in Figure 5.1 not only the body is rectangular but also the cover on the top of the mirror has a rectangular shape. The purpose of this cover is to avoid that the camera is blinded by the lights on the ceiling, but it also shadows the Perspex cylinder preventing most of the reflection on it. Because the cover is rectangular, it shields better some region of the Perspex cylinder than others. When the robot rotates it sees the same points in the world through regions of the cylinders with different shadowing from the cover and so different reflections occur at the cylinder surface. The final effect is that the colours appear to change. This effect is made even worst by the reflections occurring on the top cover of the robot body. See Figure 5.33 for an example in which these reflections are particularly strong. Notice the bright spot that seems to move on the left part of the robots body.

The explanation provided for the failure of the tracking algorithm in the rotations is consistent with the fact that this effect does not occur when the robot moves along a straight line. In fact, in this case the change in the reflection is not sharp.

The solution to the problem of reliably detect the colour of the edges could be solved changing the colour space. In fact, the RGB space is not perceptually uniform. As such, the proximity of colours in RGB colour space does not indicate colour similarity. It would probably be a good idea to

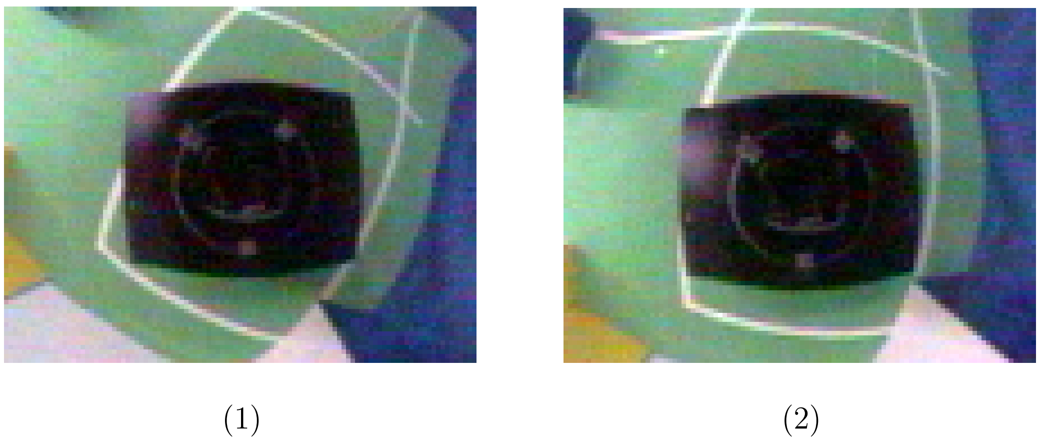
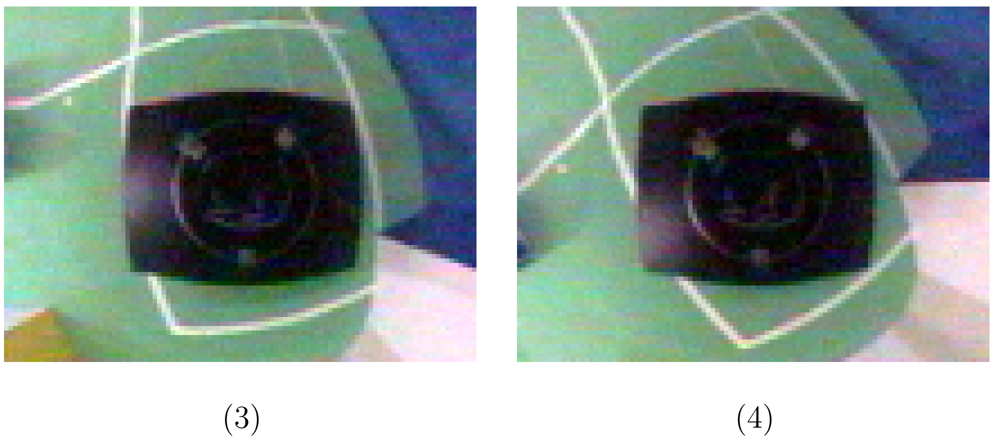

Figure 5.33: A close up of a sequence showing an example of strong reflection on the body of the robot. Notice the bright spot on the left of the robot's body that appears to move from one frame to the next.

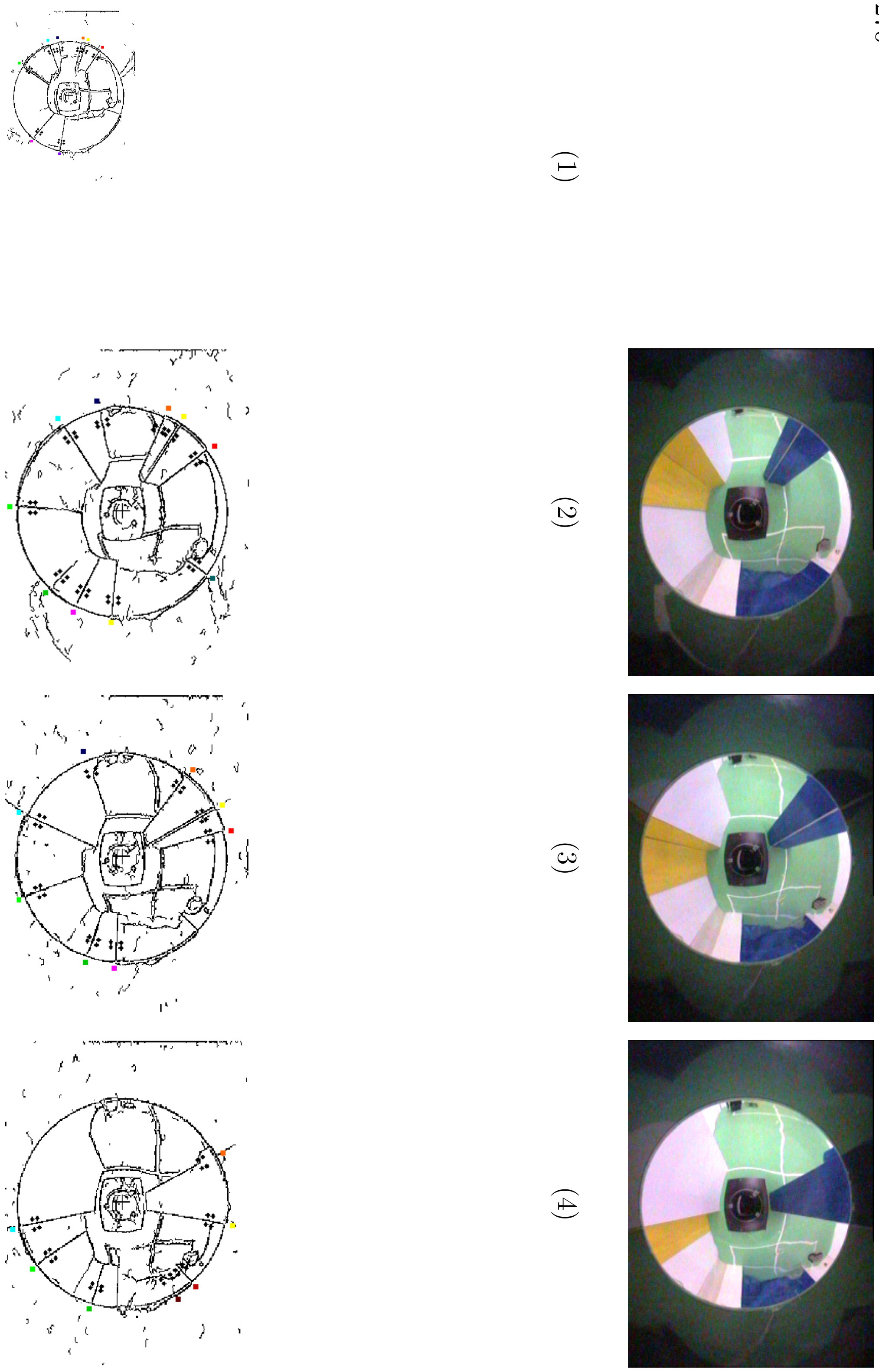

Figure 5.34: (Top) The camera view of a real image sequence for a translation of the robot. (Bottom) The tracking of the edges in this sequence.

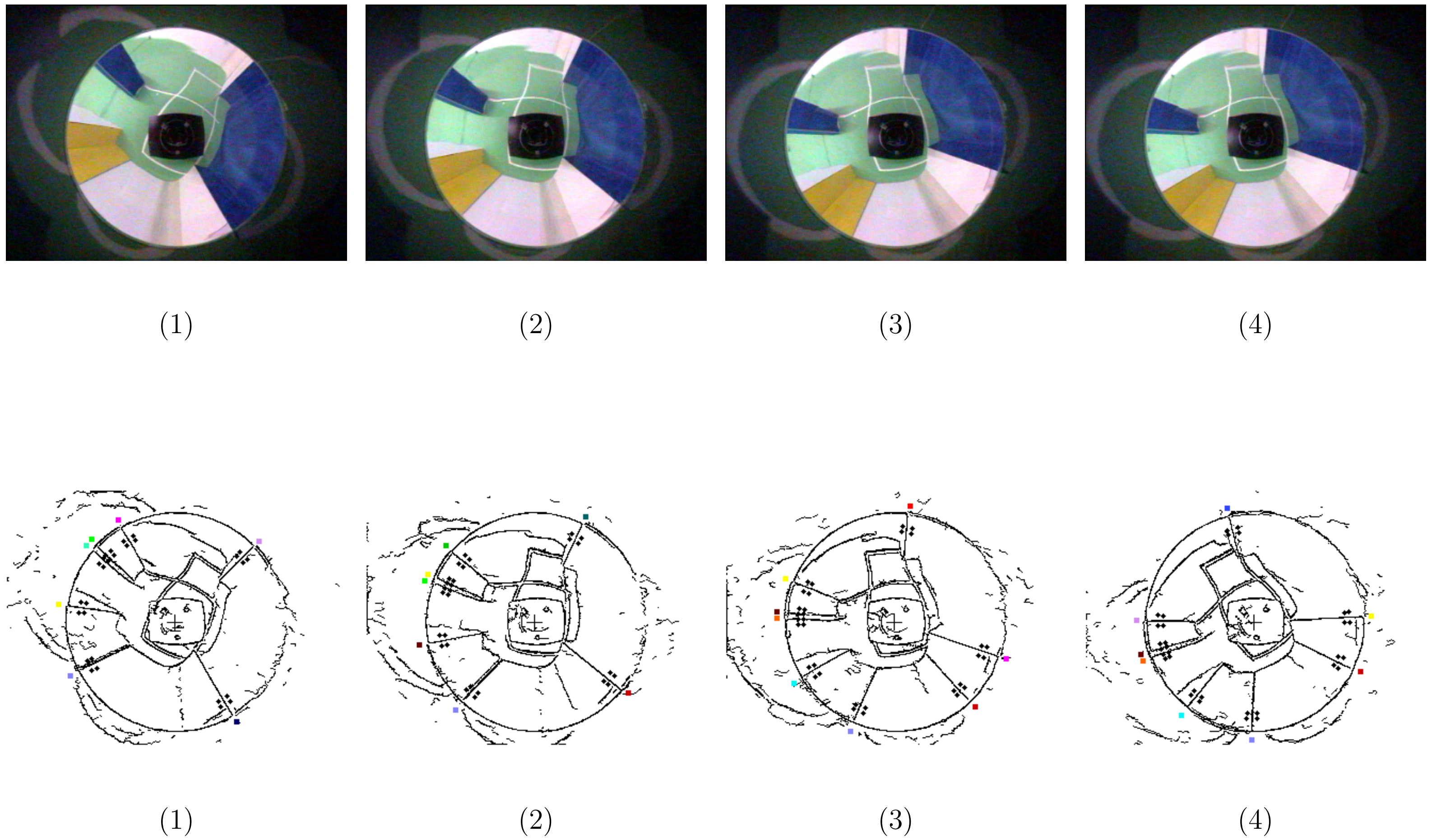

Figure 5.35: (Top) The camera view of a simulated image sequence for a rotation of the robot. (Bottom) The tracking of the edges in this sequence.

transfer the image to the HSI colour space. In this space, colour pixels are defined as triplets representing hue (H), saturation (S) and intensity (I). This colour space has the advantage of being approximately perceptually uniform. Therefore, colour similarity implies proximity in this colour space [80]

5.8 Conclusions

This work implemented the Spatial Semantic Hierarchy on a real robot. We realised the sensory level with an omni-directional vision system. This is the first step toward the construction of an agent able to draw a topological map of the environment it travels through. Experiments were performed both in simulation and with a real robot.

In this work, we showed that an omni-directional vision system is a good sensor for the SSH. We pointed out which of the features present in a omni-directional image can be used to detect the *transitions of state* needed by the control level of the SSH. We showed the existence of a strict link between the *views* of the SSH and the image taken by an omnidirectional sensor. We built a vision system able to extract these features from the images. We showed that the software runs properly in a virtual environment and finally, we tested the same software on a real robot discovering that what worked in the simulations does not work in the real world. This confirms what Ronald Arkin said, which might seem self-evident but is often forgotten:

> *To conduct robotics research, robots are needed*
> —Ronald Arkin 'Behaviour-Based Robotics' MIT Press

At the time of writing, we are working to solve this implementational problem. The work presented in this chapter was presented in [70] [71].

At the same time we are working also to extend to multi-robot systems our approach to the mapping problem. The basic idea is every robot build the local map of the portion of environment it visited. When two robots meet they share their portions of the map, fusing them in a global map. This idea was presented in [65], preliminary experiments were presented in [67].

Chapter 6

Distributed Omnidirectional Vision

In the previous chapter, we showed the synergy that can be implemented between an omnidirectional vision sensor and the theory of the *Spatial Semantic Hierarchy* (SSH) proposed by Kuipers. In this chapter we will present our current works on the distributed omnidirectional vision. In the first part of the chapter we will explain the concept of distributed vision system and we will illustrate some of the research lines we are following. In the second part of the chapter we will present an experiment where a distributed vision system is autonomously learning how to control a mobile robot. The works presented in this chapter are in progress and the experiments we are performing are giving new hints and new insights on the investigated topics.

6.1 Distributed Vision in Robotics

Our work has been inspired by the work of Ishiguro [36]. He proposed an infrastructure called *Perceptual Information Infrastructure* (PII). In his paper, he proposed an implementation of the PII composed by static Vision Agents, i.e. fixed cameras with a certain amount of computational power.

This realisation of the *Perceptual Information Infrastructure* was called Distributed Vision System (DVS). The DVS presented in [36] has 16 cameras, strategically placed in the environment, that navigate two mobile robots. The robots are not autonomous, in the sense that they need the DVS to navigate, but they has a certain amount of deliberative power, in the sense that they can decide which Vision Agent provides them the more reliable information on the surroundings. The assumption that every Vision Agents is static simplifies the problem and allows to use very simple vision algorithms. In fact, to detect the moving objects (the robots) Ishiguro used the background subtraction algorithm. This implies that the whole system is not scalable to include Mobile Vision Agents, as we will see in the following.

A parallel but independent work is the one of Matsuyama [54]. Matsuyama explicitly introduced mobile robots in the theoretical frame of its Cooperative Vision System. In the experiments presented in [54], he used active cameras mounted on a special tripod. The active cameras were pan-tilt-zoom cameras modified in order to have a fix view point. This allowed, again, the use of a simple vision algorithm, not very different from the case of static cameras.

As far as we know, no attempt has been tried to realise a DVS with truly mobile robots running robot vision algorithms.

Mobile robots are more and more fitted with vision systems. The popularity of such sensors arises from their capability of gathering a huge amount of information from the environment surrounding the robot.

In multi-robot systems there are two possibilities to acquire visual information, i.e. a centralised vision system or a distributed vision system.

The first approach consists in controlling a robot team with a unique camera that monitors the whole environment where the robots move. This has been applied in well structured and relatively small environments [14], but it is unfeasible for large environments. If this is the case, we are compelled to move toward the second approach, a distributed vision system. Nowadays, the relatively low cost of the required hardware allows to equip every robot with a vision sensor mounting a camera on each robot of the team.

In the second approach, each robot can gather a detailed information on its surrounding and the system is more versatile. In fact, fix camera positioned in *a priori* location in the environment limits the flexibility and robustness of the system, even if we dispose of several fixed cameras. As an example think of an industrial site watched with a video monitoring system composed only of cameras with fixed locations (even pan-tilt-zoom cameras). If an alarm or a meaningful event happens outside the field of view of any camera, the system cannot "see" this event. This is because the system has a *predetermined field of view.* If we have also some cameras mounted on mobile robots, the system can send a robot to inspect the new location of interest. With such a solution the system is more flexible and we realise what we call a *dynamic field of view.*

Introducing mobile robots fitted with cameras distributes the sensors in the environment, but this is not enough: we aim to the creation of a Distributed Vision System. A set of cameras scattered in the environment (fixed or mounted on mobile robots) needs to communicate over a network in order to became a unique Distributed System. If not, they are just a set of different vision sensors of pertinence of the single vision system.

In the following we will prefer the term *Vision Agent* instead of "vision system". The term Vision Agent emphasises that the vision system is not just one of the several sensors of a single robot, but that it interacts with the other vision systems to create an intelligent distributed system.

The final goal

The aim of this work is to introduce a real Mobile Vision Agent in the DVS architecture, i.e. to apply the ideas and the concepts of Distributed Vision

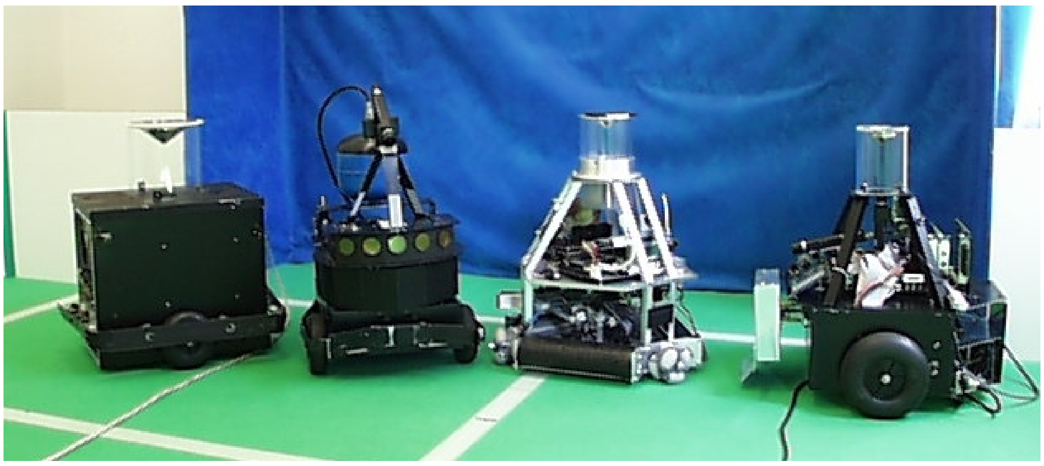

Figure 6.1: Our team of heterogeneous robots

to a mobile robot equipped with a camera.

The domain in which we are testing our ideas is the RoboCup competition. We are on the way to create a Distributed Vision System within a team of heterogeneous robots fitted with heterogeneous vision sensors. We want to create a dynamic model of the environment, which can be used by mobile robots or humans to monitor the environment or to navigate through it. The model of the environment is built fusing the data collected by every Vision Agent. The redundancy of observers (and observations) is a key issue for system robustness.

6.2 Mobile Robot DVS

6.2.1 VAs on the same robot

The first implemental step is to realise a Cooperative behaviour between two heterogeneous vision agents embodied in the same robot. Exploiting the knowledge acquired in our previous research [56] [71], we want to create a

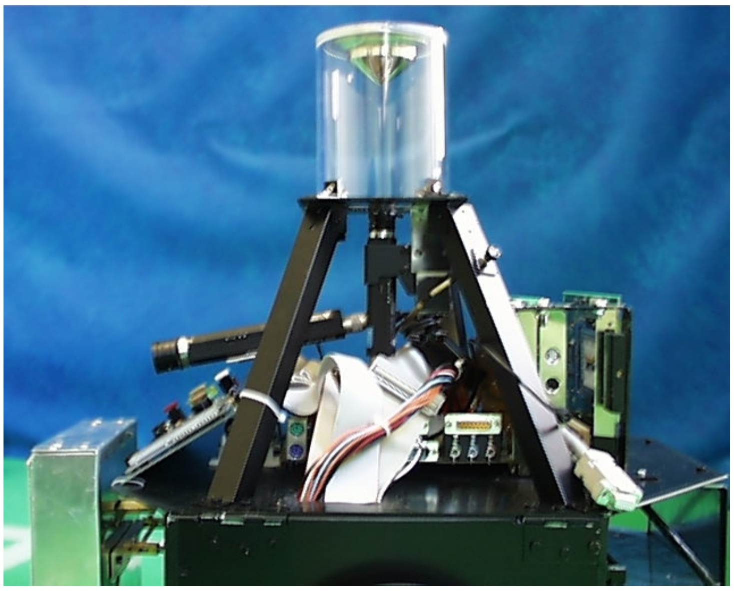

Figure 6.2: A close view of the vision system of Nelson. On the left, the perspective camera. In the middle, pointed up-ward the omnidirectional camera

Cooperative Vision System using an omnidirectional and a perspective vision system mounted on the same robot. The robot is our football player robot, called Nelson, that we entirely built starting from a Pioneer2 base[1] . The omnidirectional vision sensor is a catadioptric system composed of a standard colour camera pointing up-ward and an omnidirectional mirror, see Figure 6.1. The omnidirectional mirror presents a custom profile. We designed such a profile to improve the performances of the vision sensor in the RoboCup domain[2] .

The omnidirectional camera is mounted on the top of the robot and offers a complete view of the surroundings of the robot [88] [8]. The perspective camera is mounted in the front of the robot and offers a more accurate view of objects in front of it. These two cameras mimic the relationship

[1]For some nice picture of this robot go to the web page www.dei.unipd.it/~robocup

[2]For details on the procedure we used to design the custom profile of the mirror, please refer to [59]

between the peripheral vision and the foveal vision in humans. The peripheral vision gives a general, and less accurate, information on what is going on around the observer. The foveal vision determines the focus of attention and provides more accurate information on a narrow field of view. So, the omnidirectional vision is used to monitors the surroundings of the robot to detect the occurrence of particular events. Once one of these events occurs, the Omnidirectional Vision Agent (OVA) send a message to the Perspective Vision Agent (PVA). If the PVA is not already focused on a task, it will move the robot in order to put the event in the field of view of the perspective camera. This approach was suggested by our previous researches presented in [20].

Experiments on such a system are running and they will provide more insight on the cooperation of the two heterogeneous vision agents.

6.2.2 VAs on different robots

Another stream of research is the creation of a Cooperative Distributed Vision System for our team of football player robots[3] , depicted in Figure 6.1.

Our aim is to implement the idea of the Cooperative Object Tracking Protocol proposed by Matsuyama [54]. In the work of Matsuyama the central notion is the concept of *agency.*

An **agency**, in the definition of Matsuyama, is *the group of the VAs that see the objects to be tracked and keeps an history of the tracking.* This group is neither fixed nor static. In fact, a VA exits the agency, if it is not able to see the tracked object anymore and a new VA can joint the agency as soon as the tracked object comes in its field of view. To reflect the dynamics of the agency we need a dynamic data structure with a dynamic role assignment [55].

[3]For a detailed description of the robots employed in these experiments, please refer to [75] [76].

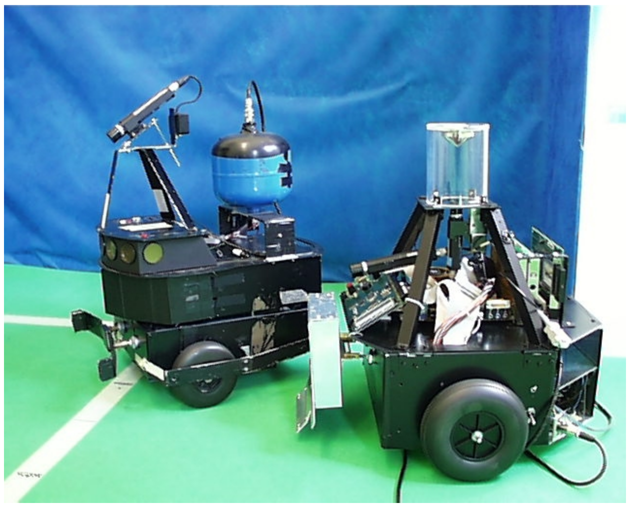

Figure 6.3: A close view of two of our robots. Note the different vision systems

Let us sketch how the agency works, using an example draw from our application field: the RoboCup domain. Suppose to have a team of robots in the field of play. Each robot is fitted with a Vision Agent. None of the Vision Agents is seeing the ball. In such a situation no agency exists. As soon as a Vision Agent see the ball, it creates the agency sending a broadcast message to inform the other Vision Agents the agency has been created and it is the master of the agency. After this message a second message follows, telling the other Vision Agents the estimated position of the ball. All the other Vision Agents manoeuvre the robots in order to see the ball. Once a Vision Agent has the ball in its field of view, it asks permission to joint the agency and send to the master its estimation of the ball position. If this information is compatible with the information of the master, i.e. if the new Vision Agent has seen the *correct ball*, it is allowed to joint the agency.

The described algorithm has been realised by Matsuyama with his fixed vied point cameras. His system was composed of four pan tilt zoom cameras mounted on a special active support in order to present a fixed view point.

The system was able to track a radio controlled toy car in a small indoor environment. As mentioned before, in such a system there is not a truly mobile agent. Moreover, the vision algorithm used is typical of static Vision Agents. In fact, it is a smart adaptation of the background subtraction technique.

Our novel approach is to implement the Cooperative Object Tracking Protocol within a team of mobile robots equipped with Vision Agents. This requires a totally new vision approach. In fact, the point of view of the Vision Agent changes all the time. The changes in the image are due not only to the changes in the world (as in the Matsuyama testbed), but also to the change of position of the Vision Agent. Therefore, we need a vision algorithm able to identify the different objects of interest and not only to reveal the objects that are moving. Moreover, we have to introduce a measure of uncertainty in the estimation of the position of these objects, because the location of the Vision Agents is not known exactly anymore and there are errors in the determination of the relative distance between the objects the Vision Agents.

To explain these issues, let us come back to our RoboCup example. Above we said that if a new Vision Agent sees the ball, it sends a message to the master that checks if it has seen the correct ball. In a RoboCup match there is just one ball, but sometimes what a robot identifies as a ball is not the correct one. This can result either because the robot sees objects resembling the ball, and erroneously interprets them as a ball (like spectators hands or reflex of the ball on walls), or because it is not properly localised and so it reports the ball to be in a fallacious position.

To cope with the uncertainty in the objects position, every Vision Agent transmits to the master the calculated ball position with the confidence of this estimation. The master dispatches to the other robot a position calculated as an average of the different position estimations, weighted by the confidences reported by every Vision Agent (if there is more than one Vision Agents in the agency).

Especially in the described dynamic system, the master role is crucial in the correct functioning of the agency. The master role cannot be statically assigned. The ball is continuously moving during the game. The first robot that sees the ball will not have the best observational position for long. So, the master role must pass from robot to robot. The processes of swapping the master role is critical. If the master role is passed to a robot that sees an *incorrect ball* the whole agency will fail in the *ball tracking* task.

The simplest solution could be to pass the master role to the robot with the highest confidence on the ball position. This means to shift the problem to identify a reliable confidence function. This makes sense, because the confidence function will be used for two services that are two sides of the same coin. In fact, if a robot is correctly localised and correctly calculates the relative distance of the ball, it will have strong weight in the calculation of the ball position. Given this, it can reliably take the role of master.

The confidence function

The confidence function ψ_{abs} associated to the reliability of the estimation of the absolute ball position is a combination of several factors. It has to account for the different aspects that contributes to a correct estimation of the ball position. In fact, the position of the ball in the field of play is calculated by a vectorial sum of the relative distance of the ball from the robot and the absolute position of the robot in the pitch. So, the confidence of the estimation of the absolute position of the ball is the sum of the confidences function associated to the self-localisation, ψ_{sl}, and of the confidence function associated to the estimation of the relative position of the ball with respect to the robot, ψ_{rel}.

$$\psi_{abs} = \psi_{sl} + \psi_{rel} \tag{6.1}$$

The self-localisation process uses the vision system to locate landmarks in the field of play. The process is run only by time to time and if the landmarks are visible. Between two of these process the position is calculated with the odometers. This means that the localisation information degrades with time. The confidence function associated with the self-localisation is the result of the following contribution:

- type of vision system (perspective, omnidirectional, etc.);
- a priori estimated absolute error made from the vision system in the calculation of the landmarks position;
- time passed after the last self-localisation process;

The relative position of the ball with respect to the robot is calculated as in [59]. The confidence function in this process presents the following contribution:

- type of vision system;
- distance from the ball;

At the moment the exact definition of the confidence function is under testing. The experiments will tell us how much every contribution should weight in the final function.

In the next section, we will present some experiments we realised on Distributed Vision Systems that can learn to control a mobile robot.

6.3 Learning DVS

Nowadays the applications of networks of sensors are more and more common. There is an increasing need for intelligent sensors able to dialogue one to the other in order to exchange information and to perform intelligent tasks. For instance, networks of cameras are something we are used in every-day-life, but in most cases these are just a set of dummy sensors (e.g. multi-camera video surveillance systems in banks or airports). They collect a huge amount of videotape data that human operators need to interpret. In the scientific community, there is a strong will to integrate these sensors into an intelligent system. Several researchers are working on autonomous system of surveillance [24] [73] or on intelligent environments [12] [83], like intelligent rooms. In the robotics community as well, the interest of the researchers is shifting form a single agent working in a cell-space to multiple agents working in the real world. For these kind of applications a single camera is not enough and multiple cameras are needed to observe the scene. Again, the aim is to provide an intelligent infrastructure able to support robots' activities [38] [36].

In this chapter, we present a network of uncalibrated omnidirectional vision sensors able to autonomously learn to control a mobile robot in a large scale environment. The cameras in the network can communicate among them and with the mobile robot. To stress that the camera network is more than a simple bunch of sensors scattered in the environment, we called it a **Distributed Vision System** (DVS). The term DVS (Distributed Vision System) emphasises that the camera network acts as a whole, as a single *"super-sensor"*, able to navigate the robot. The DVS is composed of several **Vision Agent** (VA). A VA (Vision Agent) is a vision sensor able to acquire images, to process them and to communicate with other VAs over a network. In the taxonomy of Weiss, a Vision Agent can be defined as a *Smart Agent*,

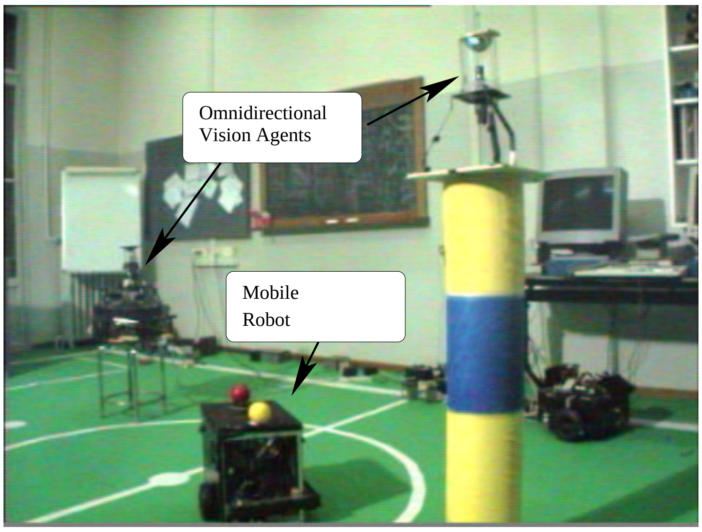

Figure 6.4: A picture of the whole system showing two Vision Agents and the robot used in the experiments.

because it is autonomous, it is able to learn from experience and it can cooperate with other agents to achieve a global goal [85]. In our implementation, everyone of these agents is *embodied* in a different sensor and is *situated* at a different position. Form a hardware point of view, the DVS presented in this chapter looks like a set of uncalibrated omnidirectional cameras distributed in the environment, see Fig. 6.4. The omnidirectional cameras are catadioptric omnidirectional cameras composed of a standard perspective camera and a convex mirror [37]. The camera is pointed upward to the mirror that is reflecting the light gathered by the surroundings of the sensor, see Fig. 6.6. Every camera is connected to a PC that provides computational power for image processing and network communication.

Ishiguro showed how a Distributed Vision System can navigate a robot in a toy-scale real-world environment [36]. In that work the learning phase required the intervention of a human operator guiding the robot in the free space in the toy town reproduction. In this chapter, we propose a totally autonomous Distributed Vision System able to learn how to control a mobile robot by autonomously generating a set of examples and by propagating the knowledge through the network.

In Section 2, we will discuss in further detail the task of the DVS. In Section 3, we will explain the structure of an Omnidirectional Vision Agents. In Section 4, the learning procedure is discussed and experimental results are presented. Finally, future work are hinted and conclusions are drawn.

6.3.1 The task to be learnt

As we said in the introduction the task of the DVS is to learn to drive a mobile robot. This knowledge is first acquired by a single VA and then is propagated to other VAs in the network. The distributed learning is composed of four steps:

1. a Vision Agent learns the mapping between its image space and the robot's motor space;
2. the Vision Agent transmits the learnt mapping to a second Vision Agent;
3. the second Vision Agent checks if the received mapping is valid, if not starts a re-learning phase guided by the first Vision Agent;
4. the knowledge is propagated from the second Vision Agent to the third Vision Agent, and so on;

The bridge to propagate the knowledge among the Vision Agents is the robot. The first Vision Agents controls a robot by sending to the robots a set of random motion commands, see Fig. 6.5. Looking at the motion of the robot, the system learns the mapping between the position of the robot in the image space and the robot's motor space, see Fig. 6.8. As we said, the acquired knowledge is then propagated to the other Vision Agents on the

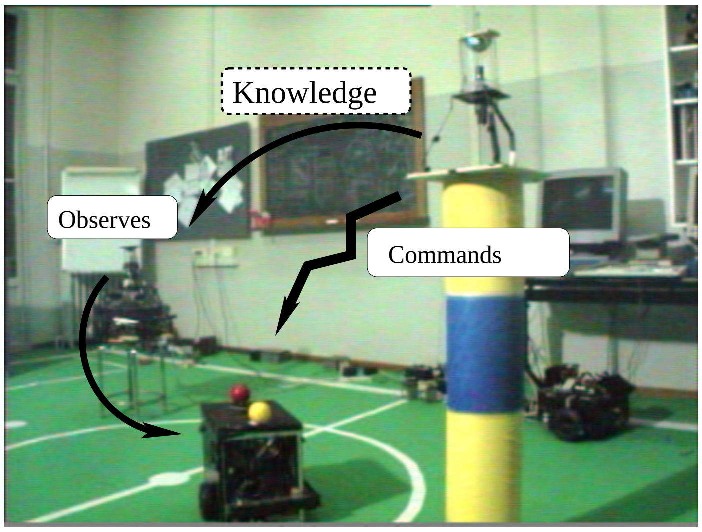

Figure 6.5: The knowledge propagation process: the VA on the right send commands to the robot, the VA on the left observing the robot evaluates the knowledge received by the first VA.

network, Fig. 6.5. Because the vision sensors are not previously calibrated, the propagated knowledge cannot be immediately used and a certain amount of re-learning can be needed. In fact, if the vision sensors are not previously calibrated, the mapping between the image space and the motor space might be different: the cameras could be located at different heights or at different distances from the mirrors, the poles supporting the cameras could be not exactly vertical, etc. In addition, the Vision Agents could mount heterogeneous vision sensors and so the mapping function have to be relearned. Examples of heterogeneous vision sensors can be omnidirectional vision sensors with mirrors with different profiles customised for different tasks [59].

Omnidirectional Vision Agent

Every sensor in the network is composed of hardware and software resources. We discussed the hardware resources in which the VA is embodied in the introduction. In Fig. 6.6, the hardware resources of the VA are depicted. In

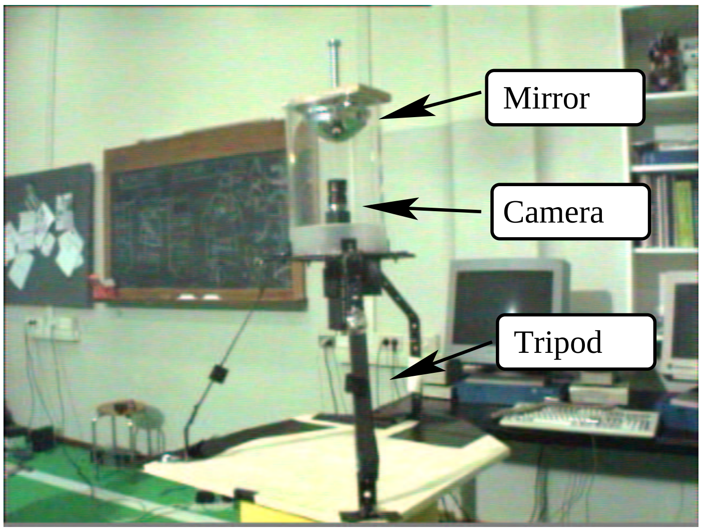

Figure 6.6: A picture of the hardware resource of the Vision Agent. On the top the omnidirectional mirror (here a hyperbolic mirror), under the mirror the camera and the tripod supporting the system.

this section we will discuss the software resources called **Vision Agent**.

The Omnidirectional Vision Agents used in this work are composed of the following modules:

- a vision system
- a neural network called *navigator*
- a neural network called *supervisor*
- a communication network module

In the next section we will discuss in detail the single modules of the Vision Agent.

6.3.2 Vision System

The vision system is the sensorial module of the Vision Agent. The Vision Agent gathers information on the world using the vision system.

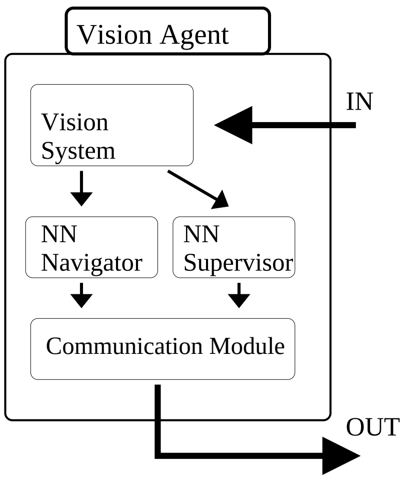

Figure 6.7: The simplified scheme of a Vision Agents. The drawing highlights the main blocks composing the VA.

The task of the vision system is to calculate the position and the heading of the robot in the image. To easily detect the position and the heading of the robot, two coloured balls are fixed on the top of the robot and the vision system looks for these two coloured blobs. The midpoint between the centres of gravity of the two balls gives the position of the robot and the line passing by the centres of gravity of the two balls gives the heading of the robot. In order to avoid to search the whole image for the coloured blobs, the vision system uses a background subtraction algorithm to detect the broad region of image in which is located the robot.

The background subtraction algorithm can be used because we are assuming the Vision Agent is static (i.e. its view of the environment does not change) and the robot is the only moving object in the filed of view of the camera. The current image with the robot moving in the environment is subtracted from a reference image in which the robot is not in the field of view of the Vision Agents. The difference image is thresholded. The centre of gravity and the vertical and horizontal standard deviations of the *"different"* pixels are calculated. A region of interest (ROI) is created in a region centred in the calculated COG (centre of gravity) and spanning an area wide as six times the horizontal standard deviation and height as six times the vertical standard deviation. This choice for the width and height of the ROI assures that all pixels belonging to the robot are included in the ROI (region of interest). The current image is searched only within this ROI for the blue and red pixels of the two balls.

The selected ROI is searched twice for the blue pixels and twice for the red pixels, in order to increase the robustness of the calculation of the blobs' COGs. In the first scan of the ROI, narrow colour thresholds are used, i.e. only pixels strictly blue or strictly red are found. The COGs and standard deviations of the found pixels are calculated and the pixels farther than twice the standard deviations from the COGs are discarded as false matches. Two ROIs are created around the calculated COGs and these two ROIs are searched again with broad colour thresholds for blue and red pixels. In the end the two COGs of this new blue and red blobs are calculated. This algorithm proved to be very robust against the image noise and the COGs of the blobs are steadily detected.

Once the COGs of the blue and red blobs are calculated, we can calculate the position of the robot as the midpoint between the COGs of the blobs. The heading of the robot is calculated as the angle between the line going from the blue blob to the red blob and the image's frame of reference.

The final output of the vision system is the heading and the position of the robot calculated both in the polar coordinates centred in the image centre and the Cartesian coordinates in the usual frame of reference for the images.

Neural Networks

The output of the vision system is passed to the two neural networks. In the learning stage the two neural nets are trained using the robot positions

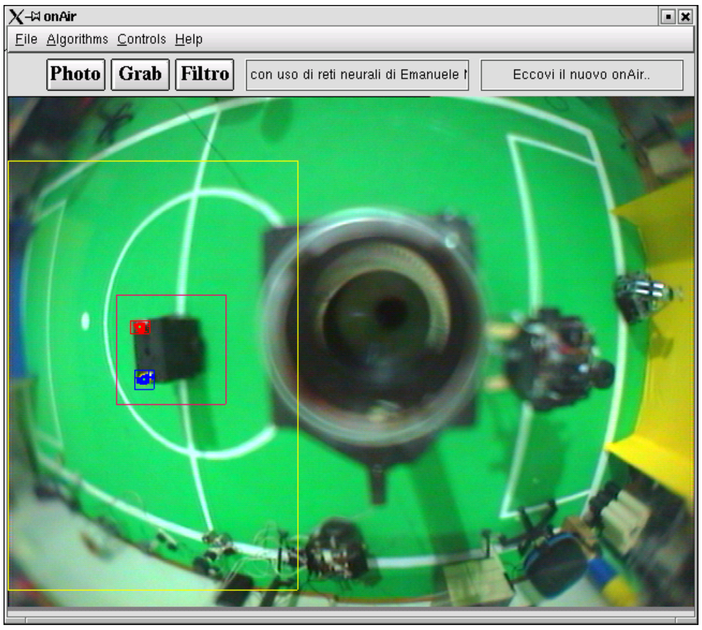
onAir
File Algorithms Controls Help
Photo
Grab
Filtro
con uso di reti neurali di Emanuele I
Eccovi il nuovo onAir..

Figure 6.8: A snapshot of the image processing software that detects the position and heading of the robot in the image.

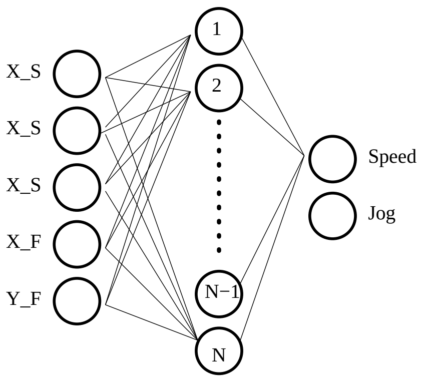

Figure 6.9: The structure of the used neural network.

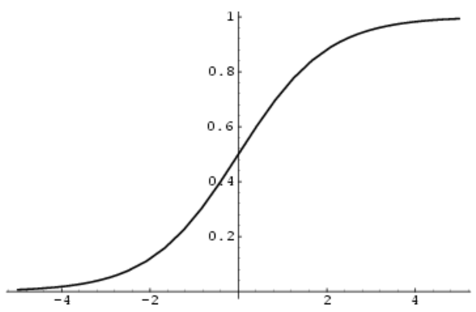

Figure 6.10: A plot of the sigmoid function.

and the robot speeds of the autonomously generated training examples. In the running stage, the task of the *navigator network* is to calculate the instantaneous translational and rotational speeds necessary to reach the target position. The task of the *supervisor network* is to check if the commands sent to the robot have been successfully executed.

In this first implementation of our system we used a very simple structure for the neural networks. These are three layer networks with an input layer, an hidden layer and an output layer, see Fig. 6.9. The units of the networks are sigmoid units and the networks are trained with the back-propagation algorithm [72]. The sigmoid function is plotted in Fig. 6.10 and it is defined as:

$$\sigma(x) = \frac{1}{1 + e^{-x}} \tag{6.2}$$

Navigator Network

As depicted in Fig. 6.9, the network has five input units, four hidden units and two output units. The input units take the three parameters of the initial position and heading of the robot and the two parameters of the final position of the robot, respectively named:

$$\begin{aligned} input &\rightarrow \{(x_S, y_S, h_S), (x_F, y_F)\} \\ output &\rightarrow \{(Speed, Jog)\} \end{aligned} \tag{6.3}$$

Note that in the first part of this work we are not considering the final heading of the robot, i.e. the robot has only to reach the final position, but the final heading is not important.

The outputs of the network are the values of linear speed and angular speed to be set on the motors of the robot, respectively.

These values are the instant speeds necessary to move the robot from the starting position to the final position. These values are sent at every cycle of the Vision Agent to the Agent on the robot through the network module.

Supervisor Network

The *supervisor network* takes as input the starting position of the robot and the speeds set on the motors and predicts the final position of the robot. The topology of the Supervisor Network is the same of the Navigator Network, but inputs and outputs are respectively:

$$\begin{aligned} input &\rightarrow \{(x_S, y_S, h_S), (Speed, Jog)\} \\ output &\rightarrow \{(x_P, y_P)\} \end{aligned} \tag{6.4}$$

If the actual final position of the robot, as reported from the vision system, is not compatible with the predicted position an exception is raised. This exception means that the learnt control of the robot is no longer valid and a re-learning is needed. As we said, in our experiment this mean that the knowledge received from another Vision Agents cannot be used and a certain amount of re-learning is needed..

Communication Network Module

The network subsystem used here is a part of the ADE library, a software suite written in C++ and used by our RoboCup[4] team: *Artisti Veneti*[5] . ADE provides basic C++ classes implementing thread scheduling, message passing and seamless network communication [17].

The protocol used for data transmission is the connectionless User Datagram Protocol (UDP) over IP. This protocol allows fast network responses even in case of a temporary failure (as it is often the case in noisy wireless networks). Packet loss for our application is not an issue since packets are self-contained and repeatedly sent.

The messages sent via the ADE network (ANet), from a programmers' point of view, are objects descending from a common virtual base class; this allows the library to find out at runtime, via the C++ RTTI facilities, the actual object class and its size. This information is then sent, together with the real object data, to the receiver network port, where the object is reconstructed in memory and cast to the correct type.

In this application, we send two types of messages: the motor commands to the robot and the messages between the Vision Agents.

6.3.3 Training the Neural Networks

The first problem in training a neural net is to have a rich set of unbiased training examples. In the learning phase, the Vision Agent generates a set of random commands for the motors of the robot. The Vision Agent stores in a file the initial pose of the robot, its final pose and the command that moved the robot from the starting position to the finish position. These data are used to train the two networks. In the first experiments we performed

[4]RoboCup: the Robotics Soccer Championship, URL www.robocup.org

[5]*Artisti Veneti* is the RoboCup team of the University of Padua for the Middle-Size League [76]

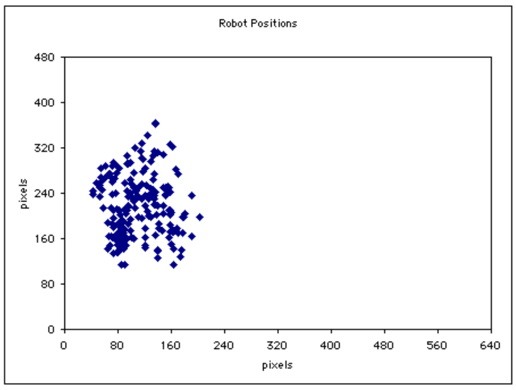

Figure 6.11: The positions of the robot in the image for the training data.

the motion of the robot was constrained in a portion of the field of view of the Omnidirectional VA. Fig. 6.11 shows the position of the robot for each training example. As you can see, the robot moved in the left field of view of the camera, approximately. Every motion had random speed and jog in order to present to the network a set of examples of velocity and jog values not biased by the choices of the user. The linear speed was randomly chosen between -400 mm/s and 400 mm/s. The angular speed was randomly chosen between -1 rad/s and 1 rad/s. We collected sets of about 200-300 examples and we used about 160-260 examples as training examples and the rest as validation examples. The training errors for a set of examples is reported in Fig. 6.12 and in Fig. 6.13. The two figures respectively refer to the error in the linear speed determination (called *speed*) and in the angular speed (called *jog*).

6.4 Conclusions

In the first part of the chapter, we introduced the concept of Vision Agent and Distributed Vision System and we presented some of the experiments we are carrying on these topics. These works on Omnidirectional Distributed

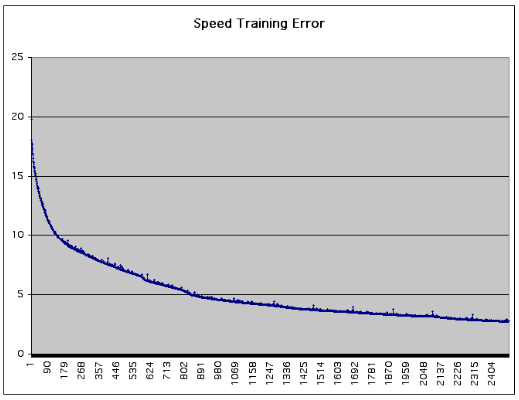

Figure 6.12: A plot of the learning error on the speed output.

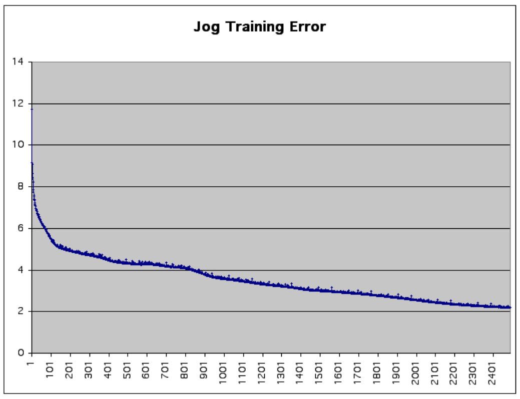

Figure 6.13: A plot of the learning error on the jog output.

Vision have been presented in [63] [62] [61] [60].

In the second part of the chapter, we presented a new idea in the creation of an intelligent network of sensor. We proposed a Distributed Vision System that is able to navigate a mobile robot in a large space. The DVS is composed of several Vision Agents that are able to autonomously learn how to control the robot. This knowledge is acquired locally and is distributed through the network from a Vision Agent to the rest of the Vision Agents using as a bridge the mobile robot for this *knowledge propagation*. This work has been presented in [69].

Bibliography

[1] H. Aihara, N. Iwasa, N. Yokoya, and H. Takemura. Memory-based self-localisation using omnidirectional images. In A. K. Jain, S. Venkatesh, and B. C. Lovell, editors, *Proc. of the 14th International Conference on Pattern Recognition*, volume vol. I, pages 1799–1803, 1998.

[2] S. Arulampalam, S. Maskell, N. Gordon, and T. Clapp. A tutorial on particle filters for on-line non-linear/non-gaussian bayesian tracking. *IEEE Transactions on Signal Processing*, 50(2):174–188, Feb. 2002.

[3] S. Baker and S. Nayar. A theory of single-viewpoint catadioptric image formation. *International Journal of Computer Vision*, vol. 35(no. 2):pp. 1–2, 1999.

[4] S. Baker and S. K. Nayar. A theory of catadioptric image formation. In *Proceeding of the 6th Intern. Conf. on Computer Vision*, January 1998.

[5] A. Basu and D. Southwell. Omni-directional sensor for pipe inspection. In *Proc. of IEEE Int. Conf. Systems, Man and Cybernetics*, volume 4, pages pp. 3107–3112, 1995.

[6] R. Benosman and S. B. Kang, editors. *Panoramic Vision.* Springer, 2001.

[7] G. Bianco and A. Zelinsky. Biologically-inspired visual landmark learning and navigation for mobile robots. *Proceedings of the 1999 IEEE/RSJ Int. Conf. on Intelligent Robots and Systems*, 1999.

[8] A. Bonarini. The body, the mind or the eye, first? In M. Veloso, E. Pagello, and H. Kitano, editors, *RoboCup99: Robot Soccer World Cup III*, volume 1856 pp. 210-221 of *LNCS*. Springer, 2000.

[9] A. Bonarini, P. Aliverti, and M. Lucioni. An omnidirectional vision sensor for fast tracking for mobile robot. *Proceedings of the IEEE IMTC99*, 1999.

[10] A. Bonarini, P. Aliverti, and M. Lucioni. An omnidirectional vision sensor for fast tracking for mobile robot. *IEEE Transaction of Instrumentation and Measurements*, 49(3):pp. 509–512, 2000.

[11] T. Boult, C. Qian, W. Yin, A. Erkin, P. Lewis, C. Power, and R. Micheal. Applications of omnidirectional imaging: Multi-body tracking and remote reality. In *IEEE Workshop on Applications of Computer Vision*, Dec 1998.

[12] R. A. Brooks. The intelligent room project. In *Proceedings of the Second International Cognitive Technology Conference (CT'97), Aizu, Japan*, August 1997.

[13] G. Browitt. Virtual reality telepresence using a mobile robot. Master's thesis, University of Edinburgh, Department of Artificial Intelligence, 1997.

[14] J. Bruce, T. Balch, and M. M. Veloso. Fast and inexpensive color image segmentation for interactive robots. In *Proceedings of the 2000 IEEE/RSJ Int. Conf. on Intelligent Robots and Systems (IROS '00)*, volume 3, pages 2061 – 2066, October 2000.

[15] R. Bunschoten and B. Krse. 3-d scene reconstruction from cylindrical panoramic images. *Robotics and Autonomous Systems (special issue)*, 2002. (to appear).

[16] W. Burgard, D. Fox, M. Moors, R. Simmons, and S. Thrun. Collaborative multi-robot exploration. In *Proceedings of the IEEE International Conference on Robotics and Automation (ICRA)*. IEEE, 2000.

[17] L. Burrelli, S. Carpin, F. Garelli, E. Menegatti, and E. Pagello. Ade: a software suite for multi-threading and networking. Technical report, Intelligent Autonomous Systems Laboratory, Department of Information Engineering, University of Padova, ITALY, 2002.

[18] J. Canny. A computational approach to edge detection. In *Transactions on Pattern Analysis and Machine Intelligence*, volume 8, pages 679–697. IEEE, 1986.

[19] J. Carpenter, P. Clifford, and P. Fearnhead. An improved particle filter for non-linear problems. In *IEEE Proc. Radar, Sonar and Navigation*, volume vol. 146, 1999.

[20] S. Carpin, C. Ferrari, E. Pagello, and P. Patuelli. Bridging deliberation and reactivity in cooperative multi-robot systems through map focus. In M.Hannebauer, J. Wendler, and E. Pagello, editors, *Balancing Reactivity and Social Deliberation in Multi-Agent Systems,*, LNCS. Springer, 2001.

[21] R. Cassinis, D. Duina, S. Inelli, and A. Rizzi. Unsupervised matching of visual landmarks for robotic homing unsing fourier-mellin transform. *Robotics and Autonomous Systems*, 40(2-3), August 2002.

[22] H. Choset and K. Nagatani. Topological simultaneous localisation and mapping (slam): Toward exact localization without explicit localization.

IEEE Transaction on Robotics and Automation, 17(2):125–137, April 2001.

[23] T. Collett, E. Dillmann, A. Giger, and R. Wehner. Visual landmarks and route following in desert ants. *Journal of Comparative Physiology A*, 170:pp. 435–442, 1992.

[24] R. Collins, A. Lipton, and T. Kanade. A system for video surveillance and monitoring. Technical report, Robotics Institute at Carnagie Mellon University, 2000.

[25] R. Cutler, Y. Rui, A. Gupta, J. C. I. Tashev, L. wei He, A. Colburn, Z. Zhang, Z. Liu, and S. Silverberg. Distributed meetings: A meeting capture and broadcasting system. In *ACM Multimedia*, 2002.

[26] S. Derrien and K. Konolige. Approximating a single effective viewpoint in panoramic imaging devices. In *Proceedings IEEE Workshop on OmniDirectional Vision*, pages pp. 85–96., June 2000.

[27] M. O. Franz, B. Schölkopf, H. A. Mallot, and H. H. Bülthoff. Learning view graph for robot navigation. *Autonomous Robots*, 5:pp. 111–125, 1998.

[28] J. Gaspar, C. Decco, J. Okamoto, and J. Santos-Victor. Constant resolution omnidirectional cameras. In *To Appear in Omnivis'02 Workshop on Omnidirectional Vision*, June 2002.

[29] J. Gaspar, N. Winters, and J. Santos-Victor. Vision-based navigation and environmental representations with an omnidirectional camera. *IEEE Transaction on Robotics and Automation*, Vol 16(number 6), December 2000.

[30] P. Greguss. The tube peeper: A new concept in endoscopy. In *Optics and Laser Technologies*, pages pp. 41–45, 1985.

[31] P. Greguss. Pal-optic based instruments for for space research and robotics. *Laser and Optoelektronik*, 28:43–49, 1996.

[32] D. Gutchess, A. K. Jain, and Sei-Wang. Automatic surveillance using omnidirectional and active cameras. In *Asian Conference on Computer Vision (ACCV)*, January 2000.

[33] A. Hicks and R. Bajcsy. Reflective surfaces as computational sensors. In *Proc. of the Second Workshop on Perception for Mobile Agents, Fort Collins*, pages pp. 82–86, 1999.

[34] P. Hough. Method for recognizing complex patterns. Technical report, US Patent 3069654, 1962.

[35] Hu and Gu. Landmark-based localisation of industrial mobile robots. *International Journal of Industrial Robot*, Vol. 27(No. 6):pp. 458 – 467, November 2000.

[36] H. Ishiguro. Distributed vision system: A perceptual information infrastructure for robot navigation. In *Proceedings of the Int. Joint Conf. on Artificial Intelligence (IJCAI97)*, pages 36–43, 1997.

[37] H. Ishiguro. Development of low-cost compact omnidirectional vision sensors. In R. Benosman and S. Kang, editors, *Panoramic Vision*, chapter 3, pages pp. 23–38. Springer, 2001.

[38] H. Ishiguro and M. Trivedi. Integrating a perceptual information infrastructure with robotic avatars: A framework for tele-existence. In *Proceedings of the IEEE/RSJ International Conference on Intelligent Robots and Systems (IROS-99)*, October 1999.

[39] H. Ishiguro and S. Tsuji. Image-based memory of environment. In *Proceedings of the IEEE/RSJ International Conference on Intelligent Robots and Systems (IROS-96)*, pages pp. 634–639, 1996.

[40] H. Ishiguro, M. Yamamoto, and S. Tsuji. Omni-directional stereo. *IEEE Transaction on Pattern Analysis and Machine Intelligence*, VOL. 14(NO. 2):pp. 257–262, February 1992.

[41] M. Jogan and A. Leonardis. Robust localization using panoramic view-based recognition. In *Proc. of the 15th Int.Conference on Pattern Recognition (ICPR00)*, volume 4, pages pages 136–139. IEEE Computer Society, September 2000.

[42] T. Kanade, P. Rander, S. Vedula, and H. Saito. Virtualized reality: Digitizing a 3d time-varying event as is and in real time. In Y. Ohta and e. Hideyuki Tamura, editors, *Mixed Reality, Merging Real and Virtual Worlds*, pages pp. 41–57. Springer-Verlag, 1999.

[43] D. Kortenkamp, P. Bonasso, and R. Murphy, editors. *Artificial Intelligence and Mobile Robotics*. AAAI Press/ MIT Press, 1998.

[44] B. Kröse, N. Vlassis, R. Bunschoten, and Y. Motomura. Feature selection for appareance-based robot localization. *Proceedings 2000 RWC Symposium*, 2000.

[45] B. Kröse, N. Vlassis, R. Bunschoten, and Y. Motomura. A probabilistic model for appareance-based robot localization. *Image and Vision Computing*, vol. 19(6):pp. 381–391, April 2001.

[46] B. Kuipers. The spatial semantic hierarchy. *Artificial Intelligence*, 119:191–233, February 2000.

[47] B. J. Kuipers and Y.-T. Byun. A robot exploration and mapping strategy based on a semantic hierarchy of spatial representations. *Journal of Robotics and Autonomous Systems*, 8:47–63, 1991.

[48] B. J. Kuipers and Y.-T. Byun. A robot exploration and mapping strategy based on a semantic hierarchy of spatial representations. *Journal of Robotics and Autonomous Systems*, 8:47–63, 1991.

[49] B. J. Kuipers and T. Levitt. Navigation and mapping in large scale space. *AI Magazine*, 9(2):25–43, 1988. Reprinted in *Advances in Spatial Reasoning, Volume 2*, Su-shing Chen (Ed.), Norwood NJ: Ablex Publishing, 1990, pages 207–251.

[50] W. Y. Lee, Ph.D. *Spatial Semantic Hierarchy for a Physical Mobile Robot*. PhD thesis, The University of Texas at Austin, 1, 1996.

[51] T. S. Levitt and D. T. Lawton. Qualitative navigation for mobile robots. *Artificial Intelligence Journal*, 44(3):305–361, 1990.

[52] F. Marchese and D. G. Sorrenti. Omni-directional vision with a multipart mirror. In P. Stone, T. Balch, and G. Kraetzschmar, editors, *RoboCup 2000: Robot Soccer World Cup IV*, LNCS. Springer, 2001.

[53] C. F. Marques and P. U. Lima. Vision-based self-localization for soccer robots. In *Proceedings of the 2000 IEEE/RSJ Int. Conf. on Intelligent robots and systems*, 2000.

[54] T. Matsuyama. Cooperative distributed vision: Dynamic integration of visual perception, action, and communication. In W. Burgard, T. Christaller, and A. B. Cremers, editors, *Proc. of the Annual German Conf. on Advances in Artificial Intelligence (KI-99)*, volume 1701 of *LNAI*, pages 75–88, Berlin, Sept. 1999. Springer.

[55] T. Matsuyama, S. Hiura, T.Wada, K.Murase, and A.Yoshioka. Dynamic memory: Architecture for real time integration of visual perception, camera action, and network communication. In W. Burgard,

T. Christaller, and A. B. Cremers, editors, *Proc. of Computer Vision and Pattern Recognition Conference*, pages pp. 728–735, June 2000.

[56] E. Menegatti. The caboto project. Master's thesis, MSc in Artificial Intelligence - Informatics Graduate School - University of Edinburgh, September 2000.

[57] E. Menegatti, T. Maeda, and H. Ishiguro. Image-based memory for robot navigation using properties of the omnidirectional images. *submitted to an International Journal*, 2002.

[58] E. Menegatti, F. Nori, and E. Pagello. Design of omnidirectional mirrors for mobile robotics based on robot's task. In *Submitted to an International Journal*, 2002.

[59] E. Menegatti, F. Nori, E. Pagello, C. Pellizzari, and D. Spagnoli. Designing an omnidirectional vision system for a goalkeeper robot. In A. Birk, S. Coradeschi, and S. Tadokoro, editors, *RoboCup-2001: Robot Soccer World Cup V.*, pages pp. 78–87. Springer, 2002.

[60] E. Menegatti and E. Pagello. Cooperation of heterogeneous vision agents for mobile robots. *Workshop of the Gruppo di Lavoro Robotica of Italian Association for Artificial Intelligence (AI*IA) Milan*, December 2001. (on the web only URL: http://aiia.elet.polimi.it/Workshop.html).

[61] E. Menegatti and E. Pagello. Cooperative distributed vision for mobile robots. *Workshop on Artificial Intelligence, Vision and Pattern Recognition 7th Conference of the Italian Association for Artificial Intelligence (AI*IA) September*, pages pp. 75–82, September 2001. Printed on AIIA Notizie, Anno 15, No. 1, 2002, pp. 11- 14.

[62] E. Menegatti and E. Pagello. Designing omnidirectional vision systems and inserting them in a distributed vision system for mobile robots. In

S. Taraglio and V. Nanni, editors, *Enabling Technologies for the PRASSI Autonomous Robot*, pages pp. 98–108. ENEA, 2001.

[63] E. Menegatti and E. Pagello. Cooperation between omnidirectional vision agents and perspective vision agents for mobile robots. In *Proceedings of the 7th International Conference on Intelligent Autonomous Systems (IAS-7)*, pages pp. 231–235, Los Angeles, USA, March 2002.

[64] E. Menegatti and E. Pagello. Howto design omnidirectional mirrors for different robotic applications. In *submitted to an international magazine*, 2002.

[65] E. Menegatti and E. Pagello. Omnidirectional distributed vision for multi-robot mapping. In *Proceedings of the 6th International Symposium on Distributed Autonomous Robotic Systems (DARS02)*, pages pp.279–288, Fukuoka, Japan, June 2002.

[66] E. Menegatti and E. Pagello. Omnidirectional mirror design based on the vision task. In *Proceeding of 1a Conferenza Nazionale su "Sistemi Autonomi Intelligenti e Robotica Avanzata*, Frascati - Roma, Ottobre 2002. (to be printed).

[67] E. Menegatti and E. Pagello. Toward a topological mapping with a multi-robot team. In *Proc. of the Workshop on Cooperative Robotics, A. Saffiotti Organizer IEEE/RSJ International Conference on Intelligent Robots and Systems (IROS02-WS7)*, pages pp.V/1–V/7, Lausanne, October 2002.

[68] E. Menegatti, E. Pagello, and H. Ishiguro. Hierarchical image-based localisation for mobile robots
with monte-carlo localisation. In *submitted to an International Conference*, 2002.

[69] E. Menegatti, E. Pagello, T. Minato, T. Nakamura, and H. Ishiguro. Toward knowledge propagation in an omnidirectional distributed vision system. In *submitted to an International Conference*, 2002.

[70] E. Menegatti, E. Pagello, and M. Wright. Using omnidirectional vision sensor within the spatial semantic hierarchy. In *IEEE International Conference on Robotics and Automation (ICRA2002)*, pages pp. 908–914, Washinton, USA, May 2002.

[71] E. Menegatti, M. Wright, and E. Pagello. A new omnidirectional vision sensor for the spatial semantic hierarchy. In *IEEE/ASME Int. Conf. on Advanced Intelligent Mechatronics (AIM '01)*, pages 93–98, July 2001.

[72] T. Mitchell. *Machine Learning*. McGraw-Hill, 1997.

[73] A. Nakazawa, H. Kato, S. Hiura, and S. Inokuchi. Tracking multiple people using distributed vision systems. In *Proceedings of the IEEE International Conference on Robotics and Automation (ICRA2002)*, pages pp. 2974–2981, May 2002.

[74] S. Nayar and V. Peri. Folded catadioptric cameras. In R. Benosman and S. B. Kang, editors, *Panoramic Vision*, pages pp.103–119. Springer, 2001.

[75] E. Pagello, M. Bert, M. Barbon, E. Menegatti, C. Moroni, C. Pellizzari, D. Spagnoli, and S. Zaffalon. Artisti veneti: an heterogeneous robot team for the 2001 middle-size league. In A. Birk, S. Coradeschi, and S. Tadokoro, editors, *RoboCup-2001: Robot Soccer World Cup V.*, volume 2377 of *L. N. on A. I*, pages pp. 599–602. Springer, 2001.

[76] E. Pagello, M. Bert, M. Barbon, E. Menegatti, C. Moroni, C. Pellizzari, D. Spagnoli, and S. Zaffalon. Artisti veneti 2002: evolving an heteroge-

neous robot team for the middle-size league. In G. A. Kaminka, P. U. Lima, and R. Rojas, editors, *RoboCup-2002: Robot Soccer World Cup VI.*, L. N. on A. I. Springer, 2002.

[77] T. Pajdla and V. Hlaváč. Zero phase representation of panoramic images for image based localization. In F. Solina and A. Leonardis, editors, *8-th International Conference on Computer Analysis of Images and Patterns*, number 1689 in Lecture Notes in Computer Scinence, pages 550–557, Tržaška 25, Ljubljana, Slovenia, September 1999. Springer Verlag.

[78] V. N. Peri and S. K. Nayar. Generation of perspective and panoramic video from omnidirectional video. In *Proc. of DARPA Image Understanding Workshop*, May 1997.

[79] K. Pierce and B. Kuipers. Map learning with uninterpreted sensors and effectors. *Artificial Intelligence*, 92:169–227, 1997.

[80] J. R. Smith. Integrated spatial and feature image systems: Retrieval, analysis and compression. Technical report, Columbia University, 1997. Available at the URL:disney.ctr.columbia.edu/jrsthesis/thesissmall.html.

[81] T. Sogo, H. Ishiguro, and T. Ishida. Acquisition and propagation of spatial constraints based on qualitative information. *IEEE Trans. Pattern Analysis and Machine Intelligence*, Vol.23:pp.268–278, 2001.

[82] T. Svoboda, T. Pajdla, and V. Hlavac. Motion estimation using central panoramic cameras. *IEEE Conf. on Intelligent Vehicles, Stuttgart, Germany*, October 1998.

[83] H. Takeda, N. Kobayashi, Y. Matsubara, and T. Nishida. A knowledge-level approach for building human-machine cooperative environment. In A. Drogoul, M. Tambe, and T. Fukuda, editors, *Collective Robotics*,

volume 1456 of *Lecture Notes in Artificial Intelligence*, pages pages 147–161. Springer, 1998.

[84] S. Thrun, M. Beetz, M. Bennewitz, W. Burgard, A. Cremers, F. D. Fox, D. Haehnel, C. Rosenberg, N. Roy, J. Schulte, and D. Schulz. Probabilistic algorithms and the interactive museum tour-guide robot minerva. In *International Journal of Robotics Research*, volume Vol. 19, pages pp. 972–999, November 2000.

[85] G. Weiss. *Multiagent Systems.* MIT Press, 1999.

[86] N. Winters and J. Santos-Victor. Mobile robot navigation using omnidirectional vision. *3rd Irish Machine Vision and Image Processing Conf. IMVIP99, Dublin, Ireland*, September 1999.

[87] J. Wolf, W. Burgard, and H. Burkhardt. Robust vision-based localization for mobile robots using an image retrieval system based on invariant features. In *Proc. of the IEEE International Conference on Robotics & Automation (ICRA)*, 2002.

[88] Y. Yagi. Omni directional sensing and its applications. *IEICE TRANS. INF. & SYST.*, VOL. E82-D(NO. 3):pp. 568–579, MARCH 1999.

[89] Y. Yagi, Y. Nishizawa, and M. Yachida. Map-based navigation for a mobile robot with omnidirectional image sensor copis. *IEEE Transaction on Robotics and automation*, VOL. 11(NO. 5):pp. 634–648, October 1995.